Real-Time Configuration Control System for Redundant Manipulators and Analysis of Avoidance Space

福　井　大　学

学位論文［博士（工学）］

A Dissertation Submitted to the
University of Fukui for the Degree of
Doctor of Engineering

Real-Time Configuration Control System for Redundant Manipulators and Analysis of Avoidance Space

冗長マニピュレータの実時間形状制御システム
と回避空間の分析

2009年9月

Tongxiao Zhang

Contents

Real-Time Configuration Control System for Redundant Manipulators and Analysis of Avoidance Space

Abstract

This research is concerned with a real-time control system of trajectory tracking and obstacle avoidance using an avoidance manipulability measure for redundant manipulators. To perform predetermined end-effector trajectory-tracking task adaptively without path-planning for avoidance, information on the local environment is naturally restricted by limited recognition time. This means adaptive configuration control has to manage its shape in real-time and without adequate information on its surroundings. Therefore, when the manipulator executes a task adaptively in a dynamic environment, its avoidance manipulability should always be kept as high as possible to prepare for sudden avoidance action. As a measure to gauge the avoidance manipulability based on non-collision, we firstly propose a new index, "AMSIP". By combining a concept of "preview control" with real-time optimization of AMSIP distribution found by "1-step GA", we propose a new real-time configuration control method, with future information being referred locally but effectively. The proposed system has been shown that it is feasible and practical by simulations in terms of real-time configuration optimization.

Avoidance manipulability is a new important concept in this research, which is inspired from manipulability. The manipulability represents the ability to generate velocity at the tip of each link without any designated end-effector task. The avoidance manipulability represents the shape-changeability (avoidance ability) of intermediate links when a prior end-effector task is given. Here, the intermediate links denote the all links of the redundant manipulator except the top link with the end-effector since the top link is used to execute

the prior task. The avoidance matrix, ${}^1\boldsymbol{M}_i$ $(i = 1, \cdots, n-1)$, is used for analyzing avoidance manipulability of the i-th intermediate link, $rank({}^1\boldsymbol{M}_i)$ indicates the shape-changeable space expansion and the singular values of ${}^1\boldsymbol{M}_i$ indicate the avoidance ability in the typical direction in the shape-changeable space. As the most essential condition to devise the robot's configuration controller that can always keep the avoidance manipulability high and to build the framework discussing shape-changeability under the prior end-effector task, we analyze what assumption guarantees mathematically the sustainability of the shape-changeable space, that is $rank({}^1\boldsymbol{M}_i)$. Then we prove that "Non-Singular Configuration Assumptions" we presented can assure $rank({}^1\boldsymbol{M}_i)$ through detailed decomposition analysis of ${}^1\boldsymbol{M}_i$. Non-Singular Configuration Assumptions have not been integrated into our current configuration control system, but they have an ability for presenting yardstick to maintain the sustainability of avoidance space expansion.

1 Introduction

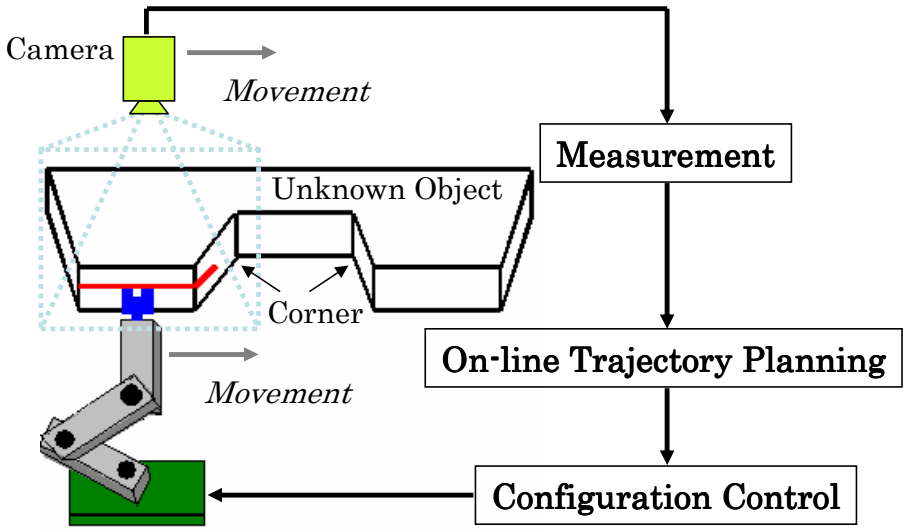

Fig. 1.1: Processing system for unknown object

Kinematically redundant manipulators have more Degrees of Freedom (DoF) than necessary for accomplishing a given end-effector task. Nowadays, redundant manipulators are used for various tasks, such as welding, sealing, grinding and other contact tasks, where the irregular shape of the object worked on may hinder the robot's successful completion of task. These kinds of tasks require that the manipulator plan its end-effector onto the desired trajectory and avoid its intermediate links, meaning all comprising links of robot except the top link with the end-effector, from obstacles existing near the target object as well as from the target object itself. Based on this situation, this research considers the real-time control system shown in Fig.1.1, this system is able to operate any working object of any shape without any preparation for production in factories.

There have been many researches on configuration control and obstacle avoidance of kinematically redundant manipulators discussing how to use the redundancy. The proposed solutions so far can roughly be categorized as Global Methods and Local Methods. Within the Global Methods, a Newton-Raphson type algorithm together with a penalty function

method has been presented [1)], which is capable of handling various goal task definitions as well as incorporating both joint and task space constraints, where a method added potential field around things in the environment has been discussed [2)]. A time-optimal control scheme for kinematically redundant manipulators has been presented to track a predefined geometric path, subjected to joint torque limits [3)], and kinematic failure tolerance has been analyzed in the environment with obstacles [4)]. A Factor-Guided algorithm that finds plans of motion from initial arm configuration to a goal arm configuration in 2D space has been presented [5)], which utilized topology of the arm and obstacles to factor search space and reduce complexity of the planning problem. In reference [6)], Ahuactzin and Gupta have proposed a global method (Kinematic Roadmap) to find a series of reachable configurations (a feasible path) from a given initial configuration to goal position based on a concept of "reachability". For travelling operation of mobile manipulator, a motion planning scheme aimed at keeping manipulability as high as possible has been presented [7)]. In general, Global Methods are used to choose the best path beginning initial posture of the manipulator to goal position from all possible paths in the full configuration space. It is obvious that Global Methods are only suitable for structured and static environments and are inapplicable to dynamic environments with moving obstacles. Moreover, Global Methods are computationally expensive, and the computational cost expands rapidly as the number of manipulator's joints increases. Therefore, considering these limitations, Global Methods are utilized only as an off-line path/motion planning tool in artificially structured static environments, and are typically supervised from a high level in the control hierarchy. On the other hand, to achieve an ability that is adaptive to dynamic environments, a system must make every effort to be as flexible as possible, even in situations where information on the surroundings is limited. Such methodologies are known as Local Methods, and this adaptation requires that the system tolerate changing conditions and possess real-time measurement ability, although Local Methods can not guarantee the superiority of a chosen path or even the existence of a path to the goal. Various approaches to real-time obstacle avoidance for redundant manipulators have been presented [8)-11)] including real-time control methods to avoid singular configurations [12)]. According to the characteristics of Local Methods, they are mainly used to deal with moving obstacles in an unstructured environment.

In addition, up to now, a variety of indices have been proposed for evaluation of the performance of robot manipulators. The manipulability ellipsoid [13], [14] has been presented to evaluate the static performance of a robot manipulator as an index for evaluating the manipulator's shape in terms of how much the end-effector velocity can be generated by normalized joint velocity. Further, reference [15] has formulated the relation of the redundancy and the priority order of multiple tasks. Reference [16] has proposed a control method of the redundancy based on the priority order of tasks, and pointed out its effectiveness through actual experiments. The manipulability measure has been addressed for cooperative arms [17], [18] and for dexterous hands [19]. In addition, the manipulating force ellipsoid [20] has been presented to evaluate the static torque-force transmission from the joints to the end-effector, while the dynamic manipulability ellipsoid [21] has been presented as an index of the dynamic performance of a robot manipulator. The concept of inertia matching for a serial-link manipulator [22] has been recently proposed as a new index of the dynamic performance of the manipulator. Then, combining the dynamic manipulability ellipsoid with the manipulability force ellipsoid, the inertia matching ellipsoid [23] has been proposed to characterize the dynamic torque-force transmission efficiency. The dynamic capability equations [24] have been provided as a description of robot acceleration and force capabilities, which refer to a manipulator's ability to accelerate its end-effector and to apply forces to the environment at the end-effector.

Above researches tell us that the focuses of the researching topics about redundant manipulators have been shifted from kinematical consideration into arguments combining kinematics and dynamics for evaluating and controlling the manipulator. However, they are based on a condition assuming implicitly that multiple avoidance motions could be realized, they do not start from the point of view that tasks involving trajectory tracking of the end-effector and obstacle avoidance may be impossible to operate simultaneously, depending on the relation of the manipulator's shape, the given end-effector task, and the environment. This is because they do not care if "avoidance manipulability" is retained or not as a result of operating the higher priority tasks. Please notice that "Avoidance" in this research is used for shape-changeable motion of the manipulator while the end-effector tracks the predetermined desired pose with designated dimension space. The above mentioned researches do

not consider how much residue redundant mobility is remained at the links required to avoid the obstacle.

On the other hand, the end-effector's mobility represented by manipulability has been well-known to be decreased by singularities of Jacobian matrix, and the manipulability measure has been recognized to present a kind of distance from singular configuration of manipulator. Contrarily to above end-effector's free motion, it seems that there has been no concept to describe avoidance manipulability for the "Avoidance" task with desired end-effector task. Moreover, in our previous researches, we presented a basic concept of preview control method, which can make the current shape be close desired shape with the aim of avoiding collision effectively by referring to the future shape [25]. However, the manipulator sometimes collided with the obstacle. Then, we presented a method which consists of both the preview control and the postview control additionally considering the past shape by using its redundancy [26], with total control performance limited to some extent. What is the most defective point in these preview approaches is the lack of consideration of how many redundant avoidance abilities are leftover at the intermediate link required to avoid the obstacle. Those approaches were arguments made on the condition that an assumption guarantees the possibility that the avoidance motion could be available. Therefore, both how to measure the avoidance manipulability remaining and how to control the configuration in a residue shape-changeable margin are the themes discussed in this research.

Our research pursues a real-time control system using the Local Method. The features of our system are shown in Fig.1.1. Such systems can be seen everywhere in factories. The camera scene symbolizes the restricted information on the surroundings, and it contains future trajectory information even though the near future is restricted. In Fig.1.1, the camera and the manipulator's end-effector are supposed to move synchronously because achieving on-line operation depends on the real-time information of an unknown target object obtained by this moving camera covering a restricted area. As shown in Fig.1.2, when the camera detects the sharp corners denoted as A, B and C appearing suddenly as the obstacles in the scene of the camera as time t is t_1, t_2 and t_3, the manipulator may be in a dangerous, collision-producing situation and in such case the configuration of the manipulator must change immediately so that it can avoid this obstacle. Therefore, in the whole on-line trajectory tracking process, al-

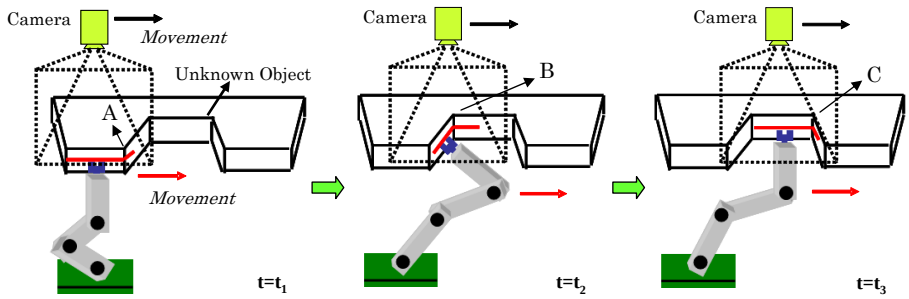

Fig. 1.2: Sharp corners appearing suddenly as the obstacles

ways keeping the avoidance manipulability (shape-changeability) of the whole manipulator as high as possible is essential to being prepared for the abrupt appearance of obstacles. In this background, we had presented a concept of the avoidance manipulability ellipsoid [27] as an index evaluating shape-changeability of the intermediate links, while the end-effector tracks the desired trajectory, which is inspired from the manipulability concept [13], [14]. In reference [27], the avoidance manipulability ellipsoid just evaluated the avoidance manipulability of each intermediate link except the end-effector, it was not enough to evaluate the avoidance manipulability of the whole manipulator. Therefore, for evaluating the avoidance manipulability of the whole manipulator, we propose an index called "AMSI" (Avoidance Manipulability Shape Index) [28]. Although "AMSI" can be used for evaluating the avoidance manipulability of the whole manipulator, it does not consider the distance between the manipulator and the target objects. By setting the potential spaces structured around the target object and combining them with "AMSI", we propose a new index called "AMSIP" (AMSI with Potential). We verify that "AMSIP" is more effective than "AMSI" through analysis and comparison. In this research, "configuration control" means a control strategy of manipulator's shape based on the optimization of "AMSIP". This definition is different from the previous concept of configuration control [29].

The emphasis of our approach is on the real-time optimization control of the manipulator's configuration using the Local Method. Here, "real-time configuration control" is defined as configuration control based on real-time recognition. Real-time recognition is to detect target working object's shape in 33$[ms]$ without delaying the video-rate 30$[frame/s]$. This has been confirmed to be realizable in our previous report on fish-catching using 1-step GA [30]. Then

"real-time configuration control" can be rewritten as to control the robot's configuration within a control period of less than 33$[ms]$ and based on on-line recognition. The Local Method has such merit as less computation burden, but local information is naturally the defect on the meaning of it being not global. On the basis of "AMSIP", combining the preview control method with 1-step GA, we successfully overcome this natural defect and realize an on-line processing system through which a manipulator's end-effector can track the desired trajectory on the working object with higher avoidance manipulability. We also verify its effectiveness through simulations.

Avoidance manipulability of the manipulator is evaluated based on the avoidance ability in each possible dimension of intermediate links in the residue redundant space. However, whether we can use the remaining redundancy to achieve desired avoidance task depends on purely whether the avoidance task lies in the range space of the avoidance matrix ${}^1\boldsymbol{M}_i$, which is defined as

$$ {}^1\boldsymbol{M}_i = \boldsymbol{J}_i(\boldsymbol{I}_n - \boldsymbol{J}_n^+\boldsymbol{J}_n), $$

where $\boldsymbol{J}_i$ and $\boldsymbol{J}_n$ are Jacobian matrices corresponding to the i-th link and the top link respectively, $\boldsymbol{J}_n^+$ is the pseudo-inverse of $\boldsymbol{J}_n$, $\boldsymbol{I}_n$ is a $n\times n$ unit matrix. The demonstration of ${}^1\boldsymbol{M}_i$ is explained in chapter 3. As the most essential condition to devise the robot's configuration controller that can always keep the avoidance manipulability high and to build the framework discussing shape-changeability under the end-effector prior task, we analyze what assumption guarantees mathematically the sustainability of the shape-changeable space, that is $rank({}^1\boldsymbol{M}_i)$. The singular values of ${}^1\boldsymbol{M}_i$ means the radius length of main axes of avoidance manipulability ellipsoids.

Maintaining $rank({}^1\boldsymbol{M}_i)$ of intermediate links as high as possible is the essential requirement for configuration control to optimize manipulator's shape with high avoidance manipulability. And we think it should be the first step to design a real-time control system of a redundant manipulator with high shape-changeability based on avoidance manipulability. We want to stress here previous researches have not paid attention to how to guarantee $rank({}^1\boldsymbol{M}_i)$ to assure the required avoidance task to be realizable. In fact, a similar concept of ${}^1\boldsymbol{M}_i$ had initially been defined and used for controlling the redundant manipulator's con-

figuration based on prioritized multiple tasks [31]. However, the proposed controller in [31] do not concern the possibility the range space of ${}^1\boldsymbol{M}_i$ could be reduced by singular configuration and it can not decouple the interacting motions of multiple tasks even though the redundant degree be much higher than the required motion degree of the multiple tasks. Even in our previous researches about avoidance manipulability optimization [28] and real-time control system [32], [33] of a redundant manipulator, we did not guarantee the sustainability of the range space of ${}^1\boldsymbol{M}_i$. So we need assumption to assert that the range space of ${}^1\boldsymbol{M}_i$ should be maitained. Then the assumption can provide a configuration control criterion as primary control objective to keep the shape-changeability by avoiding singular configuration. In chapter 7, we propose two assumptions named as "Part-Non-Singular Configuration Assumption" and "All-Non-Singular Configuration Assumption", both can guarantee that $rank({}^1\boldsymbol{M}_i)$ could be maintained without reduction by dropping into singular configuration, through analyses and proofs by decomposing ${}^1\boldsymbol{M}_i$ into singular components. These two Non-Singular Configuration Assumptions have not been integrated into our current configuration control system, but they have an ability for presenting yardstick to maintain the sustainability of avoidance space expansion.

2 Manipulability

All descriptions written in this chapter are well known in robotics field. However, we thought that careful descriptions of kinematics of redundant manipulator will help readers understand mathematical analyses described from chapter 3 and make clear discussed following chapter 3. If readers are well versed in robotics, they may start reading this thesis from chapter 3.

2.1 Redundant Manipulator's Kinematics

2.1.1 Position Space

As shown in Fig.2.1, Σ_0 is the world coordinate fixed in the task space, Σ_i $(i = 1, 2, \cdots, n)$ is a coordinate fixed at bottom-side of the i-th link, q_i is the rotational angle of the i-th link, n denotes the number of the manipulator's links. The position vector of top-side of the i-th link is denoted as $\boldsymbol{r}_{p,i+1}(\boldsymbol{q}_i) \in R^{m_p}$ with respect to Σ_0, and the position vector of bottom-side of the i-th link is denoted as $\boldsymbol{r}_{p,i}(\boldsymbol{q}_{i-1}) \in R^{m_p}$ with respect to Σ_0. m_p denotes the position dimension number of working space $(1 \leq m_p \leq 3)$. $\boldsymbol{r}_{p,n+1}(\boldsymbol{q}_n) = \boldsymbol{r}_{p,E}(\boldsymbol{q}_n)$ and we simplify as $\boldsymbol{r}_{p,1} = \boldsymbol{0}$. In this research, please notice that the all definitions will omit the left superscript "0" when they are with respect to Σ_0. When $m_p = 3$, $\boldsymbol{r}_{p,i+1}(\boldsymbol{q}_i)$ is given as a function of $\boldsymbol{q}_i$ and defined as

$$\boldsymbol{r}_{p,i+1}(\boldsymbol{q}_i) = \begin{pmatrix} x_{i+1}(\boldsymbol{q}_i) \\ y_{i+1}(\boldsymbol{q}_i) \\ z_{i+1}(\boldsymbol{q}_i) \end{pmatrix}. \tag{2.1}$$

In (2.1), $\boldsymbol{q}_i \in R^n$ and it is defined as

$$\boldsymbol{q}_i = \begin{pmatrix} q_1 \\ \vdots \\ q_i \\ 0 \\ \vdots \\ 0 \end{pmatrix}, \quad (i = 1, 2, \cdots, n). \tag{2.2}$$

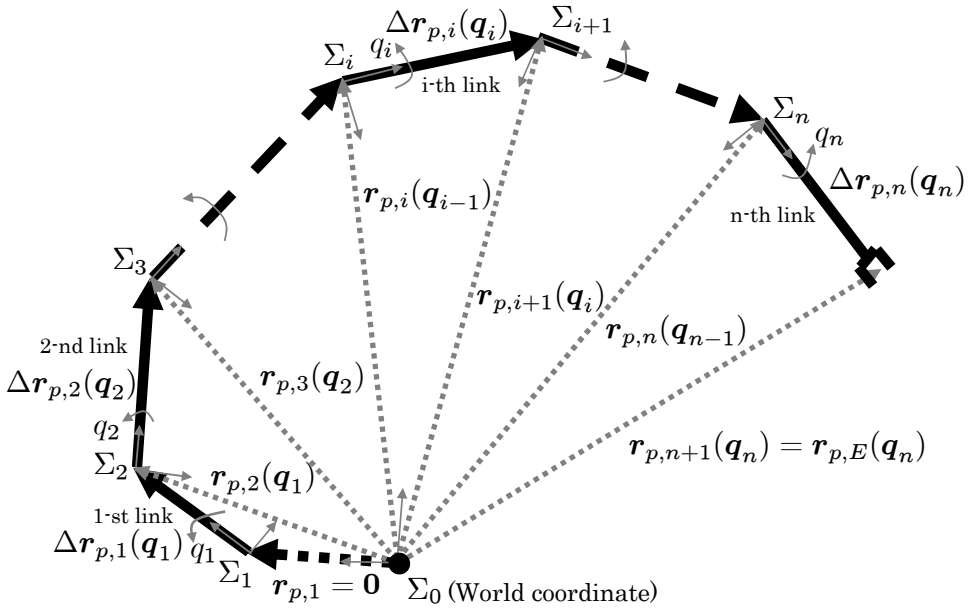

Fig. 2.1: Structure 1 of n-link redundant manipulator

In addition, as shown in Fig.2.1, $\Delta \boldsymbol{r}_{p,i}(\boldsymbol{q}_i)$ is the vector connecting bottom-side to top-side of i-th link with respect to Σ_0, so $\boldsymbol{r}_{p,i+1}(\boldsymbol{q}_i)$ can be denoted as

$$\boldsymbol{r}_{p,i+1}(\boldsymbol{q}_i) = \sum_{j=1}^{i} \Delta \boldsymbol{r}_{p,j}(\boldsymbol{q}_j). \tag{2.3}$$

By differentiating $\boldsymbol{r}_{p,i+1}(\boldsymbol{q}_i)$ in (2.3) with time, we can obtain

$$\begin{aligned}
\dot{\boldsymbol{r}}_{p,i+1}(\boldsymbol{q}_i) &= \frac{\partial \boldsymbol{r}_{p,i+1}(\boldsymbol{q}_i)}{\partial \boldsymbol{q}_n^T}\dot{\boldsymbol{q}}_n \\
&= \frac{\partial \Delta \boldsymbol{r}_{p,1}(\boldsymbol{q}_1)}{\partial \boldsymbol{q}_n^T}\dot{\boldsymbol{q}}_n + \cdots + \frac{\partial \Delta \boldsymbol{r}_{p,i}(\boldsymbol{q}_i)}{\partial \boldsymbol{q}_n^T}\dot{\boldsymbol{q}}_n \\
&= \frac{\partial \Delta \boldsymbol{r}_{p,1}(\boldsymbol{q}_1)}{\partial \boldsymbol{q}_1^T}\dot{\boldsymbol{q}}_n + \cdots + \frac{\partial \Delta \boldsymbol{r}_{p,i}(\boldsymbol{q}_i)}{\partial \boldsymbol{q}_i^T}\dot{\boldsymbol{q}}_n \\
&= \boldsymbol{J}_{p,i}\dot{\boldsymbol{q}}_n,
\end{aligned} \tag{2.4}$$

then, we can obtain the position Jacobian matrix $\boldsymbol{J}_{p,i}$ $(i = 1, 2, \cdots, n)$ in (2.4) as

$$\begin{aligned}
\boldsymbol{J}_{p,i} &= (\underbrace{\sum_{j=1}^{i}\frac{\partial \Delta \boldsymbol{r}_{p,j}(\boldsymbol{q}_j)}{\partial q_1},\ \sum_{j=2}^{i}\frac{\partial \Delta \boldsymbol{r}_{p,j}(\boldsymbol{q}_j)}{\partial q_2},\ \cdots,\ \frac{\partial \Delta \boldsymbol{r}_{p,i}(\boldsymbol{q}_i)}{\partial q_i}}_{i},\ \underbrace{\boldsymbol{0}}_{n-i})\}m_p \\
&= (\tilde{\boldsymbol{j}}_{p,i,1},\ \tilde{\boldsymbol{j}}_{p,i,2},\ \cdots,\ \tilde{\boldsymbol{j}}_{p,i,i},\ \boldsymbol{0}) \\
&= (\tilde{\boldsymbol{J}}_{p,i},\ \boldsymbol{0}).
\end{aligned} \tag{2.5}$$

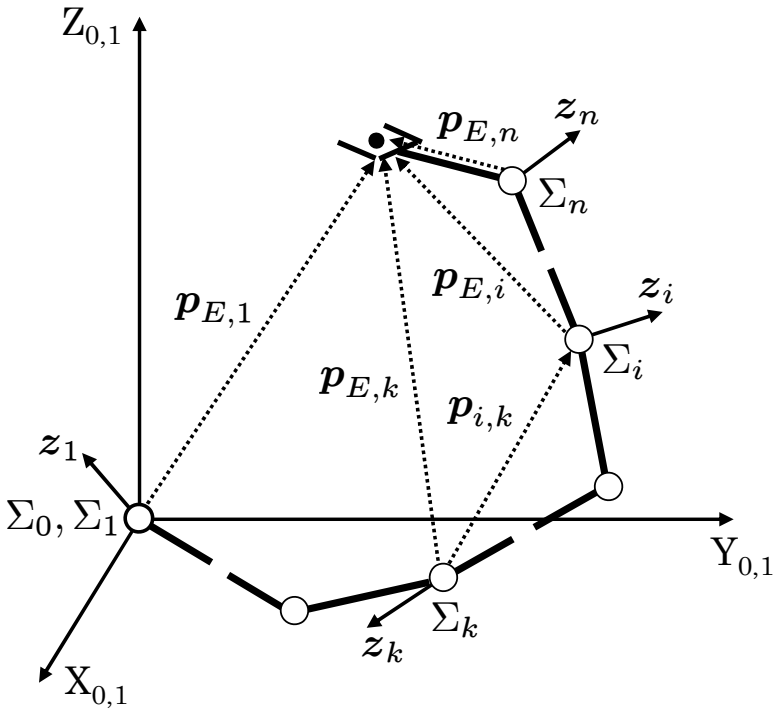

Fig. 2.2: Structure 2 of n-link redundant manipulator

If we define $\Delta \boldsymbol{J}_{p,j}$ as

$$\begin{aligned}
\Delta \boldsymbol{J}_{p,j} &= (\underbrace{\frac{\partial \Delta \boldsymbol{r}_{p,j}(\boldsymbol{q}_j)}{\partial q_1}, \cdots, \frac{\partial \Delta \boldsymbol{r}_{p,j}(\boldsymbol{q}_j)}{\partial q_j}}_{j}, \underbrace{\boldsymbol{0}}_{n-j}) \}m_p \\
&= (\Delta \tilde{\boldsymbol{j}}_{p,j,1}, \cdots, \Delta \tilde{\boldsymbol{j}}_{p,j,j}, \boldsymbol{0}) \\
&= (\Delta \tilde{\boldsymbol{J}}_{p,j}, \boldsymbol{0}),
\end{aligned} \tag{2.6}$$

then, $\boldsymbol{J}_{p,i}$ $(i = 1, 2, \cdots, n)$ can be denoted by

$$\boldsymbol{J}_{p,i} = \sum_{j=1}^{i} \Delta \boldsymbol{J}_{p,j}. \tag{2.7}$$

In this way, $\boldsymbol{J}_{p,n}$ can be represented by

$$\begin{aligned}
\boldsymbol{J}_{p,n} &= \sum_{j=1}^{n} \Delta \boldsymbol{J}_{p,j} \\
&= \boldsymbol{J}_{p,i} + \sum_{j=i+1}^{n} \Delta \boldsymbol{J}_{p,j}.
\end{aligned} \tag{2.8}$$

In addition, referring to Fig.2.2 and we define $\boldsymbol{p}_{i+1,k}$ by combining $\Delta \boldsymbol{r}_{p,i}(\boldsymbol{q}_i)$ in Fig.2.1 as

$$\boldsymbol{p}_{i+1,k} = \sum_{j=k}^{i} \Delta \boldsymbol{r}_{p,j}(\boldsymbol{q}_j). \tag{2.9}$$

In (2.9), $\boldsymbol{p}_{i+1,k}$ describes the vector connecting the origin of Σ_k to the origin of Σ_{i+1} with respect ot Σ_0.

2.1.2 Orientation Space

Representing the orientational vector of the i-th link by $\boldsymbol{r}_{o,i}(\boldsymbol{q}_i) \in R^{m_o}$. Here, m_o denotes the orientation dimension number of working space ($1 \leq m_o \leq 3$). When $m_o = 3$ and $\boldsymbol{r}_{o,i}(\boldsymbol{q}_i)$ is represented by a rather common definition of "Euler angles" $(\phi_i, \theta_i, \psi_i)$, and it is given as a function of $\boldsymbol{q}_i$ as

$$\boldsymbol{r}_{o,i}(\boldsymbol{q}_i) = \begin{pmatrix} \phi_i(\boldsymbol{q}_i) \\ \theta_i(\boldsymbol{q}_i) \\ \psi_i(\boldsymbol{q}_i) \end{pmatrix}. \tag{2.10}$$

By differentiating $\boldsymbol{r}_{o,i}(\boldsymbol{q}_i)$ in (2.10) with time, we can obtain

$$\dot{\boldsymbol{r}}_{o,i}(\boldsymbol{q}_i) = \frac{\partial \boldsymbol{r}_{o,i}(\boldsymbol{q}_i)}{\partial \boldsymbol{q}_n^T} \dot{\boldsymbol{q}}_n. \tag{2.11}$$

Providing z-axis of Σ_i represents rotational axis and it is denoted by $\boldsymbol{z}_i$, the angular velocity vector $\boldsymbol{\omega}_i$ is

$$\boldsymbol{\omega}_i = \sum_{j=1}^{i} \boldsymbol{z}_j \dot{q}_j. \tag{2.12}$$

And the relation between $\boldsymbol{\omega}_i$ and $\dot{\boldsymbol{r}}_{o,i}(\boldsymbol{q}_i)$ is

$$\begin{aligned} \boldsymbol{\omega}_i &= \begin{pmatrix} 0 & -sin\phi_i & cos\phi_i sin\theta_i \\ 0 & cos\phi_i & sin\phi_i sin\theta_i \\ 1 & 0 & cos\theta_i \end{pmatrix} \dot{\boldsymbol{r}}_{o,i}(\boldsymbol{q}_i) \\ &= \begin{pmatrix} 0 & -sin\phi_i & cos\phi_i sin\theta_i \\ 0 & cos\phi_i & sin\phi_i sin\theta_i \\ 1 & 0 & cos\theta_i \end{pmatrix} \frac{\partial \boldsymbol{r}_{o,i}(\boldsymbol{q}_i)}{\partial \boldsymbol{q}_n^T} \dot{\boldsymbol{q}}_n \\ &= \boldsymbol{J}_{o,i} \dot{\boldsymbol{q}}_n. \end{aligned} \tag{2.13}$$

From (2.12) and (2.13), $\boldsymbol{J}_{o,i}$ is denoted as

$$\begin{aligned} \boldsymbol{J}_{o,i} &= (\underbrace{\boldsymbol{z}_1, \cdots, \boldsymbol{z}_i}_{i}, \underbrace{\boldsymbol{0}}_{n-i}) \}m_o \\ &= (\tilde{\boldsymbol{J}}_{o,i},\ \boldsymbol{0}). \end{aligned} \tag{2.14}$$

Being similar with the description of (2.7), $\boldsymbol{J}_{o,i}$ $(i = 1, 2, \cdots, n)$ can be denoted as

$$\boldsymbol{J}_{o,i} = \sum_{j=1}^{i} \Delta \boldsymbol{J}_{o,j}. \tag{2.15}$$

2.1.3 Combined Position and Orientation Spaces

According to above analyses in the position space ($m_p = 3$) and orientation space ($m_o = 3$) respectively, in the maximum space of $m = m_p + m_o = 6$, we can define

$$\boldsymbol{p}_i(\boldsymbol{q}_i) = \begin{pmatrix} \boldsymbol{r}_{p,i+1}(\boldsymbol{q}_i) \\ \boldsymbol{r}_{o,i}(\boldsymbol{q}_i) \end{pmatrix} \tag{2.16}$$

and

$$\begin{aligned} \underline{\dot{\boldsymbol{r}}}_i(\boldsymbol{q}_i) &= \begin{pmatrix} \dot{\boldsymbol{r}}_{p,i+1}(\boldsymbol{q}_i) \\ \boldsymbol{\omega}_i \end{pmatrix} \\ &= \begin{pmatrix} \dot{x}_{i+1}(\boldsymbol{q}_i) \\ \dot{y}_{i+1}(\boldsymbol{q}_i) \\ \dot{z}_{i+1}(\boldsymbol{q}_i) \\ \omega_{x,i} \\ \omega_{y,i} \\ \omega_{z,i} \end{pmatrix} \\ &= \begin{pmatrix} \boldsymbol{J}_{p,i} \\ \boldsymbol{J}_{o,i} \end{pmatrix} \dot{\boldsymbol{q}}_n \\ &= \underline{\boldsymbol{J}}_i \dot{\boldsymbol{q}}_n. \end{aligned} \tag{2.17}$$

In this way, according to $\underline{\dot{\boldsymbol{r}}}_i(\boldsymbol{q}_i)$, we can define

$$\begin{aligned} \dot{\boldsymbol{r}}_i(\boldsymbol{q}_i) &= \underline{\boldsymbol{U}}_m \underline{\dot{\boldsymbol{r}}}_i(\boldsymbol{q}_i) \\ &= \underline{\boldsymbol{U}}_m \underline{\boldsymbol{J}}_i \dot{\boldsymbol{q}}_n \\ &= \boldsymbol{J}_i \dot{\boldsymbol{q}}_n. \end{aligned} \tag{2.18}$$

In (2.18), $\underline{\boldsymbol{U}}_m$ is a $m \times 6$ matrix to select end-effector's task space. For example, when the end-effector's task space is given by $m = 3$ such as $\dot{\boldsymbol{r}}_i(\boldsymbol{q}_i) = [\dot{x}_{i+1}(\boldsymbol{q}_i), \dot{y}_{i+1}(\boldsymbol{q}_i), \omega_{z,i})]^T$, $\underline{\boldsymbol{U}}_m$ is a 3×6 matrix as

$$\underline{\boldsymbol{U}}_m = \begin{pmatrix} 1 & 0 & 0 & 0 & 0 & 0 \\ 0 & 1 & 0 & 0 & 0 & 0 \\ 0 & 0 & 0 & 0 & 0 & 1 \end{pmatrix}. \tag{2.19}$$

In addition, being similar with the descriptions of (2.7) and (2.15), we can define

$$\begin{aligned} \boldsymbol{J}_i &= \sum_{j=1}^{i} \Delta \boldsymbol{J}_j \\ &= (\tilde{\boldsymbol{J}}_i,\ \boldsymbol{0}) \end{aligned} \tag{2.20}$$

and

$$\Delta \boldsymbol{J}_j = \underline{\boldsymbol{U}}_m \begin{pmatrix} \Delta \boldsymbol{J}_{p,j} \\ \Delta \boldsymbol{J}_{o,j} \end{pmatrix}. \tag{2.21}$$

2.2 Manipulability Ellipsoid

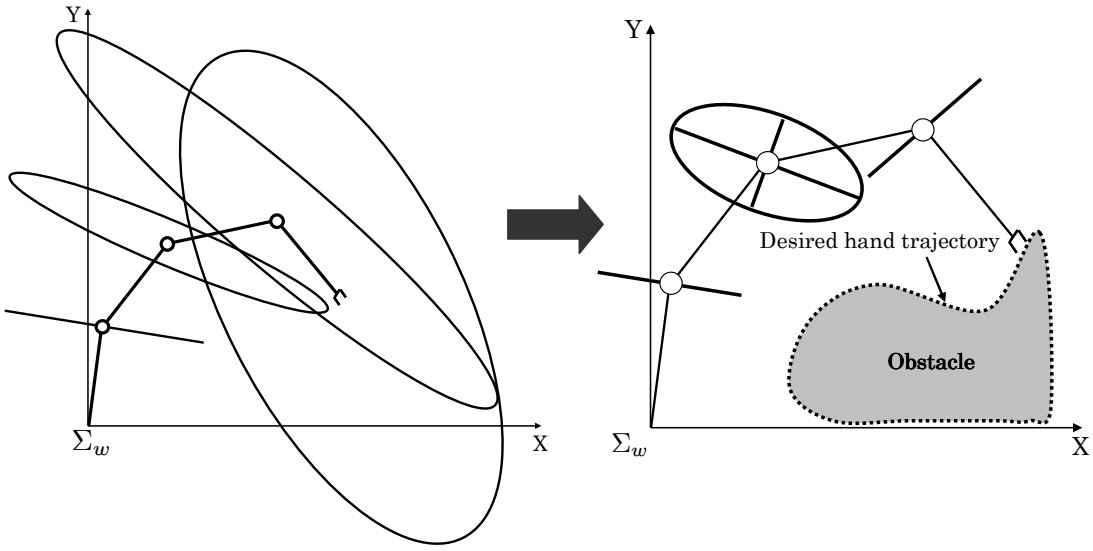

(a) Manipulability ellipsoids (b) Avoidance manipulability ellipsoids

Fig. 2.3: Manipulability ellipsoids and avoidance manipulability ellipsoids

Considering a set of tip velocities $\dot{\boldsymbol{r}}_i$ of all links being realizable by a set of joint angle velocities $\dot{\boldsymbol{q}}_i$ that satisfies an Euclidean norm condition, that is, $\|\dot{\boldsymbol{q}}_i\| = (\dot{q}_1^2+\dot{q}_2^2+\cdots+\dot{q}_i^2)^{1/2} \leq 1$, then the each tip velocity shapes an ellipsoid in range space of $\boldsymbol{J}_i$. These ellipsoids have been known as "manipulability ellipsoid"[13], [14], which are described as

$$\dot{\boldsymbol{r}}_i^T(\boldsymbol{J}_i^+)^T\boldsymbol{J}_i^+\dot{\boldsymbol{r}}_i \leq 1, \quad \dot{\boldsymbol{r}}_i \in R(\boldsymbol{J}_i). \tag{2.22}$$

In (2.22), $\boldsymbol{J}_i^+$ is the pseudo-inverse of $\boldsymbol{J}_i$, and $R(\boldsymbol{J}_i)$ represents the range space of $\boldsymbol{J}_i$. As shown in Fig.2.3(a), the singular values of $\boldsymbol{J}_i$ means the radius length of main axes of manipulability ellipsoids, that is to represent the ability to generate velocity at the tip of each link without any designated end-effector task. The avoidance manipulability ellipsoids shown in Fig.2.3(b) are inspired from manipulability ellipsoids and represent the shape-changeability of each intermediate link when a prior end-effector task is given. The detailed explanation of avoidance manipulability is shown in chapter 3 and the detailed comparison is shown in subsection 7.5.1.

3 Avoidance Manipulability

Here we assume that the desired trajectory $\boldsymbol{r}_{nd}$ and the desired velocity of the manipulator's end-effector $\dot{\boldsymbol{r}}_{nd}$ are given as primary task in m dimensional space, so $rank(\boldsymbol{J}_n) = m$. Giving $i = n$ into (2.18) and abbreviating $\dot{\boldsymbol{r}}_n(\boldsymbol{q}_n)$ to $\dot{\boldsymbol{r}}_n$, the desired $\dot{\boldsymbol{r}}_n$ is denoted by $\dot{\boldsymbol{r}}_{nd}$, then,

$$\dot{\boldsymbol{r}}_{nd} = \boldsymbol{J}_n \dot{\boldsymbol{q}}_n, \tag{3.1}$$

where $\boldsymbol{J}_n$ is a Jacobian matrix, $m \times n$, given by differentiating $\boldsymbol{r}_{nd}$ by $\boldsymbol{q}_n$. m denotes the number of work space and n denotes the number of links, $m < n$ is penetrated into this whole thesis as the redundancy condition, solving $\dot{\boldsymbol{q}}_n$ in (3.1) as

$$\dot{\boldsymbol{q}}_n = \boldsymbol{J}_n^+ \dot{\boldsymbol{r}}_{nd} + (\boldsymbol{I}_n - \boldsymbol{J}_n^+ \boldsymbol{J}_n)\ {}^1\boldsymbol{l}. \tag{3.2}$$

In (3.2), $\boldsymbol{J}_n^+$ is the pseudo-inverse of $\boldsymbol{J}_n$. Because $rank(\boldsymbol{J}_n) = m$, then

$$\boldsymbol{J}_n^+ = \boldsymbol{J}_n^T (\boldsymbol{J}_n \boldsymbol{J}_n^T)^{-1}. \tag{3.3}$$

If $rank(\boldsymbol{J}_n) = r < m$, then please refer to the definition shown from (7.1) to (7.4). (7.2) is the general definition of pseudo-inverse for all conditions. $\boldsymbol{I}_n$ is a $n \times n$ unit matrix, and ${}^1\boldsymbol{l}$ is an arbitrary vector satisfying ${}^1\boldsymbol{l} \in R^n$. The left superscript "1" of ${}^1\boldsymbol{l}$ means the first avoidance sub-task executed by using redundant DoF. If the rest DoF can execute the second sub-task besides the first sub-task, we define it by ${}^2\boldsymbol{l}$, which indicates the avoidance action in higher dimension [34]. The following definitions about the left superscript "1" are also. In the right side of (3.2), the first term denotes the solution making $\|\dot{\boldsymbol{q}}_n\|$ minimize in the full space of $\dot{\boldsymbol{q}}_n$ while realizing $\dot{\boldsymbol{r}}_{nd}$. The second term denotes the components of angular velocities at each joint, which can change the manipulator's shape regardless with the influence of $\dot{\boldsymbol{r}}_{nd}$ given arbitrarily as end-effector velocity for tracking the desired trajectory in m-dimensional space. Providing the first avoidance sub-task, that is the first demanded avoidance velocity ${}^1\dot{\boldsymbol{r}}_{id}$, is given to the i-th link by the geometric relation of manipulator and obstacles, shall we discuss realizability of ${}^1\dot{\boldsymbol{r}}_{id}$ in the following argument. In this research, ${}^1\dot{\boldsymbol{r}}_{id}$ is assumed to be

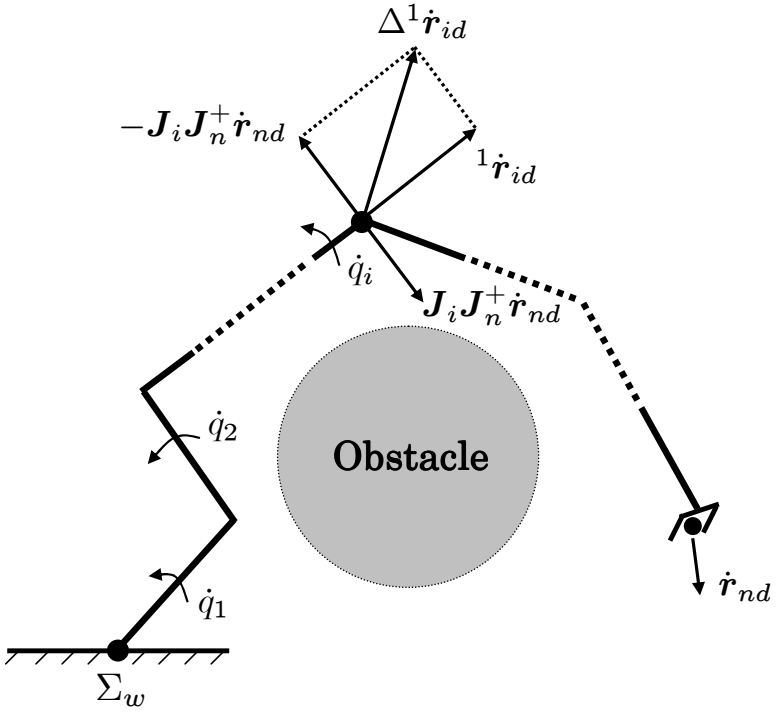

Fig. 3.1: Obstacle avoidance of intermediate links

commanded by an avoidance control system at a higher level. The relation of ${}^1\dot{\boldsymbol{r}}_{id}$ and $\dot{\boldsymbol{r}}_{nd}$ is denoted in (3.4) by substituting (3.2) into ${}^1\dot{\boldsymbol{r}}_{id} = \boldsymbol{J}_i\dot{\boldsymbol{q}}_n$.

$$ {}^1\dot{\boldsymbol{r}}_{id} = \boldsymbol{J}_i\boldsymbol{J}_n^+\dot{\boldsymbol{r}}_{nd} + \boldsymbol{J}_i(\boldsymbol{I}_n - \boldsymbol{J}_n^+\boldsymbol{J}_n)\ {}^1\boldsymbol{l}. \tag{3.4} $$

Here, we define two variables shown as

$$ \Delta^1\dot{\boldsymbol{r}}_{id} \triangleq {}^1\dot{\boldsymbol{r}}_{id} - \boldsymbol{J}_i\boldsymbol{J}_n^+\dot{\boldsymbol{r}}_{nd} \tag{3.5} $$

and

$$ {}^1\boldsymbol{M}_i \triangleq \boldsymbol{J}_i(\boldsymbol{I}_n - \boldsymbol{J}_n^+\boldsymbol{J}_n). \tag{3.6} $$

In (3.5), $\Delta^1\dot{\boldsymbol{r}}_{id}$ is called by "the first avoidance velocity". In (3.6), ${}^1\boldsymbol{M}_i$ is a $m\times n$ matrix called by "the first avoidance matrix". Then, (3.5) can be rewritten as

$$ \Delta^1\dot{\boldsymbol{r}}_{id} = {}^1\boldsymbol{M}_i{}^1\boldsymbol{l}. \tag{3.7} $$

The relation between ${}^1\dot{\boldsymbol{r}}_{id}$ and $\Delta^1\dot{\boldsymbol{r}}_{id}$ is shown in Fig.3.1.

Recipe:

Providing primarily given end-effector task $\dot{\boldsymbol{r}}_{nd}$ and avoidance task of the i-th link ${}^1\dot{\boldsymbol{r}}_{id}$, $\Delta^1\dot{\boldsymbol{r}}_{id}$ is determined by (3.5). Then the realizability of ${}^1\dot{\boldsymbol{r}}_{id}$ depends on $rank({}^1\boldsymbol{M}_i)$, meaning whether $\Delta^1\dot{\boldsymbol{r}}_{id}$ has a solution ${}^1\boldsymbol{l}$ through ${}^1\boldsymbol{M}_i$ in (3.7) relies on $rank({}^1\boldsymbol{M}_i)$.

3.1 Complete Avoidance Manipulability Ellipsoid

When ${}^1\dot{\boldsymbol{r}}_{id}$ is given as the desired velocity of the intermediate i-th link to avoid obstacle, according to (3.5), we can obtain $\Delta^1\dot{\boldsymbol{r}}_{id}$. However, the problem is whether we can realize $\Delta^1\dot{\boldsymbol{r}}_{id}$, that is, whether we can find ${}^1\boldsymbol{l}$ to realize $\Delta^1\dot{\boldsymbol{r}}_{id}$. From (3.7), we can obtain ${}^1\boldsymbol{l}$ as

$$ {}^1\boldsymbol{l} = {}^1\boldsymbol{M}_i^+\Delta^1\dot{\boldsymbol{r}}_{id} + (\boldsymbol{I}_n - {}^1\boldsymbol{M}_i^{+1}\boldsymbol{M}_i)^2\boldsymbol{l}. \tag{3.8} $$

In (3.8), ${}^1\boldsymbol{M}_i^+$ is the pseudo-inverse of ${}^1\boldsymbol{M}_i$ and ${}^2\boldsymbol{l}$ is an arbitrary vector satisfying ${}^2\boldsymbol{l} \in R^n$. From (3.8), we can obtain

$$ \begin{aligned} \|{}^1\boldsymbol{l}\|^2 &= {}^1\boldsymbol{l}^T{}^1\boldsymbol{l} \\ &= [\Delta^1\dot{\boldsymbol{r}}_{id}^T{}^1\boldsymbol{M}_i^{+T} + {}^2\boldsymbol{l}^T(\boldsymbol{I}_n - {}^1\boldsymbol{M}_i^{+1}\boldsymbol{M}_i)^T][{}^1\boldsymbol{M}_i^+\Delta^1\dot{\boldsymbol{r}}_{id} + (\boldsymbol{I}_n - {}^1\boldsymbol{M}_i^{+1}\boldsymbol{M}_i)^2\boldsymbol{l}] \\ &= \Delta^1\dot{\boldsymbol{r}}_{id}^T{}^1\boldsymbol{M}_i^{+T}{}^1\boldsymbol{M}_i^+\Delta^1\dot{\boldsymbol{r}}_{id} + \Delta^1\dot{\boldsymbol{r}}_{id}^T{}^1\boldsymbol{M}_i^{+T}(\boldsymbol{I}_n - {}^1\boldsymbol{M}_i^{+1}\boldsymbol{M}_i)^2\boldsymbol{l} \\ &\quad + {}^2\boldsymbol{l}^T(\boldsymbol{I}_n - {}^1\boldsymbol{M}_i^{+1}\boldsymbol{M}_i)^T{}^1\boldsymbol{M}_i^+\Delta^1\dot{\boldsymbol{r}}_{id} \\ &\quad + {}^2\boldsymbol{l}^T(\boldsymbol{I}_n - {}^1\boldsymbol{M}_i^{+1}\boldsymbol{M}_i)^T(\boldsymbol{I}_n - {}^1\boldsymbol{M}_i^{+1}\boldsymbol{M}_i)^2\boldsymbol{l} \\ &= \Delta^1\dot{\boldsymbol{r}}_{id}^T{}^1\boldsymbol{M}_i^{+T}{}^1\boldsymbol{M}_i^+\Delta^1\dot{\boldsymbol{r}}_{id} + \|(\boldsymbol{I}_n - {}^1\boldsymbol{M}_i^{+1}\boldsymbol{M}_i)^2\boldsymbol{l}\|^2 \\ &\geq \Delta^1\dot{\boldsymbol{r}}_{id}^T{}^1\boldsymbol{M}_i^{+T}{}^1\boldsymbol{M}_i^+\Delta^1\dot{\boldsymbol{r}}_{id}, \end{aligned} \tag{3.9} $$

since $({}^1\boldsymbol{M}_i^{+1}\boldsymbol{M}_i)^T = {}^1\boldsymbol{M}_i^{+1}\boldsymbol{M}_i$ and ${}^1\boldsymbol{M}_i^{+1}\boldsymbol{M}_i{}^1\boldsymbol{M}_i^+ = {}^1\boldsymbol{M}_i^+$. Assuming that ${}^1\boldsymbol{l}$ is restricted as $\|{}^1\boldsymbol{l}\| \leq 1$, then we obtain next relation,

$$ \Delta^1\dot{\boldsymbol{r}}_{id}^T({}^1\boldsymbol{M}_i^+)^T\ {}^1\boldsymbol{M}_i^+\Delta^1\dot{\boldsymbol{r}}_{id} \leq 1, \quad \Delta^1\dot{\boldsymbol{r}}_{id} \in R({}^1\boldsymbol{M}_i). \tag{3.10} $$

If $rank({}^1\boldsymbol{M}_i) = m$, we can obtain ${}^1\boldsymbol{M}_i{}^1\boldsymbol{M}_i^+ = \boldsymbol{I}_m$, (3.10) represents an ellipsoid expanding in m-dimensional space, that is $\Delta^1\dot{\boldsymbol{r}}_{id}$ can be arbitrarily realized in m-dimensional space and (3.7) always has the solution ${}^1\boldsymbol{l}$ corresponding to all $\Delta^1\dot{\boldsymbol{r}}_{id} \in R^m$. In this way, the ellipsoid represented by (3.10) is named "the first complete avoidance manipulability ellipsoid", which is denoted by ${}^{1C}P_i$.

3.2 Partial Avoidance Manipulability Ellipsoid

If $rank({}^1\boldsymbol{M}_i) = p < m$, ${}^1\boldsymbol{M}_i{}^1\boldsymbol{M}_i^+ \neq \boldsymbol{I}_m$, we can obtain the partial avoidance manipulability ellipsoid of reduced $\Delta^1\dot{\boldsymbol{r}}_{id}^*$ as

$$ \Delta^1\dot{\boldsymbol{r}}_{id}^{*T}({}^1\boldsymbol{M}_i^+)^{T1}\boldsymbol{M}_i^+\Delta^1\dot{\boldsymbol{r}}_{id}^* \leq 1, \quad (\Delta^1\dot{\boldsymbol{r}}_{id}^* = {}^1\boldsymbol{M}_i{}^1\boldsymbol{M}_i^+\boldsymbol{s},\ \boldsymbol{s} \in R^m). \tag{3.11} $$

(3.11) describes an ellipsoid expanded in p-dimensional space. This ellipsoid is named "the first partial reconfiguration manipulability ellipsoid", which is denoted by ${}^{1P}P_i$. Because $p < m$, the partial reconfiguration manipulability ellipsoid can be thought as regressed ellipsoid of the complete reconfiguration manipulability ellipsoid. We call ${}^1P_i$ as the first reconfiguration manipulability ellipsoid including both ${}^{1C}P_i$ and ${}^{1P}P_i$.

According to above analysis, we can generalize

Lemma 1:

The necessary and sufficient condition of $\Delta^1\dot{\boldsymbol{r}}_{id} = {}^1\boldsymbol{M}_i{}^1\boldsymbol{M}_i^+\Delta^1\dot{\boldsymbol{r}}_{id}$ *being held for all* $\Delta^1\dot{\boldsymbol{r}}_{id} \in R^m$ *is* $rank({}^1\boldsymbol{M}_i) = m$.

Lemma 2:

If $rank({}^1\boldsymbol{M}_i) = p < m$, $\Delta^1\dot{\boldsymbol{r}}_{id} \in R^m$ *does not always satisfy* $\Delta^1\dot{\boldsymbol{r}}_{id} = {}^1\boldsymbol{M}_i{}^1\boldsymbol{M}_i^+\Delta^1\dot{\boldsymbol{r}}_{id}$. *But the orthogonal projection of* $\Delta^1\dot{\boldsymbol{r}}_{id}$ *onto* $R({}^1\boldsymbol{M}_i)$, *that is, for all* $\Delta^1\dot{\boldsymbol{r}}^*_{id} \in R({}^1\boldsymbol{M}_i)$ *can be realized, avoidance manipulability in* $\Delta^1\dot{\boldsymbol{r}}^*_{id}$ *direction is possible.*

Theorem 1:

For all ${}^1\dot{\boldsymbol{r}}_{id} \in R^m$ *can be realized for any* $\dot{\boldsymbol{r}}_{nd}$ *being given primarily as end-effector task, if and only if* $rank({}^1\boldsymbol{M}_i) = m$.

Theorem 2:

If $rank({}^1\boldsymbol{M}_i) = p < m$, *for all* ${}^1\dot{\boldsymbol{r}}_{id} \in R^m$ *can not be always realized. But*

$$ {}^1\dot{\boldsymbol{r}}^\sharp_{id} \triangleq \Delta^1\dot{\boldsymbol{r}}^*_{id} + \boldsymbol{J}_i\boldsymbol{J}_n^+\dot{\boldsymbol{r}}_{nd}, \tag{3.12} $$

can be realized since $\Delta^1\dot{\boldsymbol{r}}^*_{id} \in R({}^1\boldsymbol{M}_i)$ *in* p *dimension space, that is* ${}^1\dot{\boldsymbol{r}}^\sharp_{id}$ *is contained in the affine space*

$$ R({}^1\boldsymbol{M}_i) + \boldsymbol{J}_i\boldsymbol{J}_n^+\dot{\boldsymbol{r}}_{nd}, \tag{3.13} $$

which means the summation of a vector $\Delta^1\dot{\boldsymbol{r}}^*_{id}$ *in a decreased space* $R({}^1\boldsymbol{M}_i)$ *and a constant vector* $\boldsymbol{J}_i\boldsymbol{J}_n^+\dot{\boldsymbol{r}}_{nd}$, *and the dimension number of this affine space is also* p.

The all proofs of "**Propositions**", "**Lemmas**", "**Theorems**" and "**Corollaries**" are shown in "Appendix".

3.3 Plural Avoidance Manipulability

In subsections 3.1 and 3.2, we defined the first avoidance manipulability ellipsoid ${}^1P_i$ ($i = 1, \cdots, n-1$). However, in fact, it may not be possible that these intermediate links realize their own avoidance velocities simultaneously. This subsection discusses the multi-avoidance task realization. If the first avoidance task, that is, the first avoidance velocity, $\Delta^1\dot{\boldsymbol{r}}_{id}$ or $\Delta^1\dot{\boldsymbol{r}}^*_{id}$ has been realized at the certain i-th link, we will consider the possibility to execute the secondly demanded velocity except the i-th link. Substituting (3.8) into (3.2), we can obtain

$$\dot{\boldsymbol{q}}_n = \boldsymbol{J}_n^+\dot{\boldsymbol{r}}_{nd} + (\boldsymbol{I}_n - \boldsymbol{J}_n^+\boldsymbol{J}_n){}^1\boldsymbol{M}_i^+\Delta^1\dot{\boldsymbol{r}}_{id} + (\boldsymbol{I}_n - \boldsymbol{J}_n^+\boldsymbol{J}_n)(\boldsymbol{I}_n - {}^1\boldsymbol{M}_i^{+1}\boldsymbol{M}_i){}^2\boldsymbol{l}. \tag{3.14}$$

Substituting (3.14) into ${}^2\dot{\boldsymbol{r}}_{jd} = \boldsymbol{J}_j\dot{\boldsymbol{q}}_n$, we can obtain

$$\begin{aligned} {}^2\dot{\boldsymbol{r}}_{jd} &= \boldsymbol{J}_j\boldsymbol{J}_n^+\dot{\boldsymbol{r}}_{nd} + \boldsymbol{J}_j(\boldsymbol{I}_n - \boldsymbol{J}_n^+\boldsymbol{J}_n){}^1\boldsymbol{M}_i^+\Delta^1\dot{\boldsymbol{r}}_{id} \\ &\quad + \boldsymbol{J}_j(\boldsymbol{I}_n - \boldsymbol{J}_n^+\boldsymbol{J}_n)(\boldsymbol{I}_n - {}^1\boldsymbol{M}_i^{+1}\boldsymbol{M}_i){}^2\boldsymbol{l}. \end{aligned} \tag{3.15}$$

By defining $\Delta^2\dot{\boldsymbol{r}}_{jd}$ and ${}^2\boldsymbol{M}_j$ as

$$\Delta^2\dot{\boldsymbol{r}}_{jd} \triangleq {}^2\dot{\boldsymbol{r}}_{jd} - \boldsymbol{J}_j\boldsymbol{J}_n^+\dot{\boldsymbol{r}}_{nd} - \boldsymbol{J}_j(\boldsymbol{I}_n - \boldsymbol{J}_n^+\boldsymbol{J}_n){}^1\boldsymbol{M}_i^+\Delta^1\dot{\boldsymbol{r}}_{id} \tag{3.16}$$

and

$${}^2\boldsymbol{M}_j \triangleq \boldsymbol{J}_j(\boldsymbol{I}_n - \boldsymbol{J}_n^+\boldsymbol{J}_n)(\boldsymbol{I}_n - {}^1\boldsymbol{M}_i^{+1}\boldsymbol{M}_i), \tag{3.17}$$

we can obtain

$$\Delta^2\dot{\boldsymbol{r}}_{jd} = {}^2\boldsymbol{M}_j{}^2\boldsymbol{l}. \tag{3.18}$$

The forms of (3.18) and (3.7) are similar. Therefore, the analysis method of the second avoidance manipulability ellipsoid ${}^2P_j$ ($j = 1, \cdots, n-1; \{j \neq i\}$) and the first avoidance manipulability ellipsoid ${}^1P_i$ are also similar. In other words, whether the second avoidance task can be realized or not depends on the rank value of the second avoidance matrix ${}^2\boldsymbol{M}_j$ ($j = 1, \cdots, n-1; \{j \neq i\}$). If $rank({}^2\boldsymbol{M}_j) \neq 0$, the second avoidance task can be realized partially at least. Otherwise, the second avoidance task can not be realized. Similarly, we can judge whether the third avoidance task can be realized or not by the third avoidance matrix ${}^3\boldsymbol{M}_k$ as

$${}^3\boldsymbol{M}_k \triangleq \boldsymbol{J}_k(\boldsymbol{I}_n - \boldsymbol{J}_n^+\boldsymbol{J}_n)(\boldsymbol{I}_n - {}^1\boldsymbol{M}_i^{+1}\boldsymbol{M}_i)(\boldsymbol{I}_n - {}^2\boldsymbol{M}_j^{+2}\boldsymbol{M}_j),$$

$$(k = 1, \cdots, n-1;\ \{k \neq i\} \cap \{k \neq j\}). \tag{3.19}$$

According to the above analyses for ${}^1\boldsymbol{M}_i$, ${}^2\boldsymbol{M}_j$ and ${}^3\boldsymbol{M}_k$, by the similar method, the realizability of the fourth or more avoidance tasks can be judged.

4 Avoidance Manipulability Shape Index

As shown in Fig.1.1, if the manipulator's end-effector operates a target object in trajectory tracking with lower avoidance manipulability, it is difficult to avoid the target object/obstacles newly detected by camera. Our research is the real-time control system, the working manipulator must possess the characteristic being able to do a quick avoidance action (shape-changing action) when it meets the target object/obstacles appearing suddenly. Therefore, for simultaneously realizing on-line trajectory tracking and obstacle avoidance, it is necessary and important to always keep the high avoidance manipulability in the whole working process.

4.1 Volume Summation

Here, we present "AMSI" (Avoidance Manipulability Shape Index) expressed by sum of avoidance manipulability of all intermediate links to evaluate avoidance manipulability of the whole manipulator. The avoidance manipulability of each intermediate link can be evaluated by the avoidance manipulability ellipsoid. The volume of avoidance manipulability ellipsoid will determine the extent of avoidance manipulability. When the volume of avoidance manipulability ellipsoid of the i-th link is the largest, the avoidance manipulability of the i-th link is the best. The volume of avoidance manipulability ellipsoid of the i-th link is defined as

$$ {}^1V_i = c_m \cdot {}^1w_i. \tag{4.1} $$

In (4.1), the right subscript "m" of c_m denotes the dimension number, c_m and ${}^1w_i$ are defined as

$$ c_m = \begin{cases} \dfrac{2(2\pi)^{(m-1)/2}}{1 \cdot 3 \cdots (m-2)m} & (m : odd) \\ \dfrac{(2\pi)^{m/2}}{2 \cdot 4 \cdots (m-2)m} & (m : even) \end{cases} . \tag{4.2} $$

and

$$ {}^1w_i = {}^1\sigma_{i1} \cdot {}^1\sigma_{i2} \ \cdots \ {}^1\sigma_{im}. \tag{4.3} $$

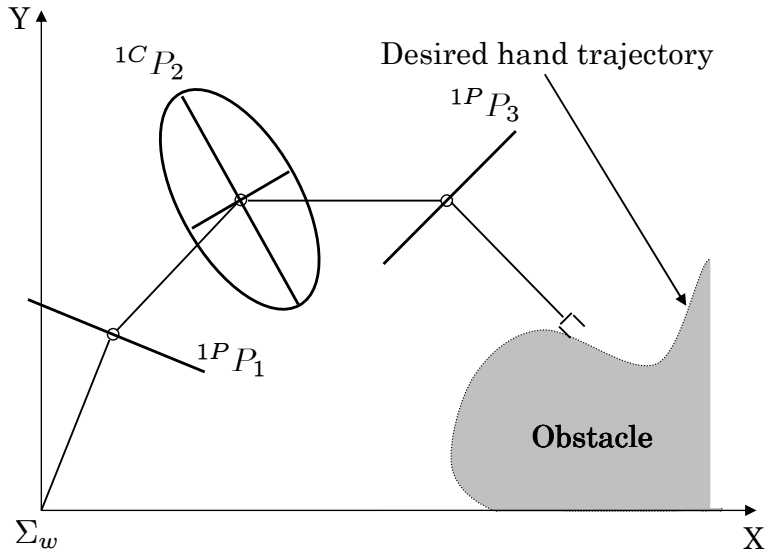

Fig. 4.1: Avoidance manipulability ellipsoids.

In (4.3), ${}^1\sigma_{i1},\ {}^1\sigma_{i2},\ \cdots,\ {}^1\sigma_{im}$ are the singular values of ${}^1\boldsymbol{M}_i$ in (3.6).

According to above discussion, the "volume" of avoidance manipulability ellipsoid is adaptable to situation that redundant manipulator works in 3-dimensional space ($m = 3$). Here, for making it comprehensive and understandable, we will analyze a multi-link redundant manipulator in 2-dimensional space ($m = 2$). In this case of 2-dimensional space, ${}^1V_i$ denotes the area measure of avoidance manipulability ellipsoid rather than volume. Moreover, the avoidance manipulability ellipsoids of the 1-st link and $(n-1)$-th link will become lines (area measures are zero). However, we can not omit the avoidance manipulability of these two links when we evaluate the avoidance manipulability of the whole manipulator although their ellipsoid areas are zero. Therefore, the lengths of these two lines will be used to denote the avoidance manipulability of them. Here, taking a 4-link redundant manipulator ($n = 4$) in 2-dimensional space ($m = 2$) for example shown in Fig.4.1. The avoidance manipulability ellipsoid of the 2-nd link is called the first complete avoidance manipulability ellipsoid evaluated by its area measure, which is denoted by $^{1C}P_2$. The avoidance manipulability ellipsoids of the 1-st link and 3-rd link are called the first partial avoidance manipulability ellipsoid evaluated by lengths of their lines, which are denoted by $^{1P}P_1$ and $^{1P}P_3$ respectively [27]. The largest ${}^1V_i$ corresponds to the highest avoidance manipulability of the i-th link. However, ${}^1V_i$ just denotes the extent of avoidance manipulability of the i-th link. Sometimes, as for a

given configuration, the i-th link possesses higher avoidance manipulability and other links possess lower avoidance manipulability, which seriously affects the avoidance manipulability of the whole manipulator. Therefore, for evaluating the avoidance manipulability of the whole manipulator, ${}^1E$ is defined as

$$ {}^1E = \sum_{i=1}^{n-1} {}^1V_i \, a_i. \tag{4.4} $$

In (4.4), when $m = 2$, ${}^1V_1$ and ${}^1V_{n-1}$ denote the lengths, ${}^1V_{2,3,\cdots,(n-2)}$ denote area measure. a_i is defined as

$$ a_1 = a_{n-1} = 1[m^{-1}], \ a_{2,3,\cdots,(n-2)} = 1[m^{-2}]. \tag{4.5} $$

By (4.5), ${}^1E$ denotes an index without unit. Evaluating the avoidance manipulability by using area measures ${}^1V_i$ is to simultaneously consider the avoidance manipulability in the both directions of the longest and the shortest axes of ellipsoid. If the shape of avoidance manipulability ellipsoid of the i-th link is slender, it indicates that the tip of the i-th link possesses very low avoidance manipulability along the direction of the shortest axis although avoidance manipulability along the longest one is high, resulting in ${}^1V_i$ being small and ${}^1E$ being small also, which is not the desired avoidance manipulability ellipsoid. In addition, if the manipulator's end-effector can not reach the desired position, we define ${}^1E$ as

$$ {}^1E = 0. \tag{4.6} $$

In this way, ${}^1E$ is a kind of index evaluating the avoidance manipulability of the whole manipulator.

4.2 Singular Value Summation

The above discussed ${}^1E$ evaluates the avoidance manipulability depending on the sum of volumes of avoidance manipulability ellipsoids. In addition, the avoidance manipulability of the whole manipulator can be evaluated by another index as

$$ {}^1E' = \sum_{i=1}^{n-1} \sum_{j=1}^{m_i} {}^1\sigma_{ij}. \tag{4.7} $$

In (4.7), m_i denote the number of the non-zero singular values of ${}^1\boldsymbol{M}_i$. This kind of index ${}^1E'$ is the sum of all singular values ${}^1\sigma_{ij}$. Here, singular value denotes the radius of main axis

of avoidance manipulability ellipsoid. In this way, although some singular values are very small, the evaluation index ${}^1E'$ will be relatively large only if others singular values are large (when $m = 2$, there are two positive singular values at most corresponding to ${}^1\boldsymbol{M}_i$). We will analyze and compare ${}^1E$ with ${}^1E'$ which criterion can give appropriate configuration for the redundant manipulator based on the avoidance manipulability next.

4.3 Comparison

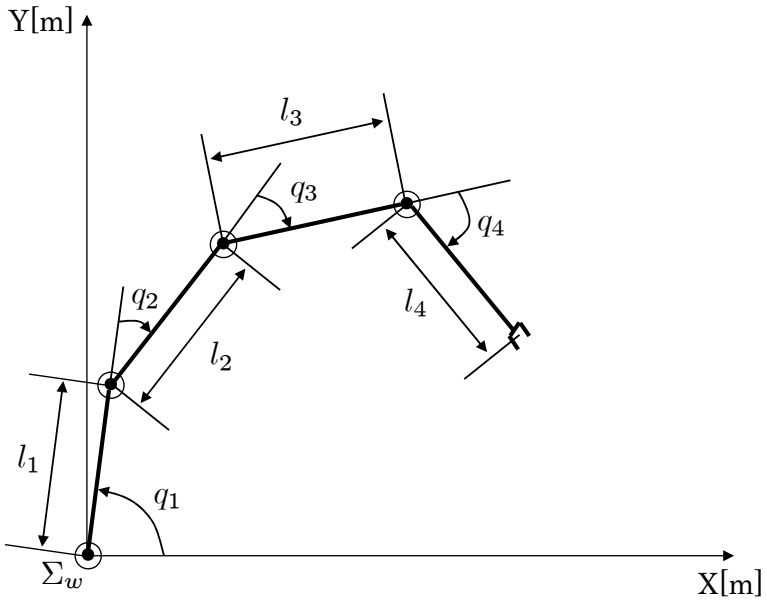

Fig. 4.2: Manipulator's configuration in this example.

From the definitions of ${}^1E$ and ${}^1E'$, we can find that ${}^1E'$ is easier to be calculated than ${}^1E$ since ${}^1E'$ calculates simply the summation of singular values. ${}^1E$ needs calculate the volumes of avoidance manipulability ellipsoids. On the other hand, ${}^1E$ can keep the balance between the longest axis and the shortest axis of avoidance manipulability ellipsoid by calculating the volume. ${}^1E'$ will lose this kind of balance when the shape of avoidance manipulability ellipsoid is very slender, that is the length of the longest axis of avoidance manipulability ellipsoid is very long and the shortest one is very short to be nearly zero. These facts suggest us that ${}^1E'$ keeps non-zero value even though the length of the shortest axis is decreased to be zero. However the value of ${}^1E$ decreases to zero in the above situation.

In the 4-link manipulator in a 2-dimensional space shown in Fig.4.2, where the length of

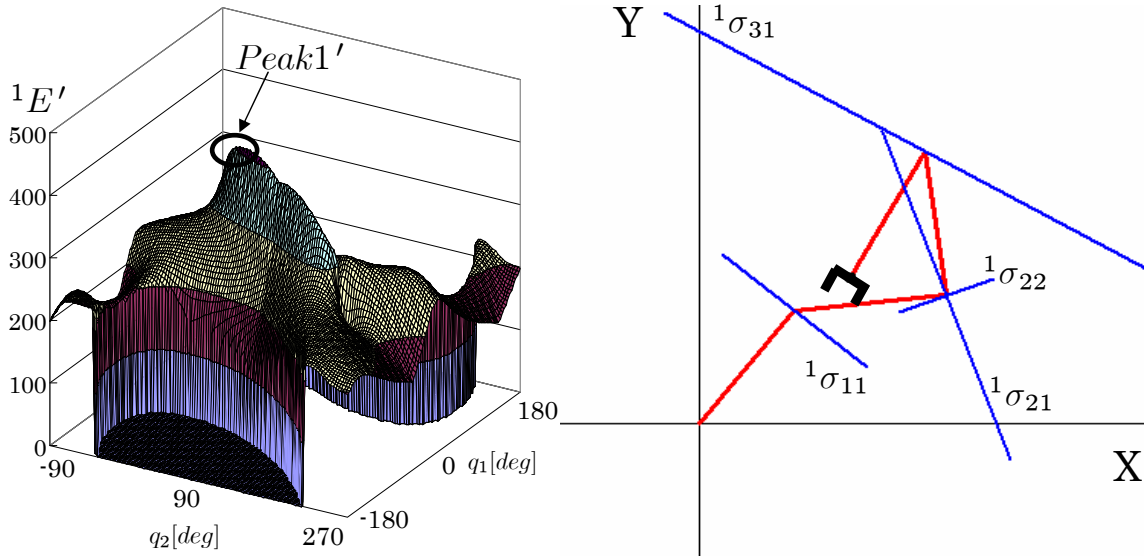

(a) $^1E'$ distribution (b) Manipulator's shape at $Peak1'$

Fig. 4.3: $^1E'$ distribution and manipulator's optimal shape when the end-effector is fixed at (x,y)=(100,100).

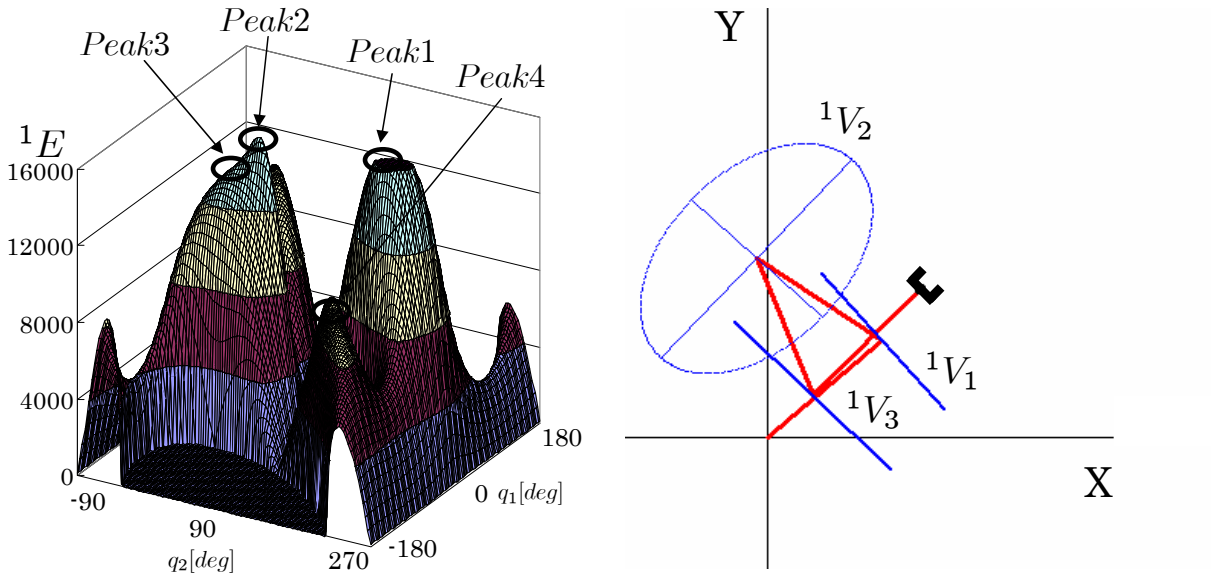

(a) ^1E distribution (b) Manipulator's shape at $Peak1$

Fig. 4.4: ^1E distribution and manipulator's optimal shape when the end-effector is fixed at (x,y)=(100,100).

each link is 100[cm], q_1, q_2, q_3 and q_4 are defined specifically. When the manipulator's end-effector is fixed in the position ($x = 100[cm]$, $y = 100[cm]$), the manipulator's configuration will be determined once q_1 and q_2 are given. When q_1 and q_2 change from 0 degree to 360 degree, which corresponds to 360×360 cases with an interval of change of 1 degree, the value of ${}^1E'$ is plotted by changing q_1 and q_2 with the resolution of 1 degree in Fig.4.3(a), and ${}^1E$ distribution is done in Fig.4.4(a). In addition, Fig.4.3(b) denotes the optimal shape of a manipulator corresponding to the largest ${}^1E'$ ($Peak1'$). Fig.4.4(b) denotes the optimal shape of a manipulator corresponding to the largest ${}^1E$ ($Peak1$). Here, please notice that we do not consider the problem of self-collision in this research. Obviously, when we compare Fig.4.3(b) with Fig.4.4(b), the manipulator's optimal shape evaluated by ${}^1E'$ is not the desired shape from the viewpoint of avoidance manipulability. The largest ${}^1E'$ in $Peak1'$ is mainly supported by the biggest value ${}^1\sigma_{31}$, which merely indicates that there exists a high avoidance velocity along the direction of ${}^1\sigma_{31}$. We can also find from Fig.4.3(b) that avoidance velocity along the direction of ${}^1\sigma_{22}$ is very small. Therefore, we think ${}^1E'$ is not suitable for the evaluation of the avoidance manipulability of the whole manipulator. However, in Fig.4.4(b), the manipulator's optimal shape, as evaluated by ${}^1E$, is very desirable because the largest ${}^1E$ in $Peak1$ is mainly supported by the biggest area measure ${}^1V_2$. Especially, from the shape of ${}^1V_2$, we can find that the avoidance velocities along arbitrary directions in the plane are average.

By comparing ${}^1E'$ (sum of ${}^1\sigma_{ij}$) with ${}^1E$ (sum of ${}^1V_i$), ${}^1E$ can effectively evaluate the avoidance manipulability of the whole manipulator in view of the balance along all directions in the working space. Therefore, we think that ${}^1E$ is more effective and accurate than ${}^1E'$ as an evaluation index of the avoidance manipulability of the whole manipulator. Therefore, we chose ${}^1E$ and named it as "Avoidance Manipulability Shape Index (AMSI)".

5 AMSI With Potential

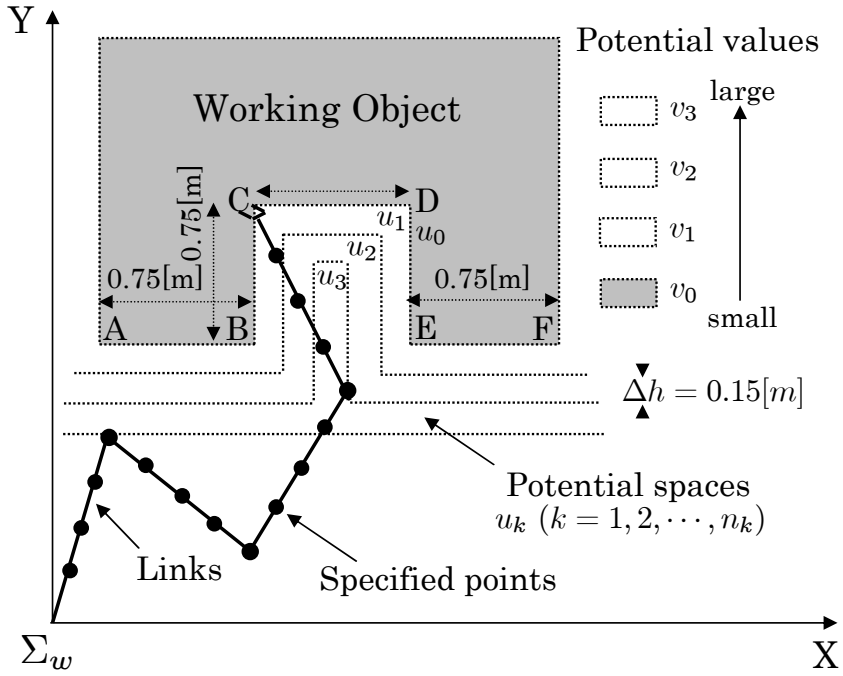

Fig. 5.1: Potential spaces and specified points.

For satisfying the requirements of real-time trajectory tracking and obstacle avoidance, just keeping higher avoidance manipulability of the whole manipulator is not enough, keeping the farther distance between the manipulator and the target object is another important thing. In chapter 4, we discussed the evaluation index of the avoidance manipulability of the whole manipulator "AMSI"(^1E), which is the sum of volumes of all avoidance manipulability ellipsoids. However, although avoidance manipulability of the whole manipulator can be evaluated by using "AMSI"(^1E), the possibility of collision may increase because it does not consider the distance between the manipulator and the target object. Here, we need to introduce the potential spaces, which are detected by camera and automatically created around the working object's shape. As shown in Fig.5.1, the potential spaces $u_k(k = 0, 1, 2, \cdots, n_k)$ are set along the working object's shape with the interval of Δh, here

n_k denotes the number of potential spaces. And the potential values $v_k(k = 0, 1, 2, 3, \cdots, n_k)$ denote the dangerous extent, which are defined by $v_0 < v_1 < v_2 < \cdots < v_{n_k} < 0$. In other words, if the distance from the working object decreases, the potential value will become smaller. In addition, the specified points are spaced evenly on each link of the manipulator besides each joint position, and the coordinates of the specified points are represented by $s_{ij}(x_{ij}, y_{ij})[i = 1, 2, 3, \cdots, n; j = 1, 2, \cdots, n_i]$ where n denotes the number of manipulator's links and n_i denotes the sum number of the specified points in the i-th link. Here, please notice that these specified points are not to be arbitrarily chosen, and obviously, the larger $\sum_{i=1}^{n} n_i$ is, the more accurate the collision avoidance will be. Evaluation values $a(s_{ij})$ of specified points are defined as

$$\begin{cases} a(s_{ij}) = v_k & s_{ij} \in u_k \\ a(s_{ij}) = 0 & s_{ij} \notin u_k \end{cases}. \tag{5.1}$$

Total potential value U of the manipulator's shape is defined as

$$U = \sum_{i=1}^{n} \sum_{j=1}^{n_i} a(s_{ij}). \tag{5.2}$$

According to the definition of U, we can think that U will be decreased once the manipulator moves into potential spaces or it approaches the working object. Moreover, please notice that all potential values are negative, and the potential value v_0 inside the working object is especially small. In this way, we can judge whether the manipulator collides with the working object or not according to U. When $U \leq v_0$, it indicates that the manipulator has collided with the working object because v_0 is the smallest potential value and is much smaller than other potential values. Therefore, the truly optimal shape of the manipulator should be determined by considering both "AMSI"(^1E) and the total potential value (U), which evaluates avoidance manipulability along with degree of vicinity between the manipulator and the working object by judging the distance between them with potential. Here, please notice that there is a trade-off between avoidance manipulability (^1E) and potential value (U).

$$^1S = k_e {}^1E + k_u U. \tag{5.3}$$

In (5.3), k_e and k_u are weight coefficients, which are also used to keep unity between ^1E and U. In this research, we hold that $k_e = k_u = 1$. In this way, for evaluating the manipulator's

shape, the multi-aim optimization of avoidance manipulability and potential is necessary [35]. Here, we define the evaluation index considering avoidance manipulability and collision possibility, which is called "AMSIP"(AMSI with Potential). However, once the problems of multi-aim optimization are considered, k_e and k_u will be determined according to the working environment. In future research, it will be necessary to discuss the method of how to select weight coefficients according to the changing, real-time environment.

Here, we will use an example to compare "AMSI" with "AMSIP". In Fig.5.2 and Fig.5.3, the length of each link is 100$[cm]$. When the manipulator's end-effector is fixed in the position ($x = 85[cm]$, $y = 215[cm]$), ${}^1E$ distribution about q_1 and q_2 is shown in Fig.5.2(a), where q_1 and q_2 are joint angles of the 1-st link and 2-nd link respectively and they constitute the redundancy space of joint angles. q_3 and q_4 are determined depending on the end-effector position once q_1 and q_2 are confirmed. ${}^1S$ distribution is shown in Fig.5.3(a). As shown in Fig.5.1, we set three potential spaces outside the working object, the potential values are set to $v_1 = -3000$, $v_2 = -25$ and $v_3 = -5$, respectively. In addition, the potential value inside the working object is set to $v_0 = -40000$. As a rule, the potential value v_0 is defined by an extremely negative value in order to conveniently judge whether the manipulator has collided with the working object or not. Comparing Fig.5.2(a) with Fig.5.3(a), the obvious difference can be found that the shapes of $Peak^*$ of ${}^1S$ are lower and thiner than the shapes of $Peak$ of ${}^1E$. Moreover, there are some ${}^1S < 0$ areas in ${}^1S$ distribution. It is of particular note that the highest position $Peak1$ of ${}^1E$ in Fig.5.2(a) almost disappears and is replaced by $Peak1^*$ in Fig.5.3(a), which indicates that collision is possible or the manipulator is very near the target object, although position $Peak1$ of ${}^1E$ corresponds to the highest avoidance manipulability. However, if we utilize the potential spaces to keep the manipulator from the target object, in other words, if we use ${}^1S$ to determine the optimal shape of the manipulator, the manipulator can be far away from the target object at little expense to avoidance manipulability (${}^1E$).

As shown in Fig.5.2(b), the manipulator collides with the target object, although the manipulator's shape corresponding to $Peak1$ possesses the highest avoidance manipulability. However, as shown in Fig.5.3(b), the manipulator's shape corresponding to $Peak1^*$ avoids the collision successfully by excluding the area of ${}^1S < 0$ in the ${}^1S$ distribution, although ${}^1S$ is somewhat smaller than ${}^1E$ (little avoidance manipulability is lost). In short, ${}^1E$ can

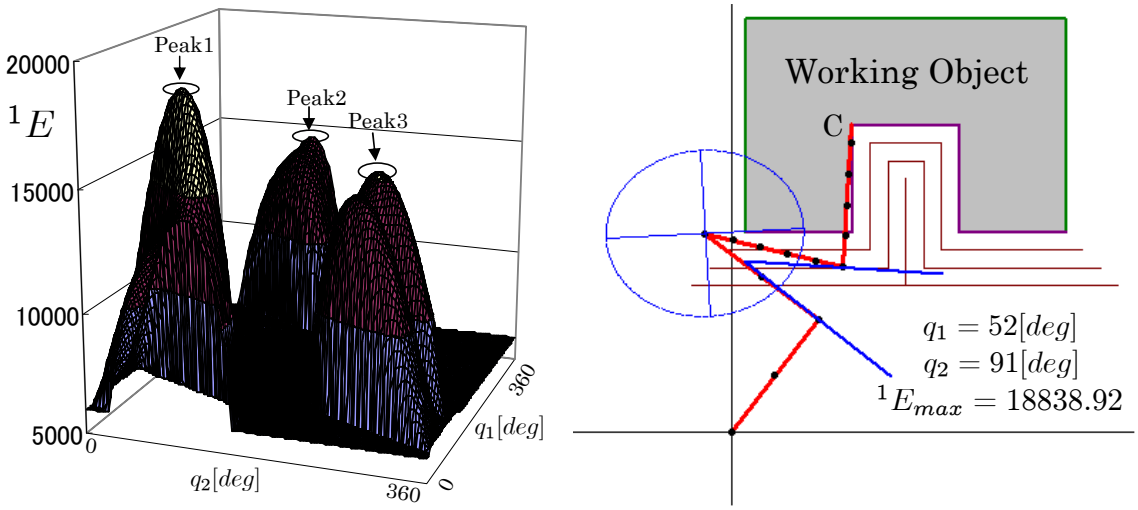

(a) ^1E distribution (b) Manipulator's shape at $Peak1$

Fig. 5.2: ^1E distribution and the manipulator's optimal shape corresponding to the maximum ^1E when the end-effector is fixed at (x,y)=(85,215).

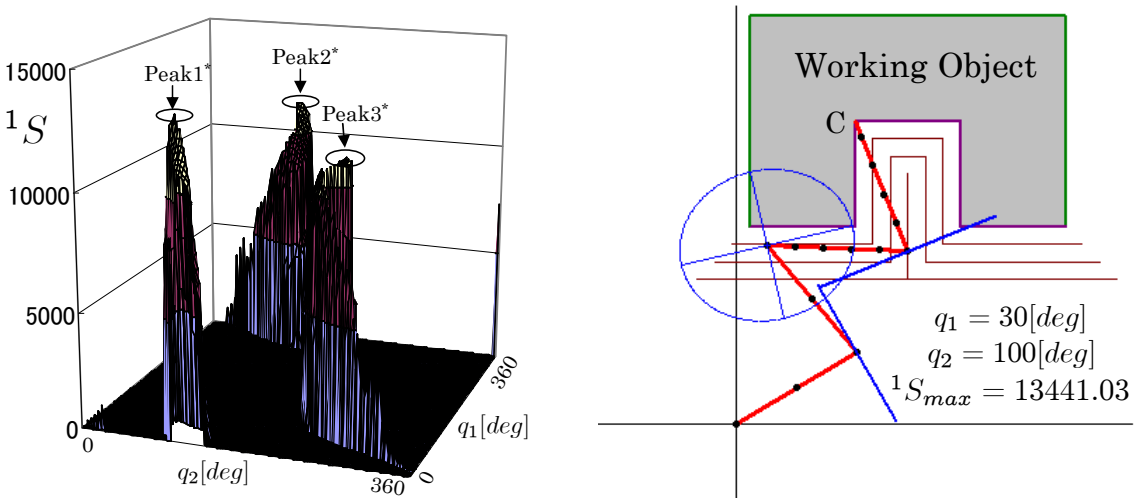

(a) ^1S distribution (b) Manipulator's shape at $Peak1^*$

Fig. 5.3: ^1S distribution and the manipulator's optimal shape corresponding to the maximum ^1S when the end-effector is fixed at (x,y)=(85,215).

just guarantee the requirement of the highest avoidance manipulability without considering the possibility of collision. ${}^1S$ is used to keep avoidance manipulability as high as possible based on non-collision (using potential spaces). Through the comparison shown in Fig.5.2 and Fig.5.3, we can verify that "AMSIP" (${}^1S$) is more effective than "AMSI" (${}^1E$) when simultaneously considering avoidance manipulability and the potential for collision.

6 Configuration Control

6.1 Reachability and Real-Time Controller

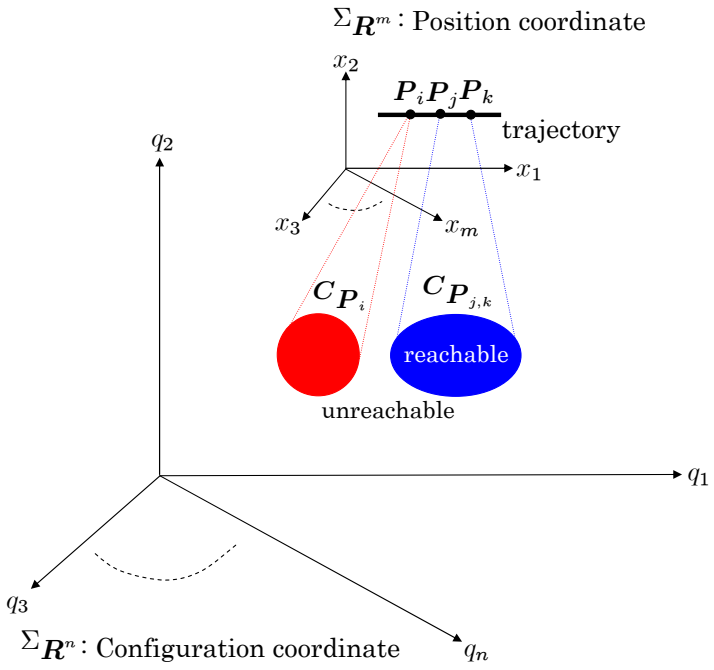

Fig. 6.1: The concepts of "unreachable" and "reachable"

The redundancy indicates that one position of the manipulator's end-effector corresponds to a sub-space in joint configuration space (redundancy solutions). Firstly and basically, it is necessary to explain the two important concepts, "unreachable" and "reachable". As shown in Fig.6.1, there are three positions as $\boldsymbol{P}_i$, $\boldsymbol{P}_j$ and $\boldsymbol{P}_k$ in the whole trajectory. The configuration space corresponding to $\boldsymbol{P}_i$, $\boldsymbol{C}_{\boldsymbol{P}_i}$ is denoted by a red circle area. And the configuration spaces corresponding to $\boldsymbol{P}_j$ and $\boldsymbol{P}_k$ are also represented by $\boldsymbol{C}_{\boldsymbol{P}_j}$ and $\boldsymbol{C}_{\boldsymbol{P}_k}$, where $\boldsymbol{C}_{\boldsymbol{P}_{j,k}} = \boldsymbol{C}_{\boldsymbol{P}_j} \cup \boldsymbol{C}_{\boldsymbol{P}_k}$, and $\boldsymbol{C}_{\boldsymbol{P}_{j,k}}$ is denoted by blue ellipsoid area. On the one hand, $\boldsymbol{C}_{\boldsymbol{P}_i}$ and $\boldsymbol{C}_{\boldsymbol{P}_{j,k}}$ are completely separated twos, which means that any configuration in red circle area can not be connected into any configuration in blue ellipsoid area by result of some natural reasons such as manipulator's fixed composition or working environment, so it is unreachable from $\boldsymbol{P}_i$ to $\boldsymbol{P}_j$ or from $\boldsymbol{P}_i$ to $\boldsymbol{P}_k$. On the other hand, configuration space

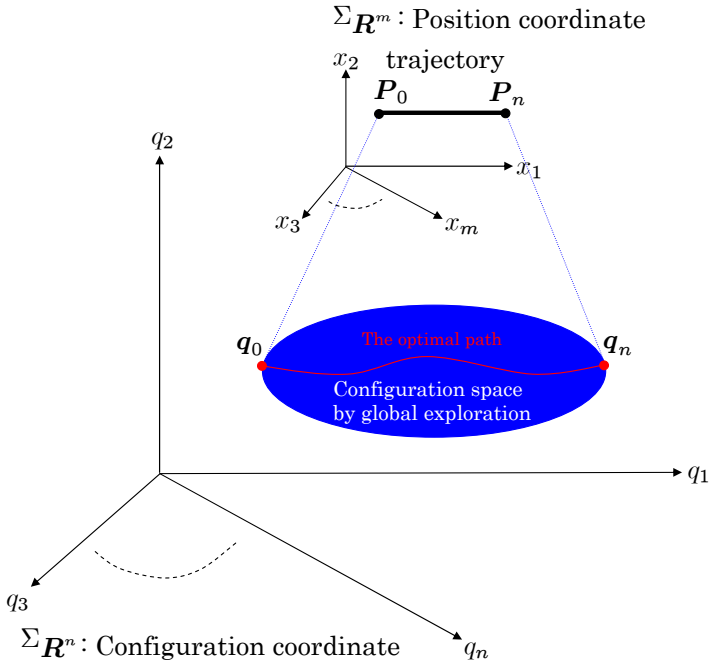

Fig. 6.2: Path/motion planning

$\boldsymbol{C}_{\boldsymbol{P}_{j,k}}$ includes the all configurations corresponding to $\boldsymbol{P}_j$ and $\boldsymbol{P}_k$. In this alone configuration space, any configuration can be changed each other, so we can think that it is reachable from $\boldsymbol{P}_j$ to $\boldsymbol{P}_k$. In this example, the relations of $\boldsymbol{P}_i \leftrightarrow \boldsymbol{P}_j$ and $\boldsymbol{P}_i \leftrightarrow \boldsymbol{P}_k$ are called by "unreachable", the relation of $\boldsymbol{P}_j \leftrightarrow \boldsymbol{P}_k$ is called by "reachable".

Consider the path/motion planning problem assuming reachability, that is classic problem as shown in Fig.6.2. Where, the trajectory in position coordinate from $\boldsymbol{P}_0$ to $\boldsymbol{P}_n$ is given, then the possible configuration space denoted by a blue ellipsoid area in the figure corresponding to the whole trajectory can be calculated by global exploration. Finally, we can find the optimal path such as the red line according to some optimization requirement.

However, our research is to use inverse kinematic knowledge in the velocity relation to solve a classic real-time trajectory tracking problem of redundant manipulators. The trajectory tracking problem in our research includes two main sub-problems: reachability problem (how to ensure continuity from start configuration to the goal configuration in all time) and real-time optimization problem (on the basis that reachability is held, how to select the optimal solution among many solutions in each varying time). That is to say, our purpose is to design an controller giving attention to reachability and real-time optimization. Therefore, preview control system is presented as a configuration control method, which is used to make current

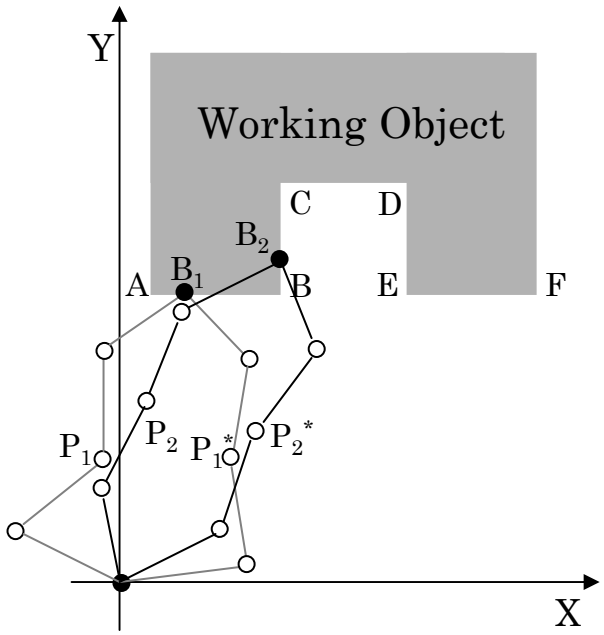

Fig. 6.3: A simple example for explaining the importance of preview control.

manipulator's shape close the future optimal shape based on an real-time measurement by referring to the future optimal shape.

This future optimal shape satisfies two requirements. One is that the manipulator's links should avoid the obstacle. The other is that the manipulator's shape should possess high avoidance manipulability as much as possible based on non-collision. This future optimal shape, corresponding to the maximum ${}^1S$, merging the high avoidance manipulability into non-collision shape, can be found by using 1-step GA in future time (please refer to [30] about the detail of 1-step GA). Fig.6.3 is used to explain the importance of preview control. When the end-effector reaches the position B_1, two kinds of the manipulator's configurations denoted by P_1 and $P_1{}^*$, representing symbolically infinite choice of configurations, both can avoid collision. However, when the end-effector reaches the position B_2, only the configuration of $P_2{}^*$ in the two configurations denoted by P_2 and $P_2{}^*$ can avoid collision. If the manipulator's configuration is selected as P_1 at end-effector point B_1, the angular velocities of joints will be high values to change its configuration like $P_2{}^*$ near the corner B. This poses a possibility that the manipulator crashes to corner B when the required high angular velocity is over maximum velocity of the joint. Therefore, the manipulator's configuration must be prepared to the configuration $P_1{}^*$ that is similar future configuration $P_2{}^*$. This requires

that the current manipulator's configuration should be determined in a consideration of future possible configuration or several future possible configurations, which is so-call preview control. If we select only one future optimal shape in one future time, we call it as "single preview control", if we select several future optimal shapes in several future times, we call it as "multiple preview control".

6.2 Preview Control

6.2.1 Single Preview Control

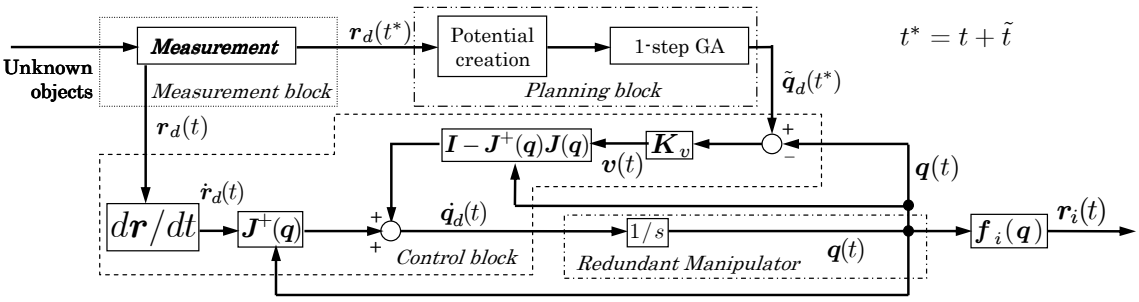

Fig. 6.4: Single preview control system.

Single preview control system is described in Fig.6.4. t denotes the current time, t^* denotes the future time and t^* is forwarder than t by $\tilde{t}$ ($\tilde{t} = t^* - t$). Here, $\tilde{t}$ is called "preview time". In addition, this preview control system consists of a real-time measurement block, a planning block, a redundancy control block and a redundant manipulator. Firstly, the measurement block can detect the desired end-effector position $\boldsymbol{r}_d(t^*)$ on the surface of working object (target object) in future time t^*. Next, the planning block outputs the future optimal joint angles $\tilde{\boldsymbol{q}}_d(t^*)$ found by 1-step GA corresponding to the future desired end-effector position $\boldsymbol{r}_d(t^*)$. This is called "imaginary manipulator". At last, once the optimal shape $\tilde{\boldsymbol{q}}_d(t^*)$ is determined, the control block outputs the desired angular velocities of each joint $\dot{\boldsymbol{q}}_d(t)$ that can make the current joint angles $\boldsymbol{q}(t)$ (actual manipulator's shape) close the future optimal joint angles $\tilde{\boldsymbol{q}}_d(t^*)$ (imaginary manipulator's shape) to satisfy requirements of high avoidance manipulability based on non-collision. The last part of Fig.6.4 represents $\boldsymbol{r}_i(t) = \boldsymbol{f}_i(\boldsymbol{q}(t))$, which means natural calculation of forward kinematics of robot's i-th link through the robot's configuration itself. Here, the key is how to determine $\dot{\boldsymbol{q}}_d(t)$. When the desired velocity of

the manipulator's end-effector $\dot{\boldsymbol{r}}_d(t)$ is given, from $\dot{\boldsymbol{r}}_d(t) = \boldsymbol{J}_n(\boldsymbol{q})\dot{\boldsymbol{q}}(t)$ we can obtain genaral solution $\dot{\boldsymbol{q}}(t)$ as

$$\dot{\boldsymbol{q}}(t) = \boldsymbol{J}_n^+(\boldsymbol{q})\dot{\boldsymbol{r}}_d(t) + [\boldsymbol{I}_n - \boldsymbol{J}_n^+(\boldsymbol{q})\boldsymbol{J}_n(\boldsymbol{q})]\boldsymbol{v}(t). \tag{6.1}$$

In (6.1), $\boldsymbol{v}(t)$ is an arbitrary vector satisfying $\boldsymbol{v}(t) \in R^n$. In this research, trajectory tracking and obstacle avoidance should be executed simultaneously through redundancy [13]. Here, $\boldsymbol{v}(t)$ is determined to make the current shape of actual manipulator $\boldsymbol{q}(t)$ close the future optimal shape of imaginary manipulator $\tilde{\boldsymbol{q}}_d(t^*)$, so it is designed as

$$\boldsymbol{v}(t) = \boldsymbol{K}_v[\tilde{\boldsymbol{q}}_d(t^*) - \boldsymbol{q}(t)]. \tag{6.2}$$

In (6.2), $\boldsymbol{K}_v$ is a positive definite diagonal matrix representing gains as

$$\boldsymbol{K}_v = diag[k_{v1}, k_{v2}, \cdots, k_{vn}]. \tag{6.3}$$

Then, substituting (6.2) into (6.1), we can obtain $\dot{\boldsymbol{q}}_d(t)$ as

$$\dot{\boldsymbol{q}}_d(t) = \boldsymbol{J}_n^+(\boldsymbol{q})\dot{\boldsymbol{r}}_d(t) + [\boldsymbol{I}_n - \boldsymbol{J}_n^+(\boldsymbol{q})\boldsymbol{J}_n(\boldsymbol{q})]\boldsymbol{K}_v[\tilde{\boldsymbol{q}}_d(t^*) - \boldsymbol{q}(t)]. \tag{6.4}$$

The first term of right side of (6.4) represents angular velocity vector that can achieve $\dot{\boldsymbol{r}}_d \in R^m$ with minimum norm of $\dot{\boldsymbol{q}}_d$, on the other hand, the second term can use the redundant degrees of $n-m$ to decrease $\tilde{\boldsymbol{q}}_d(t^*)-\boldsymbol{q}(t)$ as much as possible without intervening in realization of $\dot{\boldsymbol{r}}_d$. Thus (6.4) does not refer to what number of joint works for which task of $\dot{\boldsymbol{r}}_d$ or $\tilde{\boldsymbol{q}}_d(t^*)-\boldsymbol{q}(t)$. According to above discussion, the optimal shape of imaginary manipulator $\tilde{\boldsymbol{q}}_d(t^*)$ in future time of t^* is chosen by 1-step GA through real-time optimization of ${}^1S$, including both the shape-changeability and how much the manipulator's configuration approaching in the vicinity of the working object. Then, $\tilde{\boldsymbol{q}}_d(t^*)$ is given to the controller represented by (6.4), which is "preview control". This means our method does not control a specific link to avoid obstacle, instead of that, total configuration $\tilde{\boldsymbol{q}}_d(t^*)$ is given. In our approach, the number of the redundant degrees $n - m$ (n: manipulator's link number; m: dimension of working space) equals to the degree of the searching space found by 1-step GA. When $\boldsymbol{r}_d(t^*)$ is known, $n - m$ angles can be decided after the on-line optimization of the 1-step GA in the redundant space of R^{n-m}, then the remaining joint m angles can be decided uniquely by inverse kinematics. In this way, since n angles have been decided, that is manipulator's shape

$\tilde{\boldsymbol{q}}_d(t^*)$ has been decided to realize $\boldsymbol{r}_d(t^*)$. So, in our strategy, there is no concept to select which link should be avoided, in spite of that the whole configuration $\tilde{\boldsymbol{q}}_d(t^*)$ represents the shape with best avoidance changeability and best avoidance position against working object through ${}^1S$, which is composed of ${}^1E$ (avoidance changeability) and U (avoidance position against working object).

6.2.2 Multiple Preview Control

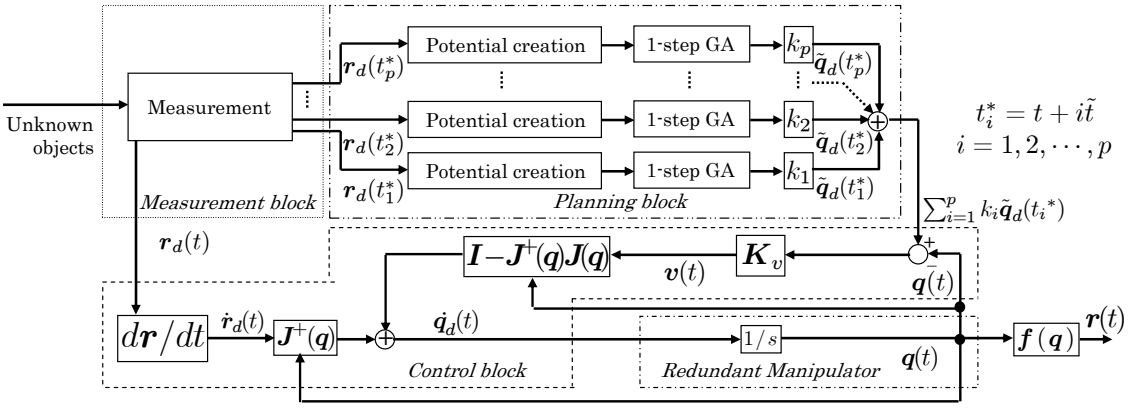

Fig. 6.5: Multiple preview control system

Multiple preview control system depicted in Fig.6.5 consists of a real-time measurement block, a path planning block, a redundancy control block and a redundant manipulator. On the assumption that current time is represented by t, and the future times are defined as $t_i^* = t + i\tilde{t}$ where $\tilde{t}$ denotes preview time and $i = 1, 2, \cdots, p$, p denotes the number of future times. Firstly, the measurement block can detect desirable end-effector positions $\boldsymbol{r}_d(t_i^*)$ on the surface of the target object at future times t_i^*. Then, the potential spaces detected by camera are created around the target object at the planning block automatically. Next, the planning block outputs desired joint angles $\tilde{\boldsymbol{q}}_d(t_i^*)$ corresponding to future time t_i^* satisfying non-collision found by 1-step GA. Here, we make an assumption that $\tilde{\boldsymbol{q}}_d(t_i^*)$ are "imaginary manipulators" and p also denotes the number of imaginary manipulators. At last, when desired velocity $\dot{\boldsymbol{r}}_d(t)$ is given, the control block outputs desired joint angular velocity $\dot{\boldsymbol{q}}_d(t)$ as

$$\dot{\boldsymbol{q}}_d(t) = \boldsymbol{J}^+(\boldsymbol{q})\dot{\boldsymbol{r}}_d(t) + (\boldsymbol{I}_n - \boldsymbol{J}^+(\boldsymbol{q})\boldsymbol{J}(\boldsymbol{q}))\boldsymbol{v}(t) \tag{6.5}$$

In (6.5), $\boldsymbol{v}(t)$ is an arbitrary vector, which is used for making current joint angle $\boldsymbol{q}(t)$ of actual

manipulator close to future joint angles of imaginary manipulators $\tilde{\boldsymbol{q}}_d(t_i^*)$ without collision, so its definitions are very key and varied.

In the case of multiple preview control system, we use several optimal configurations of imaginary manipulators at future times ${t_i}^* = t + i\tilde{t}$ ($i = 1, 2, \cdots, p$, p is finite and $p \geq 2$) to control the current joint angle $\boldsymbol{q}(t)$ of actual manipulator to make $\boldsymbol{q}(t)$ not only close the future optimal configurations without collision but also keep high reachability. For example, when $p = 3$, it means that we adopt three future optimal configurations at three different future times $t + \tilde{t}$, $t + 2\tilde{t}$ and $t + 3\tilde{t}$ to control current configuration. Therefore, variable $\boldsymbol{v}(t)$ in multi-preview control system is defined as

$$\boldsymbol{v}(t) = \boldsymbol{K}_v[\sum_{i=1}^{p} k_i \tilde{\boldsymbol{q}}_d({t_i}^*) - \boldsymbol{q}(t)] \tag{6.6}$$

In (6.6), $\sum_{i=1}^{p} k_i \tilde{\boldsymbol{q}}_d({t_i}^*)$ indicates the synthetic evaluation of p future optimal configurations, k_i are weight coefficients satisfying $0 < k_i < 1$ and $\sum_{i=1}^{p} k_i = 1$. We can select arbitrary value of preview time $\tilde{t}$ and number of preview control p and weight coefficient k_i according to different conditions. By comparing multiple preview with single preview, multiple preview improves the limitation of single preview by more information of future dynamic environments, which is possible to realize reachability.

6.2.3 The Effectiveness of Multiple Preview Control

Fig.6.6 describes the effectiveness of multiple preview control, where the times defined by t_0, t_1, t_2, t_3 and t_4 respectively. And "•" indicates several local optimal configurations at each future time whose evaluation values ${}^1S$ given by (5.3) are plus and are denoted here by S_{1a}, S_{1b}, S_{1c} ($S_{1a} < S_{1b} < S_{1c}$) at $t = t_1$, and S_{2a}, S_{2b}, S_{2c} ($S_{2a} < S_{2b} < S_{2c}$) at $t = t_2$, and S_{3a}, S_{3b}, S_{3c} ($S_{3a} < S_{3b} < S_{3c}$) at $t = t_3$ and S_{4b}, S_{4c} ($S_{4b} < S_{4c}$) at $t = t_4$. The value S evaluates superiority of the configuration and safety concerning collision with the working object, and $S < 0$ means collision. The manipulator stays at initial configuration when time $t = t_0$. If we do not use preview control method, we almost can not know the future information, so control of the current manipulator's configuration will be blind without any reference. If we use single preview depending on only one future optimal configuration at one future time, then the configuration will be controlled to S_{1c} at time $t = t_1$, to S_{2c} at time $t = t_2$ and to S_{3c} at time $t = t_3$. Shall we provide that the value of S_{4a} has negative value represented by

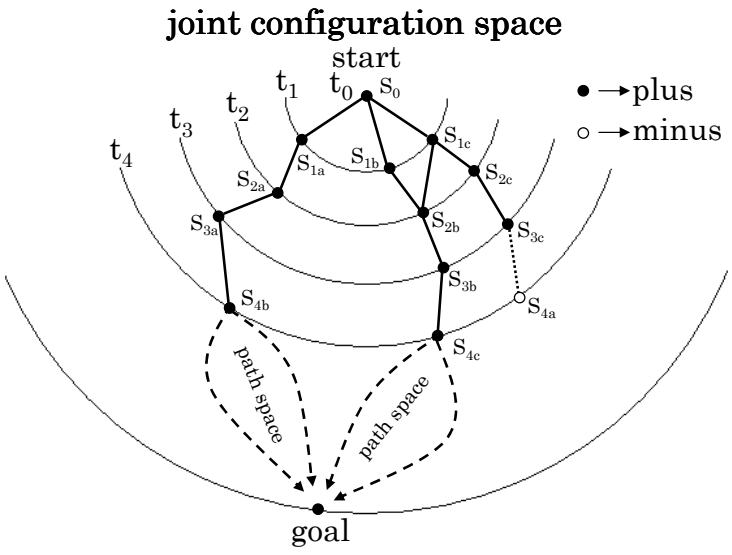

Fig. 6.6: Why the multiple preview control is effective against the unknown-shape object

"○" meaning future possible configuration from S_{3c} can not avoid collision with surroundings or target object. The configuration of redundant manipulator corresponding to S_{3c} at time $t = t_3$ is trapped in hardship because the future information at only one future time is very local. The real-time motion will have to be stopped at time $t = t_3$ for safety. However, if we expand the future information by selecting three future optimal configurations at three future times, which is multi-preview. In this example, referring to (6.6), $p = 3$. At the current time $t = t_0$, the current configuration is S_0. The configuration will be controlled to S_{1c} at time $t = t_1$ by the future optimal reachable sequences $S_{1c}\rightarrow S_{2c}\rightarrow S_{3c}$ estimated from $S_{ij}(i = 1, 2, 3; j = a, b, c)$, where the other possible sequences $S_{1a}\rightarrow S_{2a}\rightarrow S_{3a}$, $S_{1b}\rightarrow S_{2b}\rightarrow S_{3b}$ and $S_{1c}\rightarrow S_{2b}\rightarrow S_{3b}$ are inferior selection, which are composed of three future configurations because $p = 3$ in (6.6). Then, from S_{1c}, the possible future sequences are restricted to $S_{2b}\rightarrow S_{3b}\rightarrow S_{4c}$ and $S_{2c}\rightarrow S_{3c}\rightarrow S_{4a}$. The multi-preview controller can judge and exclude the unreachable sequence $S_{2c}\rightarrow S_{3c}\rightarrow S_{4a}$ because it includes the collision configuration S_{4a}, then the configuration will be controlled to S_{2b} at time $t = t_2$ according to the future optimal reachable sequences $S_{2b}\rightarrow S_{3b}\rightarrow S_{4c}$. Obviously, this multi-preview controller with $p = 3$ can detect the future collision configuration S_{4a} at the current time $t = t_1$ and avoid it forward by selecting S_{2b} rather than S_{2c} at time $t = t_2$, although $S_{2b} < S_{2c}$. By repeating such evaluation of future configuration sequences and possible route changing, multi-preview control system

Table 6.1: ${}^1S$ of $Peaki^*$ in global trajectory

$t[s]$	$Peak1^*$	$Peak2^*$	$Peak3^*$	$Peak4^*$
0	20140.69	14443.42	10762.14	14661.14
5	19650.81	14997.29	11305.17	14363.01
10	18684.81	14711.02	11350.10	13794.14
15	13067.19	12637.86	10914.79	< 0
20	13441.03	10656.65	11113.94	< 0
25	14803.23	11752.52	11539.66	< 0
30	13614.74	8505.96	7821.52	< 0
35	15327.24	11976.49	9622.34	< 0
40	16399.25	12404.49	13386.48	< 0
50	14656.65	11800.18	14204.03	< 0

will possibly avoid dangerous sequences connecting to clashing in the future and can widen out the possibility from current configuration to goal configuration. In subsection 6.3, we will compare and analyze their difference by simulations.

6.3 Simulations

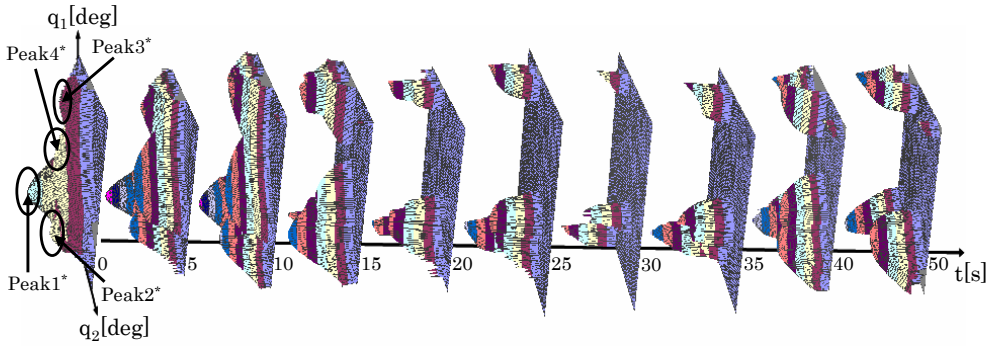

Fig. 6.7: 3-D AMSIP ${}^1S$ distribution in whole tracking process

As shown in Fig.5.1, the trajectory consists of five parts, $A-B$, $B-C$, $C-D$, $D-E$ and $E-F$ respectively. The coordinate of A is fixed at position of $(10cm, 140cm)$, the each length of trajectory is defined as $l_{A-B} = l_{B-C} = l_{C-D} = l_{D-E} = l_{E-F} = 75[cm]$ and the length of each link is defined as $l_1 = l_2 = l_3 = l_4 = 100[cm]$. The whole simulation time is set to $50[s]$. We can detect the 3-D AMSIP ${}^1S$ distributions at ten different given times in whole tracking process shown in Fig.6.7. From Fig.6.7, we can clearly find that there are four peaks of ${}^1S$ when $t = 0[s]$, $t = 5[s]$ and $t = 10[s]$ denoted by $peak1^*$, $peak2^*$,

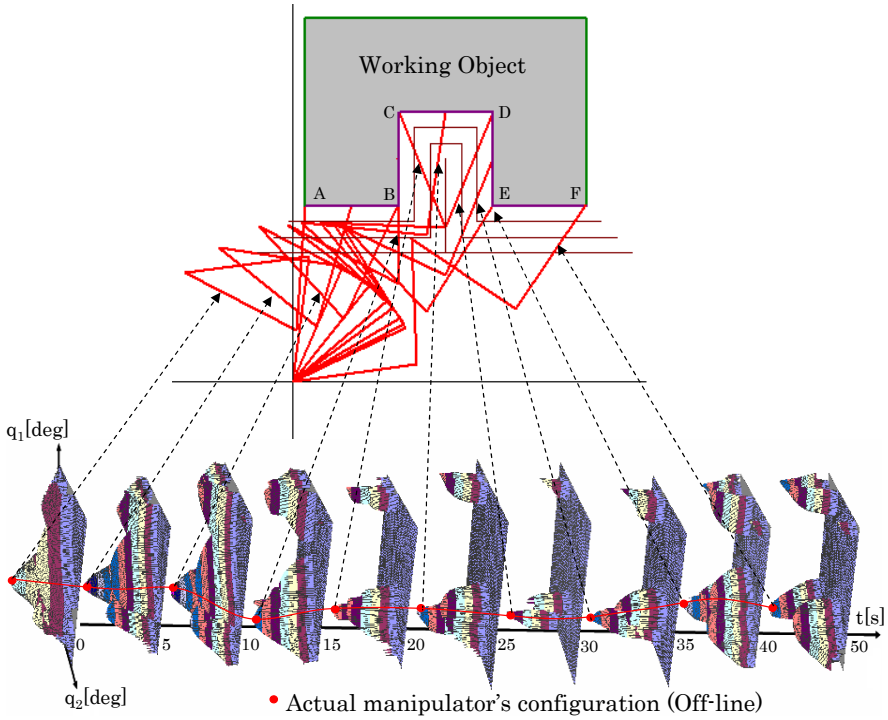

Fig. 6.8: Actual manipulator's configurations in whole tracking process based on path planning

$peak3^*$ and $peak4^*$ respectively. However, $peak4^*$ disappears from $t = 15[s]$ to end, which indicates the safe configuration around $peak4^*$ will become dangerous configuration after $15[s]$ when manipulator's end-effector tracks the trajectory indicated by $peak4^*$. In addition, according to Table 6.1 generalizing the peak values of ${}^1S$, we can think that always keeping ${}^1S$ around $peak1^*$ in whole tracking process is desired selection, which can satisfy requirement of reachability meanwhile can keep higher avoidance ability because $peak1^*$ is always exist and ${}^1S$ around $peak1^*$ is larger than ${}^1S$ of other peaks such as $peak2^*$, $peak3^*$ and $peak4^*$ in whole tracking process.

6.3.1 By Path Planning

Simulation result in the condition of path planning is shown in Fig.6.8, ${}^1S$ of actual manipulator are in the highest peaks in the whole process, which indicates ${}^1S$ are maximum and their corresponding configurations are also optimal. But this path planning is just suitable for off-line control.

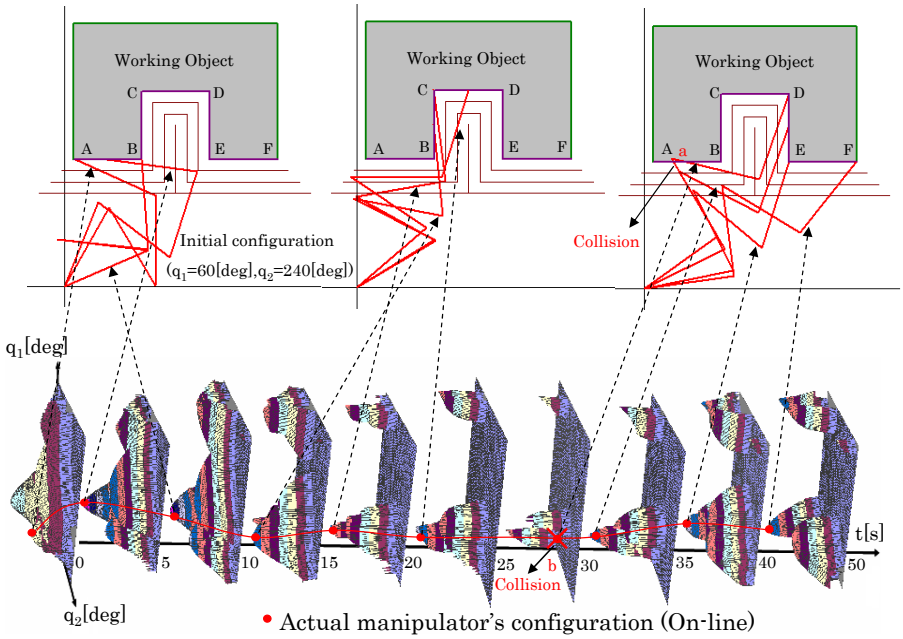

Fig. 6.9: Actual manipulator's configurations in whole tracking process based on single preview control

6.3.2 By Single Preview Control

We use single preview control to do some simulations and the single preview time $\tilde{t}$ is set to $10[s]$. ${}^1S$ of actual manipulator at ten different given times in whole tracking process denoted by red points and configurations corresponding to the highest peak of ${}^1S$ at these ten times are shown in Fig.6.9, where the red line connecting these red points denotes the trajectory change of ${}^1S$ of actual manipulator in whole tracking process. From Fig.6.9, we can find that actual manipulator almost can achieve real-time trajectory tracking except for the collision with working object when $t = 30[s]$ because the future information is very local. Collision position is described as "a" and corresponding ${}^1S$ is negative described as "b" in Fig.6.9.

6.3.3 By Multiple Preview Control

Here, we adopt three-preview control to do the same simulations, three future times are defined by ${t_1}^* = t + \tilde{t}$, ${t_2}^* = t + 2\tilde{t}$ and ${t_3}^* = t + 3\tilde{t}$ respectively (here, $\tilde{t} = 5[s]$). Then, we define $k_1 = 0.3$, $k_2 = 0.65$ and $k_3 = 0.05$ (notice that weight coefficients k_i has been presented in (6.6)). In this way, we use these three future optimal configurations of imaginary manipulators, that is $0.3\tilde{\boldsymbol{q}}_d(t_1^*) + 0.65\tilde{\boldsymbol{q}}_d(t_2^*) + 0.05\tilde{\boldsymbol{q}}_d(t_3^*)$ from (6.6), to control current configuration of actual manipulator. The simulation result is shown in Fig.6.10. From Fig.6.10, we can

find that collision occurred at 30[s] in the case of single preview control has been avoided by three-points preview control and actual manipulator can achieve real-time trajectory tracking without collision meanwhile keeping higher avoidance manipulability.

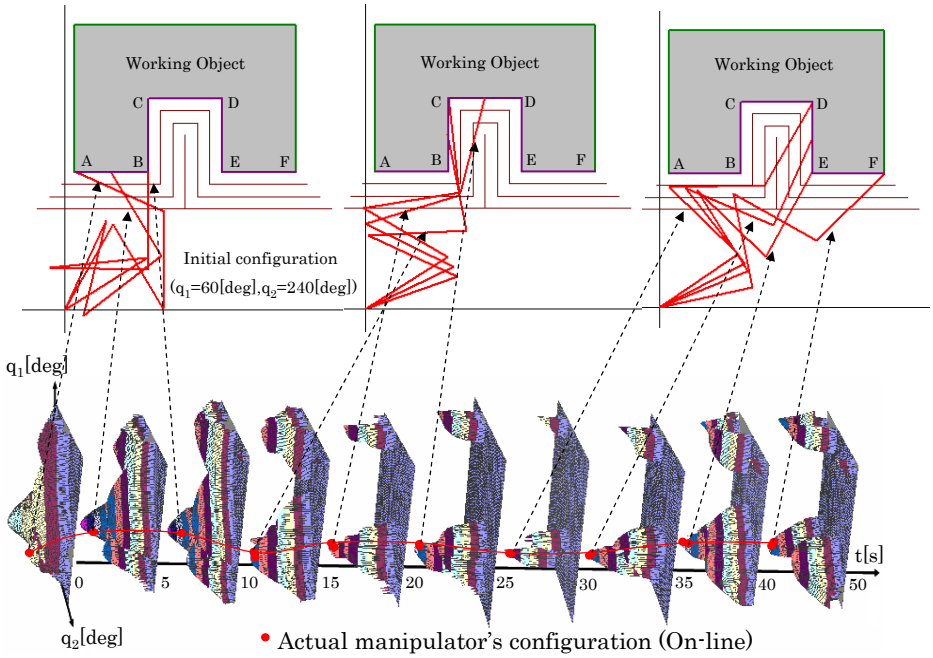

Fig. 6.10: Actual manipulator's configurations in whole tracking process based on multiple preview control

6.3.4 Simulation of Real Machine

For further verifying our proposed methods, here we use the real machine named "PA10" to realize trajectory tracking and obstacle avoidance. "PA10" is a 7-link redundant manipulator and its end-effector can execute the task in 3-dimensional space. The photo of "PA10" is shown in Fig.6.11. Its coordinate system is shown in Fig.6.12. Where, the first, third, fifth and seventh joints are revolute ones with self-rotation, the second, fourth and sixth joints are revolute ones with up-and-down or back-and-forth rotation as looking from the different directions, the length of links is also shown. The desired trajectory is shown in Fig.6.13, which is described by mathematical equations as

$$\begin{cases} r_{dx} = -0.8[m] \\ r_{dy} = -0.5 + 0.05t[m] \\ r_{dz} = 0.6[m] \end{cases}, \quad 0 \leq t \leq 20 \tag{6.7}$$

and

$$\begin{cases} r_{dx} = -0.8 + 0.05(t - 20.0)[m] \\ r_{dy} = 0.5[m] \\ r_{dz} = 0.6[m] \end{cases} , \quad t > 20. \tag{6.8}$$

The velocity of manipulator's end-effector is $0.05[m/s]$ and the whole tracking time is $36[s]$. As the time is varying, the changing process of the singular values of avoidance matrices corresponding from the 3-rd link to 7-th link are shown from Fig.6.14 to Fig.6.18. The 1-st and 2-nd links are fixed in root of "PA10", so their singular values are not existing. Avoidance manipulability ellipsoids of "PA10" at $0[s]$, $4[s]$, $8[s]$, $12[s]$, $16[s]$, $20[s]$, $24[s]$, $28[s]$, $32[s]$ and $36[s]$ are shown from Fig.6.19 to Fig.6.28 respectively.

From Fig.6.14 to Fig.6.16 where there are some peaks appear from $15[s]$ to $21[s]$. The reason is that "PA10" is near the corner position after from $15[s]$, for passing this corner position without collision, "PA10" is required to change its shape quickly, resulting in the changing of singular values. Moreover, the singular values corresponding from the 3-rd link to 5-th link are increasing as the time is varying.

In addition, according to Fig.6.17 and Fig.6.18 where the singular values corresponding to the 6-th and 7-th links are very small. On the one hand, the manipulator's end-effector can be thought as being given the fixed task when it is tracking the desired trajectory, so theoretically the 7-th link does not possess the avoidance manipulability. On the other hand, the 6-th link is very near the end-effector, that is the length of the 7-th link is almost zero, so we can approximately think that the 6-th link of "PA10" does not possess the avoidance manipulability because its singular values are not existing.

Fig. 6.11: PA10

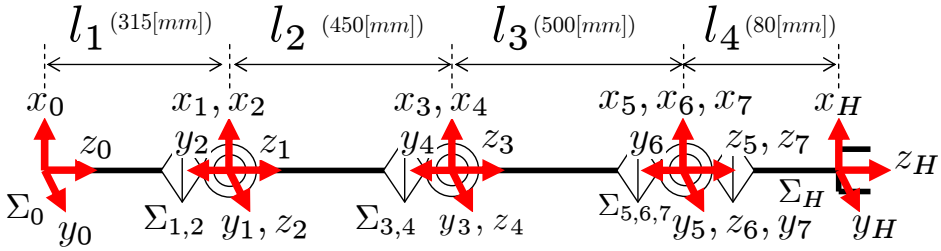

Fig. 6.12: The coordinate system of PA10

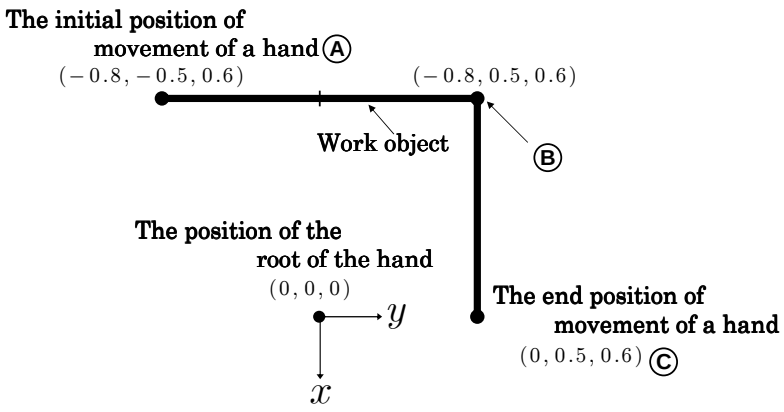

Fig. 6.13: The desired trajectory

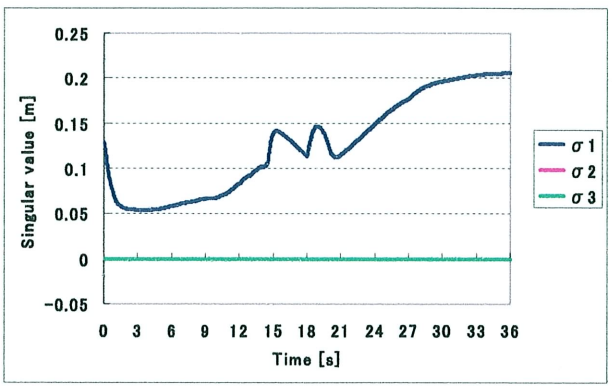

Fig. 6.14: The singular values of the 3-rd link

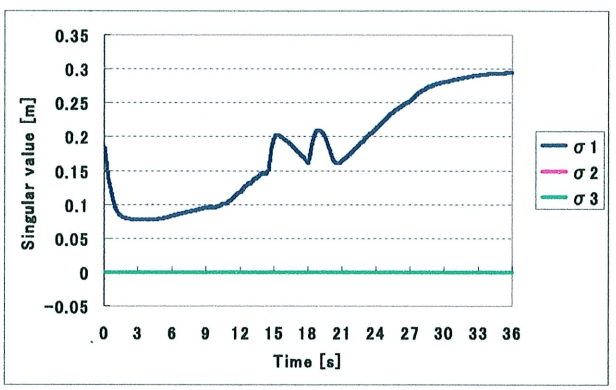

Fig. 6.15: The singular values of the 4-th link

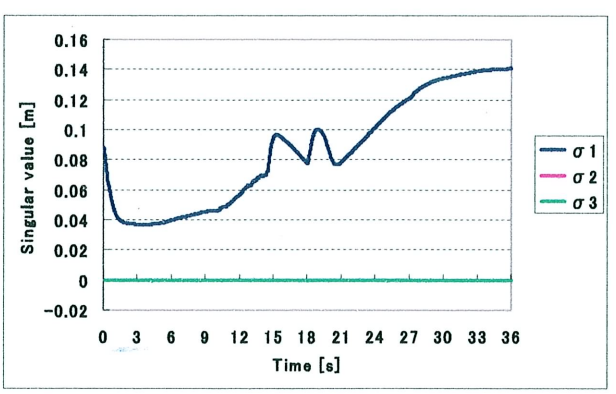

Fig. 6.16: The singular values of the 5-th link

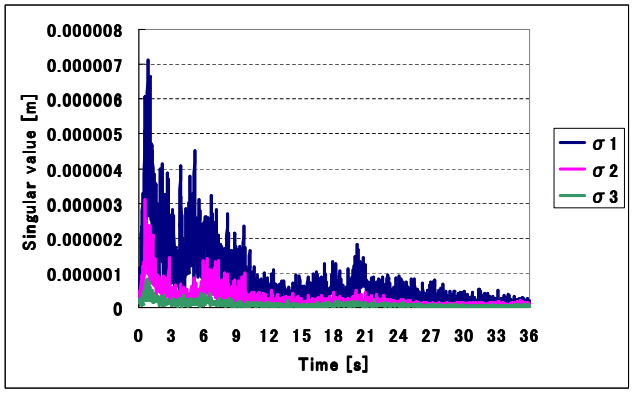

Fig. 6.17: The singular values of the 6-th link

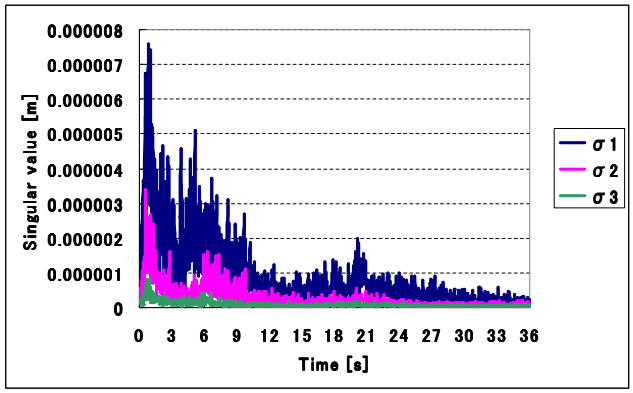

Fig. 6.18: The singular values of the 7-th link

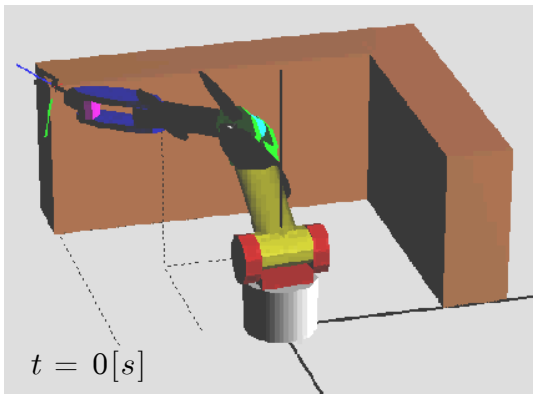

Fig. 6.19: Avoidance manipulability ellipsoids at 0[s]

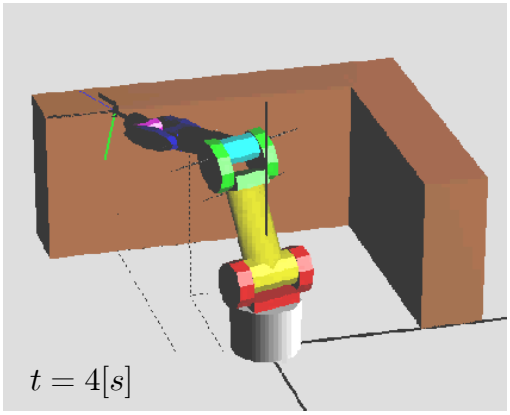

Fig. 6.20: Avoidance manipulability ellipsoids at 4[s]

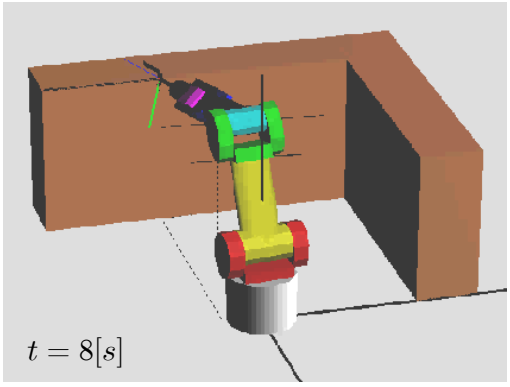

Fig. 6.21: Avoidance manipulability ellipsoids at 8[s]

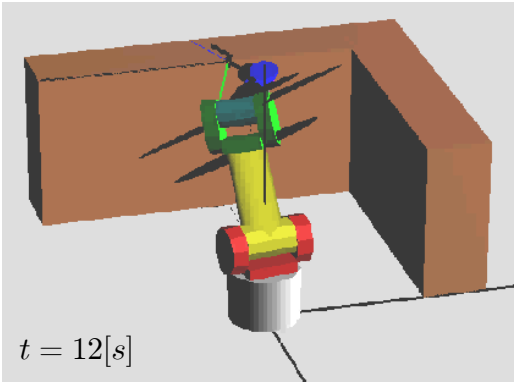

Fig. 6.22: Avoidance manipulability ellipsoids at 12[s]

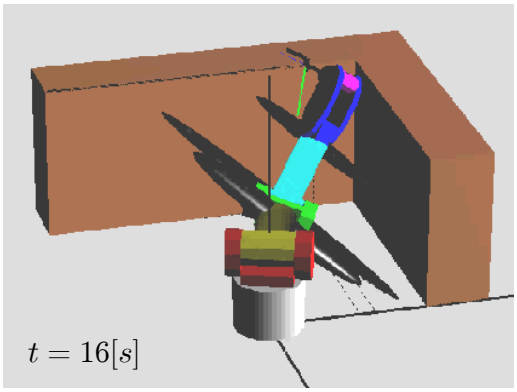

Fig. 6.23: Avoidance manipulability ellipsoids at 16[s]

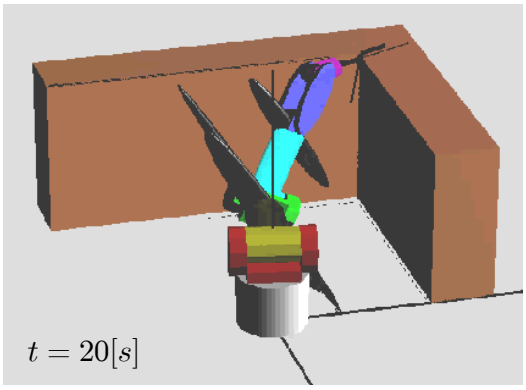

Fig. 6.24: Avoidance manipulability ellipsoids at 20[s]

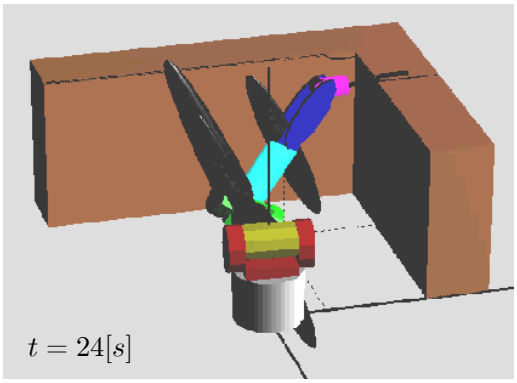

Fig. 6.25: Avoidance manipulability ellipsoids at 24[s]

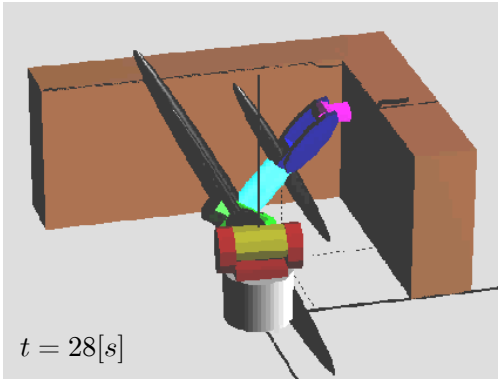

Fig. 6.26: Avoidance manipulability ellipsoids at 28[s]

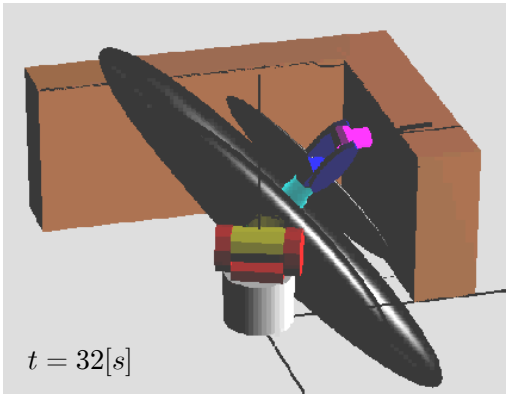

Fig. 6.27: Avoidance manipulability ellipsoids at 32[s]

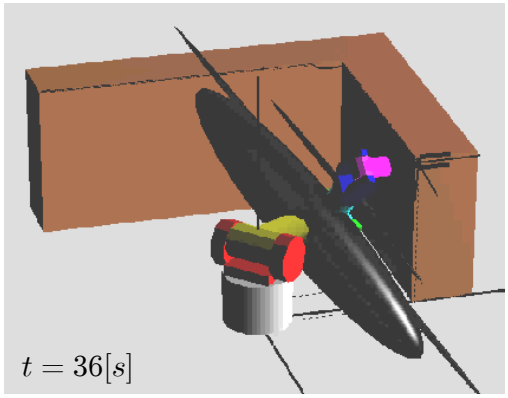

Fig. 6.28: Avoidance manipulability ellipsoids at 36[s]

7 Analysis of Avoidance Space

7.1 Importance and Significance

In above chapters, we explained the concept of avoidance manipulability ellipsoid and presented "AMSIP" to evaluate manipulator's shape (the largest ${}^1S$ corresponds to the optimal shape in the consideration of high avoidance manipulability and non-collision), finally we realized the simulations of a real-time control system by combining preview control (real-time configuration controller) with 1-step GA (real-time configuration optimization).

As for the concept of avoidance manipulability, we have known that avoidance manipulability of the manipulator was evaluated based on the avoidance ability in each possible dimension of intermediate links in the residue redundant space, we also have known that $rank({}^1\boldsymbol{M}_i)$ denotes the shape-changeable space dimension of the i-th link and the singular values of ${}^1\boldsymbol{M}_i$ means the radius length of main axes of avoidance manipulability ellipsoids, that is to indicate the shape-changeability of the i-th link. However, whether we can use the remaining redundancy to achieve desired avoidance task depends on purely whether the avoidance task lies in the range space of ${}^1\boldsymbol{M}_i$. In other words, only if the all shape-changeable spaces of every intermediate links are sustained can the manipulator acquire possibilities to achieve desired avoidance task. Therefore, it is necessary to analyze what assumption guarantees mathematically the sustainability of the shape-changeable space of the i-th link, that is $rank({}^1\boldsymbol{M}_i)$. Maintaining $rank({}^1\boldsymbol{M}_i)$ of intermediate links to be as high as possible is the essential requirement for configuration control to optimize manipulator's shape with high avoidance manipulability. And it is the first step to design a real-time control system of a redundant manipulator with high shape-changeability based on avoidance manipulability. In this chapter, we will propose two assumptions named as "Part-Non-Singular Configuration Assumption" and "All-Non-Singular Configuration Assumption", both can guarantee that $rank({}^1\boldsymbol{M}_i)$ could be maintained without reduction by dropping into singular configuration, through analyses and proofs by decomposing ${}^1\boldsymbol{M}_i$ into singular components. Here, we want

to stress previous researches have not paid attention to how to guarantee $rank({}^1\boldsymbol{M}_i)$ to assure the required avoidance task to be realizable. Even that these two Non-Singular Configuration Assumptions have not been integrated into our current configuration control system, but they have an ability for presenting yardstick to maintain the sustainability of avoidance space expansion.

7.2 Mathematical Descriptions

7.2.1 Definitions

A $m \times n$ matrix $\boldsymbol{J}$ can be decomposed by

$$\boldsymbol{J} = \boldsymbol{U}\boldsymbol{\Sigma}\boldsymbol{V}^T \tag{7.1}$$

and $\boldsymbol{J}^+$, the pseudo-inverse of $\boldsymbol{J}$, can be decomposed by

$$\boldsymbol{J}^+ = \boldsymbol{V}\boldsymbol{\Sigma}^+\boldsymbol{U}^T. \tag{7.2}$$

In (7.1) and (7.2), $\boldsymbol{U}$ is a $m\times m$ orthogonal matrix satisfying $\boldsymbol{U}\boldsymbol{U}^T = \boldsymbol{U}^T\boldsymbol{U} = \boldsymbol{I}_m$, $\boldsymbol{V}$ is a $n\times n$ orthogonal matrix satisfying $\boldsymbol{V}\boldsymbol{V}^T = \boldsymbol{V}^T\boldsymbol{V} = \boldsymbol{I}_n$, $\boldsymbol{\Sigma}$ is a $m\times n$ matrix, which includes a diagonal matrix composing of the non-zero singular values of $\boldsymbol{J}$ and the rest parts are all zero elements. $\boldsymbol{\Sigma}^+$ is a $n\times m$ matrix. $\boldsymbol{\Sigma}$ and $\boldsymbol{\Sigma}^+$ are denoted by

$$\boldsymbol{\Sigma} = \begin{array}{c} \\ r \\ \\ m-r \end{array} \begin{array}{c} \begin{array}{cc} r & n-r \end{array} \\ \begin{pmatrix} \sigma_1 & & \mathbf{0} & \\ & \ddots & & \mathbf{0} \\ \mathbf{0} & & \sigma_r & \\ & \mathbf{0} & & \mathbf{0} \end{pmatrix} \end{array} \tag{7.3}$$

and

$$\boldsymbol{\Sigma}^+ = \begin{array}{c} \\ r \\ \\ n-r \end{array} \begin{array}{c} \begin{array}{cc} r & m-r \end{array} \\ \begin{pmatrix} \sigma_1^{-1} & & \mathbf{0} & \\ & \ddots & & \mathbf{0} \\ \mathbf{0} & & \sigma_r^{-1} & \\ & \mathbf{0} & & \mathbf{0} \end{pmatrix} \end{array}. \tag{7.4}$$

In (7.3) and (7.4), r denotes the number of the non-zero singular values of $\boldsymbol{J}$ and $\sigma_1 \geq \cdots \geq \sigma_r > 0$. In addition, $rank(\boldsymbol{J}) \leq m$ because $r \leq m$. In the following, we will discuss the

condition that $rank(\boldsymbol{J}) = m$ $(r = m)$. In this way, $\boldsymbol{\Sigma}$ and $\boldsymbol{\Sigma}^+$ can be denoted by

$$\boldsymbol{\Sigma} = \begin{array}{c} \\ m \\ \\ \end{array} \begin{array}{c} \begin{array}{ccc} m & & n-m \end{array} \\ \begin{pmatrix} \sigma_1 & & \mathbf{0} \\ & \ddots & & \mathbf{0} \\ \mathbf{0} & & \sigma_m & \end{pmatrix} \end{array} \tag{7.5}$$

and

$$\boldsymbol{\Sigma}^+ = \begin{array}{c} \\ m \\ \\ n-m \end{array} \begin{array}{c} \begin{array}{ccc} & m & \end{array} \\ \begin{pmatrix} \sigma_1^{-1} & & \mathbf{0} \\ & \ddots & \\ \mathbf{0} & & \sigma_m^{-1} \\ & \mathbf{0} & \end{pmatrix} \end{array}. \tag{7.6}$$

In (7.5) and (7.6), $\sigma_1 \geq \ \cdots \ \geq \sigma_m > 0$.

Generally, $\boldsymbol{V}$ can be defined with the column vectors $\hat{\boldsymbol{v}}_i$ $(i = 1, 2, \cdots, n)$ by

$$\boldsymbol{V} = (\hat{\boldsymbol{v}}_1 \ \ \hat{\boldsymbol{v}}_2 \ \ \cdots \ \ \hat{\boldsymbol{v}}_n). \tag{7.7}$$

In (7.7), these column vectors $\hat{\boldsymbol{v}}_j$ $(j = 1, \cdots, m)$ are obtained by

$$\boldsymbol{J}^T \boldsymbol{J} \hat{\boldsymbol{v}}_j = \hat{\boldsymbol{v}}_j \sigma_j^2 \tag{7.8}$$

and $\boldsymbol{V}$ can be redefined with the row vectors $\check{\boldsymbol{v}}_i$ $(i = 1, 2, \cdots, n)$ by

$$\boldsymbol{V} = \begin{pmatrix} \check{\boldsymbol{v}}_1 \\ \check{\boldsymbol{v}}_2 \\ \vdots \\ \check{\boldsymbol{v}}_n \end{pmatrix}. \tag{7.9}$$

In addition, when $rank(\boldsymbol{J}) = m$, we know that $\boldsymbol{J}$ can be also decomposed by

$$\boldsymbol{J} = \boldsymbol{U}_m \boldsymbol{\Sigma}_m \boldsymbol{V}_m^T \tag{7.10}$$

and $\boldsymbol{J}^+$ can be decomposed by

$$\boldsymbol{J}^+ = \boldsymbol{V}_m \boldsymbol{\Sigma}_m^+ \boldsymbol{U}_m^T. \tag{7.11}$$

In (7.10) and (7.11), $\boldsymbol{U}_m$ is a $m \times m$ matrix satisfying $\boldsymbol{U}_m \boldsymbol{U}_m^T = \boldsymbol{U}_m^T \boldsymbol{U}_m = \boldsymbol{I}_m$, $\boldsymbol{V}_m^T$ is a $m \times n$ matrix satisfying $\boldsymbol{V}_m^T \boldsymbol{V}_m = \boldsymbol{I}_m$, $\boldsymbol{\Sigma}_m$ is a $m \times m$ matrix, which is a diagonal matrix including

m non-zero singular values of $\boldsymbol{J}$. $\boldsymbol{\Sigma}_m^+$ is also a $m \times m$ diagonal matrix. So, $\boldsymbol{\Sigma}_m$ and $\boldsymbol{\Sigma}_m^+$ are denoted by

$$\boldsymbol{\Sigma}_m = \begin{array}{c} \\ m \end{array} \overset{\begin{array}{ccc} m & & \end{array}}{\begin{pmatrix} \sigma_1 & & \mathbf{0} \\ & \ddots & \\ \mathbf{0} & & \sigma_m \end{pmatrix}} \tag{7.12}$$

and

$$\boldsymbol{\Sigma}_m^+ = \begin{array}{c} \\ m \end{array} \overset{\begin{array}{ccc} m & & \end{array}}{\begin{pmatrix} \sigma_1^{-1} & & \mathbf{0} \\ & \ddots & \\ \mathbf{0} & & \sigma_m^{-1} \end{pmatrix}}. \tag{7.13}$$

According to above discussion, we can clearly obtain the relations of $\boldsymbol{U}$ and $\boldsymbol{U}_m$, $\boldsymbol{V}$ and $\boldsymbol{V}_m$, $\boldsymbol{\Sigma}$ and $\boldsymbol{\Sigma}_m$, $\boldsymbol{\Sigma}^+$ and $\boldsymbol{\Sigma}_m^+$ as

$$\boldsymbol{U} = \boldsymbol{U}_m, \tag{7.14}$$

$$\boldsymbol{V} = \begin{pmatrix} \boldsymbol{V}_m & \boldsymbol{V}_{n-m} \end{pmatrix}, \tag{7.15}$$

$$\boldsymbol{\Sigma} = \begin{pmatrix} \boldsymbol{\Sigma}_m & \mathbf{0} \end{pmatrix}, \tag{7.16}$$

$$\boldsymbol{\Sigma}^+ = \begin{pmatrix} \boldsymbol{\Sigma}_m^+ \\ \mathbf{0} \end{pmatrix}. \tag{7.17}$$

In (7.15), $\boldsymbol{V}_m$ is defined using the first m column vectors $\hat{\boldsymbol{v}}_j$ $(j = 1, 2, \cdots, m)$ in (7.7) as

$$\boldsymbol{V}_m = \begin{array}{c} \\ n \end{array} \overset{\begin{array}{ccc} m & & \end{array}}{\begin{pmatrix} \hat{\boldsymbol{v}}_1 & \cdots & \hat{\boldsymbol{v}}_m \end{pmatrix}}, \tag{7.18}$$

$\boldsymbol{V}_m$ is redefined referring to the row vectors $\check{\boldsymbol{v}}_i$ $(i = 1, 2, \cdots, n)$ in (7.9) as

$$\boldsymbol{V}_m = \begin{array}{c} \\ n \end{array} \overset{\begin{array}{c} m \end{array}}{\begin{pmatrix} \check{\boldsymbol{v}}_{1,m} \\ \vdots \\ \check{\boldsymbol{v}}_{n,m} \end{pmatrix}}. \tag{7.19}$$

$\boldsymbol{V}_{n-m}$ is the rest block part of $\boldsymbol{V}$ except $\boldsymbol{V}_m$. So, $\boldsymbol{V}_{n-m}$ can be denoted using the column vectors $\hat{\boldsymbol{v}}_j$ $(j = m+1, \cdots, n)$ in (7.7) as

$$\boldsymbol{V}_{n-m} = (\hat{\boldsymbol{v}}_{m+1} \ \cdots \ \hat{\boldsymbol{v}}_n), \tag{7.20}$$

$\boldsymbol{V}_{n-m}$ can be redenoted referring to the row vectors $\check{\boldsymbol{v}}_i$ $(i = 1, 2, \cdots, n)$ in (7.9) as

$$\boldsymbol{V}_{n-m} = \begin{pmatrix} \check{\boldsymbol{v}}_{1,(n-m)} \\ \vdots \\ \check{\boldsymbol{v}}_{n,(n-m)} \end{pmatrix}. \tag{7.21}$$

We can divide $\boldsymbol{V}_{n-m}$ as

$$\boldsymbol{V}_{n-m} = \begin{matrix} \\ i \\ n-i \end{matrix} \begin{matrix} n-m \\ \begin{pmatrix} \boldsymbol{V}_{i,(n-m)} \\ \boldsymbol{V}_{(n-i),(n-m)} \end{pmatrix} \end{matrix}. \tag{7.22}$$

In (7.22), $\boldsymbol{V}_{i,(n-m)}$ is

$$\boldsymbol{V}_{i,(n-m)} = \begin{matrix} \\ i \end{matrix} \begin{matrix} n-m \\ \begin{pmatrix} \check{\boldsymbol{v}}_{1,(n-m)} \\ \vdots \\ \check{\boldsymbol{v}}_{i,(n-m)} \end{pmatrix} \end{matrix} \tag{7.23}$$

and $\boldsymbol{V}_{(n-i),(n-m)}$ is

$$\boldsymbol{V}_{(n-i),(n-m)} = \begin{matrix} \\ n-i \end{matrix} \begin{matrix} n-m \\ \begin{pmatrix} \check{\boldsymbol{v}}_{(i+1),(n-m)} \\ \vdots \\ \check{\boldsymbol{v}}_{n,(n-m)} \end{pmatrix} \end{matrix}. \tag{7.24}$$

Then, if we divide $\boldsymbol{V}_m$ into two block matrices ($\boldsymbol{V}_{(n-m),m}$ and $\boldsymbol{V}_{m,m}$) and divide $\boldsymbol{V}_{n-m}$ into two block matrices ($\boldsymbol{V}_{(n-m),(n-m)}$ and $\boldsymbol{V}_{m,(n-m)}$). Therefore, $\boldsymbol{V}$ can be redenoted by

$$\begin{aligned} \boldsymbol{V} &= (\boldsymbol{V}_m \ \ \boldsymbol{V}_{n-m}) \\ &= \begin{matrix} \\ n-m \\ m \end{matrix} \begin{matrix} \begin{matrix} m & n-m \end{matrix} \\ \begin{pmatrix} \boldsymbol{V}_{(n-m),m} & \boldsymbol{V}_{(n-m),(n-m)} \\ \boldsymbol{V}_{m,m} & \boldsymbol{V}_{m,(n-m)} \end{pmatrix} \end{matrix} \\ &= \begin{matrix} \\ n-m \\ m \end{matrix} \begin{matrix} \begin{matrix} m & n-m \end{matrix} \\ \begin{pmatrix} \boldsymbol{A} & \boldsymbol{C} \\ \boldsymbol{B} & \boldsymbol{D} \end{pmatrix} \end{matrix}. \end{aligned} \tag{7.25}$$

7.2.2 Avoidance Matrix

Here, we have defined the first avoidance matrix ${}^1\boldsymbol{M}_i$ $(i = 1, 2, \cdots, n-1)$ as (3.6). Here, ${}^1\boldsymbol{M}_i$ is redefined as

$${}^1\boldsymbol{M}_i = \boldsymbol{J}_i \boldsymbol{L}_n, \tag{7.26}$$

where,

$$\boldsymbol{L}_n = \boldsymbol{I}_n - \boldsymbol{J}_n^+ \boldsymbol{J}_n. \tag{7.27}$$

7.2.3 Decomposition of Null Space of end-effector Jacobian

Discussion of $\boldsymbol{J}$ in 7.2.1 can be adopted to $\boldsymbol{J}_n$ in (3.1) since $\boldsymbol{J}_n$ is $m \times n$ matrix. Because $rank(\boldsymbol{J}_n) = m$, then, according to (7.1) and (7.2) and referring to (7.25), $\boldsymbol{L}_n$ can be decomposed by

$$\begin{aligned}
\boldsymbol{L}_n &= \boldsymbol{I}_n - \boldsymbol{J}_n^+ \boldsymbol{J}_n \\
&= \boldsymbol{I}_n - \boldsymbol{V}\boldsymbol{\Sigma}^+ \boldsymbol{U}^T \boldsymbol{U}\boldsymbol{\Sigma}\boldsymbol{V}^T \\
&= \boldsymbol{I}_n - \boldsymbol{V} \begin{array}{c} \\ m \\ n-m \end{array} \begin{array}{c} \begin{array}{cc} m & n-m \end{array} \\ \begin{pmatrix} \boldsymbol{I}_m & \boldsymbol{0} \\ \boldsymbol{0} & \boldsymbol{0} \end{pmatrix} \end{array} \boldsymbol{V}^T \\
&= \boldsymbol{V}\boldsymbol{V}^T - \boldsymbol{V} \begin{array}{c} \\ m \\ n-m \end{array} \begin{array}{c} \begin{array}{cc} m & n-m \end{array} \\ \begin{pmatrix} \boldsymbol{I}_m & \boldsymbol{0} \\ \boldsymbol{0} & \boldsymbol{0} \end{pmatrix} \end{array} \boldsymbol{V}^T \\
&= \boldsymbol{V} \begin{array}{c} \\ m \\ n-m \end{array} \begin{array}{c} \begin{array}{cc} m & n-m \end{array} \\ \begin{pmatrix} \boldsymbol{0} & \boldsymbol{0} \\ \boldsymbol{0} & \boldsymbol{I}_{n-m} \end{pmatrix} \end{array} \boldsymbol{V}^T \\
&= n \begin{array}{c} \begin{array}{cc} m & n-m \end{array} \\ \begin{pmatrix} \boldsymbol{V}_m & \boldsymbol{V}_{n-m} \end{pmatrix} \end{array} \begin{array}{c} \\ m \\ n-m \end{array} \begin{array}{c} \begin{array}{cc} m & n-m \end{array} \\ \begin{pmatrix} \boldsymbol{0} & \boldsymbol{0} \\ \boldsymbol{0} & \boldsymbol{I}_{n-m} \end{pmatrix} \end{array} \boldsymbol{V}^T \\
&= n \begin{array}{c} \begin{array}{cc} m & n-m \end{array} \\ \begin{pmatrix} \boldsymbol{0} & \boldsymbol{V}_{n-m} \end{pmatrix} \end{array} \begin{array}{c} \\ m \\ n-m \end{array} \begin{array}{c} n \\ \begin{pmatrix} \boldsymbol{V}_m^T \\ \boldsymbol{V}_{n-m}^T \end{pmatrix} \end{array} \\
&= n \begin{array}{c} n-m \\ \begin{pmatrix} \boldsymbol{V}_{n-m} \end{pmatrix} \end{array} \quad n-m \begin{array}{c} n \\ \begin{pmatrix} \boldsymbol{V}_{n-m}^T \end{pmatrix} \end{array}.
\end{aligned} \tag{7.28}$$

In (7.28), because $rank(\boldsymbol{V}_{n-m}) = rank(\boldsymbol{V}_{n-m}^T) = n - m$, we can obtain

$$rank(\boldsymbol{L}_n) = n - m. \tag{7.29}$$

7.3 Description of Avoidance Space

Proposition a:

$rank({}^1\boldsymbol{M}_n) = 0$, since ${}^1\boldsymbol{M}_n = \boldsymbol{0}$.

Proposition b:

When $m < n$ and $1 \leq i \leq n-1$, then

$$ {}^1\boldsymbol{M}_i = \tilde{\boldsymbol{J}}_i \boldsymbol{V}_{i,(n-m)} \boldsymbol{V}_{n-m}^T, \tag{7.30} $$

so that

$$ rank(\tilde{\boldsymbol{J}}_i) + rank(\boldsymbol{V}_{i,(n-m)}) - i \leq rank({}^1\boldsymbol{M}_i) \leq $$
$$ min\{rank(\tilde{\boldsymbol{J}}_i), rank(\boldsymbol{V}_{i,(n-m)}), n-m\}. \tag{7.31} $$

Proposition c:

If $rank(\boldsymbol{J}_i) = min\{i, m\}$, then

$$ min\{i,m\} + rank(\boldsymbol{V}_{i,(n-m)}) - i \leq rank({}^1\boldsymbol{M}_i) \leq $$
$$ min\{min\{i,m\}, rank(\boldsymbol{V}_{i,(n-m)}), n-m\}. \tag{7.32} $$

Lemma a:

Firstly, we give the definition of matrix $\boldsymbol{J}_i^{a\to b}$ ($1 \leq i \leq n$ and $1 \leq a \leq b \leq n$). From (2.20), we know that $\boldsymbol{J}_i$ is a $m \times n$ matrix composed of column vectors $\tilde{\boldsymbol{j}}_{ij}$ ($1 \leq j \leq i$) and $\boldsymbol{0}$ as

$$ \boldsymbol{J}_i = [\tilde{\boldsymbol{j}}_{i1}, \cdots, \tilde{\boldsymbol{j}}_{ii},\ \boldsymbol{0}], \tag{7.33} $$

then, $\boldsymbol{J}_i^{a\to b}$ is a $m \times (b-a+1)$ matrix, which only includes the a-th to the b-th column vectors of $\boldsymbol{J}_i$ as

$$ \boldsymbol{J}_i^{a\to b} = [\tilde{\boldsymbol{j}}_{ia}, \cdots, \tilde{\boldsymbol{j}}_{ib}]. \tag{7.34} $$

In this way, $\boldsymbol{J}_n^{n-m+1\to n}$ is defined as a block matrix comprising the last m column vectors sequentially chosen from $\boldsymbol{J}_n$. When $m < n$ and assuming $rank(\boldsymbol{J}_n^{n-m+1\to n}) = m$,

$$ rank(\boldsymbol{V}_{i,(n-m)}) = min\{i, n-m\},\ (1 \leq i \leq n). \tag{7.35} $$

Lemma b:

Assuming $rank(\boldsymbol{J}_n^{n-m+1\to n}) = m$ *and* $rank(\boldsymbol{J}_i) = min\{i, m\}$, *then*

$$min\{i, m\} + min\{i, n-m\} - i \leq rank({}^1\boldsymbol{M}_i) \leq min\{i, m, n-m\}. \tag{7.36}$$

Theorem a:

Given "Part-Non-Singular Configuration Assumption" as

$$\begin{cases} (a). & rank({\boldsymbol{J}_n}^{n-m+1\to n}) = m \\ (b). & rank(\boldsymbol{J}_i) = min\{i, m\} \end{cases},$$
$$(for\ arbitrary\ i\ satisfying\ 1 \leq i \leq n-1; m < n). \tag{7.37}$$

Then, if $n \geq 2m$,

$$rank({}^1\boldsymbol{M}_i) = \begin{cases} i & (1 \leq i < m) \\ m & (m \leq i \leq n-m) \\ n-i{\sim}m & (n-m < i \leq n-1) \end{cases}. \tag{7.38}$$

If $m < n < 2m$,

$$rank({}^1\boldsymbol{M}_i) = \begin{cases} i & (1 \leq i < n-m) \\ n-m & (n-m \leq i \leq m) \\ n-i{\sim}n-m & (m < i \leq n-1) \end{cases}. \tag{7.39}$$

Corollary a:

Given "All-Non-Singular Configuration Assumption" as

$$rank({\boldsymbol{J}_i}^{\nu\to\nu+m-1}) = min\{i, m\},$$
$$(for\ all\ i\ satisfying\ 1 \leq i \leq n; m < n; \nu = max\{i-m+1, 1\}). \tag{7.40}$$

In (7.40), ${\boldsymbol{J}_i}^{\nu\to\nu+m-1}$ *indicates the matrices including the* m *column vectors sequentially chosen from* $\boldsymbol{J}_i$. *Then, the results (7.38) and (7.39) are guaranteed.*

Both the "Part-Non-Singular Configuration Assumption" and "All-Non-Singular Configuration Assumption" can guarantee (7.38) and (7.39) from mathematical viewpoint. Here, we use a simple example shown in Fig.7.1 ($m = 2, n = 4$ and all links are unit in length) to understand their difference about structure of manipulator.

Firstly, shall we consider "Part-Non-Singular Configuration Assumption". Here, we define that $S_1 = sin(q_1)$, $C_1 = cos(q_1)$, $S_{12} = sin(q_1 + q_2)$, $C_{12} = cos(q_1 + q_2)$ and so on.

Firstly, we can calculate

$$\boldsymbol{J}_4 = \begin{bmatrix} -S_1 - S_{12} - S_{123} - S_{1234} & -S_{12} - S_{123} - S_{1234} & -S_{123} - S_{1234} & -S_{1234} \\ C_1 + C_{12} + C_{123} + C_{1234} & C_{12} + C_{123} + C_{1234} & C_{123} + C_{1234} & C_{1234} \end{bmatrix} \tag{7.41}$$

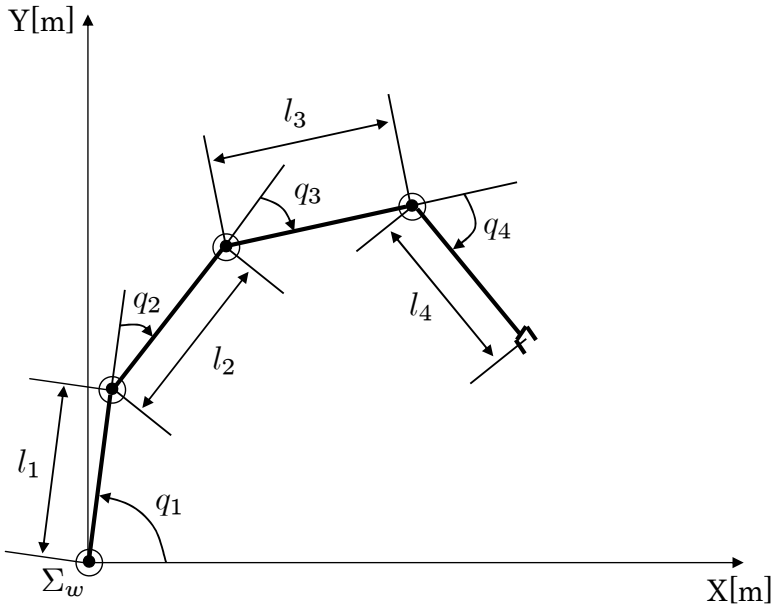

Fig. 7.1: 4-link manipulator in 2-dimensional space

From "(a)" in (7.37), we can obtain

$$rank({\boldsymbol{J}_4}^{3\to4}) = 2, \tag{7.42}$$

where

$${\boldsymbol{J}_4}^{3\to4} = \begin{bmatrix} -S_{123} - S_{1234} & -S_{1234} \\ C_{123} + C_{1234} & C_{1234} \end{bmatrix}. \tag{7.43}$$

If and only if $q_4 \neq 0$, $rank({\boldsymbol{J}_4}^{3\to4}) = 2$.

From "(b)" in (7.37), when $i = 1$, we can obtain

$$rank(\boldsymbol{J}_1) = 1, \tag{7.44}$$

where

$$\boldsymbol{J}_1 = \begin{bmatrix} -sin(q_1) & 0 & 0 & 0 \\ cos(q_1) & 0 & 0 & 0 \end{bmatrix}. \tag{7.45}$$

Whatever q_1 is, always $rank(\boldsymbol{J}_1) = 1$.

When $i = 2$, we can obtain

$$rank(\boldsymbol{J}_2) = 2, \tag{7.46}$$

where

$$\boldsymbol{J}_2 = \begin{bmatrix} -S_1 - S_{12} & -S_{12} & 0 & 0 \\ C_1 + C_{12} & C_{12} & 0 & 0 \end{bmatrix}. \tag{7.47}$$

If and only if $q_2 \neq 0$, $rank(\boldsymbol{J}_2) = 2$.

When $i = 3$, we can obtain

$$rank(\boldsymbol{J}_3) = 2, \tag{7.48}$$

where

$$\boldsymbol{J}_3 = \begin{bmatrix} -S_1 - S_{12} - S_{123} & -S_{12} - S_{123} & -S_{123} & 0 \\ C_1 + C_{12} + C_{123} & C_{12} + C_{123} & C_{123} & 0 \end{bmatrix}. \tag{7.49}$$

Only if $q_2 \neq 0$, whatever q_3 is, $rank(\boldsymbol{J}_3) = 2$.

We can understand the meaning of "Part-Non-Singular Configuration Assumption" about structure of manipulator, $q_2 \neq 0 \cap q_4 \neq 0$, it is not so important whether $q_3 \neq 0$ or not.

Secondly, shall we consider "All-Non-Singular Configuration Assumption".

When $i = 1$, then $\nu = max\{1 - 2 + 1, 1\} = 1$, then assumption in (7.40) will be

$$rank({\boldsymbol{J}_1}^{1\rightarrow 1+2-1}) = min\{1, 2\}, \tag{7.50}$$

that is

$$rank({\boldsymbol{J}_1}^{1\rightarrow 2}) = 1. \tag{7.51}$$

We know that $\boldsymbol{J}_1$ is 2×4 matrix as

$$\boldsymbol{J}_1 = \begin{bmatrix} -S_1 & 0 & 0 & 0 \\ C_1 & 0 & 0 & 0 \end{bmatrix} \tag{7.52}$$

and ${\boldsymbol{J}_1}^{1\rightarrow 2}$ is 2×2 matrix including the first and second column vectors of $\boldsymbol{J}_1$ as

$${\boldsymbol{J}_1}^{1\rightarrow 2} = \begin{bmatrix} -S_1 & 0 \\ C_1 & 0 \end{bmatrix}. \tag{7.53}$$

Whatever q_1 is, always $rank({\boldsymbol{J}_1}^{1\rightarrow 2}) = 1$.

When $i = 2$, then $\nu = max\{2 - 2 + 1, 1\} = 1$, then assumption in (7.40) will be

$$rank({\boldsymbol{J}_2}^{1\rightarrow 1+2-1}) = min\{2, 2\}, \tag{7.54}$$

that is

$$rank({\boldsymbol{J}_2}^{1\rightarrow 2}) = 2. \tag{7.55}$$

We know that $\boldsymbol{J}_2$ is 2×4 matrix as

$$\boldsymbol{J}_2 = \begin{bmatrix} -S_1 - S_{12} & -S_{12} & 0 & 0 \\ C_1 + C_{12} & C_{12} & 0 & 0 \end{bmatrix} \tag{7.56}$$

and ${\boldsymbol{J}_2}^{1\to 2}$ is 2×2 matrix including the first and second column vectors of $\boldsymbol{J}_2$ as

$$ {\boldsymbol{J}_2}^{1\to 2} = \begin{bmatrix} -S_1 - S_{12} & -S_{12} \\ C_1 + C_{12} & C_{12} \end{bmatrix}. \tag{7.57} $$

If and only if $q_2 \neq 0$, $rank({\boldsymbol{J}_2}^{1\to 2}) = 2$.

When $i = 3$, then $\nu = max\{3 - 2 + 1, 1\} = 2$, then assumption in (7.40) will be

$$ rank({\boldsymbol{J}_3}^{2\to 2+2-1}) = min\{3, 2\}, \tag{7.58} $$

that is

$$ rank({\boldsymbol{J}_3}^{2\to 3}) = 2. \tag{7.59} $$

We know that $\boldsymbol{J}_3$ is 2×4 matrix as

$$ \boldsymbol{J}_3 = \begin{bmatrix} -S_1 - S_{12} - S_{123} & -S_{12} - S_{123} & -S_{123} & 0 \\ C_1 + C_{12} + C_{123} & C_{12} + C_{123} & C_{123} & 0 \end{bmatrix} \tag{7.60} $$

and ${\boldsymbol{J}_3}^{2\to 3}$ is 2×2 matrix including the second and third column vectors of $\boldsymbol{J}_3$ as

$$ {\boldsymbol{J}_3}^{2\to 3} = \begin{bmatrix} -S_{12} - S_{123} & -S_{123} \\ C_{12} + C_{123} & C_{123} \end{bmatrix}. \tag{7.61} $$

If and only if $q_3 \neq 0$, $rank({\boldsymbol{J}_3}^{2\to 3}) = 2$.

When $i = 4$, then $\nu = max\{4 - 2 + 1, 1\} = 3$, then assumption in (7.40) will be

$$ rank({\boldsymbol{J}_4}^{3\to 3+2-1}) = min\{4, 2\}, \tag{7.62} $$

that is

$$ rank({\boldsymbol{J}_4}^{3\to 4}) = 2. \tag{7.63} $$

We know that $\boldsymbol{J}_4$ is 2×4 matrix as shown in (7.41) and ${\boldsymbol{J}_4}^{3\to 4}$ is 2×2 matrix including the third and fourth column vectors of $\boldsymbol{J}_4$ as

$$ {\boldsymbol{J}_4}^{3\to 4} = \begin{bmatrix} -S_{123} - S_{1234} & -S_{1234} \\ C_{123} + C_{1234} & C_{1234} \end{bmatrix}. \tag{7.64} $$

If and only if $q_4 \neq 0$, $rank({\boldsymbol{J}_4}^{3\to 4}) = 2$.

We can understand the meaning of "All-Non-Singular Configuration Assumption" about structure of manipulator, $q_2 \neq 0 \cap q_3 \neq 0 \cap q_4 \neq 0$, that is "Non-Singular" in each joint.

Therefore, we can obtain the conclusion according to above discussion. On the one hand, the former is lower than the latter in the consideration of restriction degree of assumptions

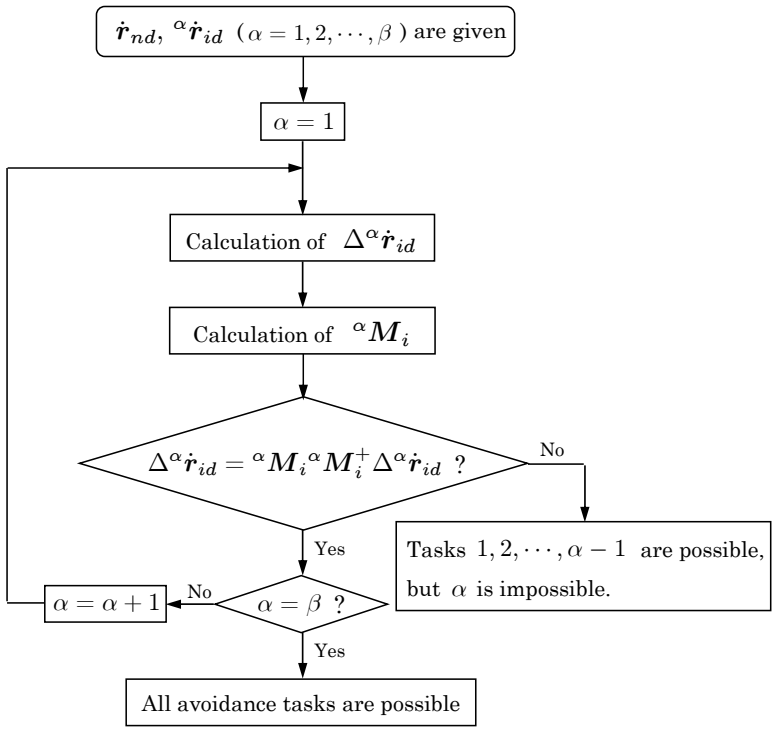

Fig. 7.2: Flow chart of judgment of avoidance possibility

themselves. On the other hand, the former is wider than the latter in the consideration of their availability.

The detailed proof is shown in "Appendix" including proofs of "**Propositions a, b, c**", "**Lemmas a, b**" and "**Theorem a**".

7.4 Avoidance Motion

7.4.1 Judgment of Avoidance Possibility

As discussed in chapter 3, under the condition that the avoidance manipulability ellipsoid of the i-th link is ${}^{1C}P_i$ expressed in (3.10) with $rank({}^1\boldsymbol{M}_i) = m$, $\Delta^1\dot{\boldsymbol{r}}_{id}$ can be realized in m-dimensional space. Under the condition that the avoidance manipulability ellipsoid of the i-th link is ${}^{1P}P_i$ expressed in (3.11) with $rank({}^1\boldsymbol{M}_i) = p$, $\Delta^1\dot{\boldsymbol{r}}^{*}_{id}$ can be realized in p-dimensional space.

Here, we show judgment sequence by a flow chart shown in Fig.7.2 when β avoidance tasks are demanded. i denotes the number of link, $\alpha(\alpha = 1, 2, \cdots, \beta)$ denotes the priority order of avoidance tasks, ${}^{\alpha}\dot{\boldsymbol{r}}_{id}$ means the demanded avoidance velocity for the i-th link as the α-th avoidance task. According to Fig.7.2, whether ${}^{\alpha}\dot{\boldsymbol{r}}_{id}$ and end-effector velocity $\dot{\boldsymbol{r}}_{nd}$ are

both realized or not can be judged through $\Delta^{\alpha}\dot{\boldsymbol{r}}_{id}$ recurrently.

7.4.2 Judgment of Stoppage Possibility

Corollary b:

For intermediate links, the simplest avoidance behavior is to stop their movement. Assumming the first demanded avoidance velocity ${}^{1}\dot{\boldsymbol{r}}_{id}$ *in (3.5) is given as* ${}^{1}\dot{\boldsymbol{r}}_{id} = 0$*, that is* $\Delta^{1}\dot{\boldsymbol{r}}_{id} = -\boldsymbol{J}_i\boldsymbol{J}_n^{+}\dot{\boldsymbol{r}}_{nd}$*. Then for* $\forall\dot{\boldsymbol{r}}_{nd} \in R^m$*, admits* ${}^{1}\boldsymbol{l} \in R^n$ *such that* $\Delta^{1}\dot{\boldsymbol{r}}_{id} = {}^{1}\boldsymbol{M}_i{}^{1}\boldsymbol{l}$ *if and only if*

$$\boldsymbol{J}_i\boldsymbol{J}_n^{+} = {}^{1}\boldsymbol{M}_i{}^{1}\boldsymbol{M}_i^{+}\boldsymbol{J}_i\boldsymbol{J}_n^{+}. \tag{7.65}$$

If we consider the case of $n - m < i \leq n$, the number of remaining links, i.e., from the $(n - m + 1)$-th link to n-th link, is $m - 1$ and the dimensional number being realized by remaining links is less than m. Then, the realizable DoF of the remaining links becomes insufficient to keep the manipulator's end-effector desired trajectory $\dot{\boldsymbol{r}}_{nd}$ in m-dimensional space. So, discussing the stopping possibility of links within $n-m < i \leq n$ is out of the extent of prerequisite condition of arbitrarily given end-effector trajectory $\boldsymbol{r}_{nd}$ and $\dot{\boldsymbol{r}}_{nd}$. Hence, here we think that the intermediate links satisfying $1 \leq i \leq n - m$ are possible to be stopped.

Corollary c:

As for redundant manipulator satisfying that $m < n$*, assuming "Part-Non-Singular Configuration Assumption" or "All-Non-Singular Configuration Assumption" for all* i *satisfying* $1 \leq i \leq n - m$*. Then the intermediate links satisfying* $1 \leq i \leq n - m$ *can be stopped as the simplest avoidance behavior while the manipulator's end-effector tracks the desired trajectory.*

7.5 Examples

7.5.1 Comparison of Manipulability and Avoidance Manipulability

Taking a 4-link redundant manipulator ($n = 4$) in 2-dimensional space ($m = m_p = 2$) for example shown in Fig.7.1, whose kinematics can be defined by $\underline{\boldsymbol{U}}_m$ of (2.19) after deleting the third row vector, thus $\underline{\boldsymbol{U}}_m$ becomes 2×6 matrix as $\begin{pmatrix} 1 & 0 & 0 & 0 & 0 & 0 \\ 0 & 1 & 0 & 0 & 0 & 0 \end{pmatrix}$. The definition of the kinematics of the manipulators used in this subsection follows the example shown in page 250 of [36] written by Yoshikawa. The origin of the working coordinate system Σ_w is fixed at the root of the first link. The joint angles, q_i ($i = 1, 2, 3, 4$ and unit is $[rad]$), are

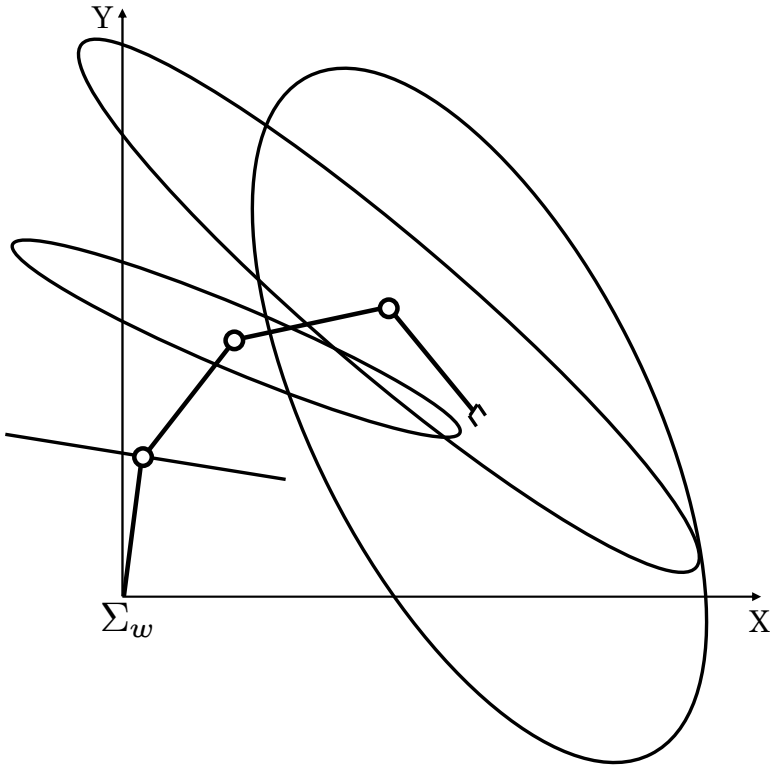

Fig. 7.3: Manipulability ellipsoids

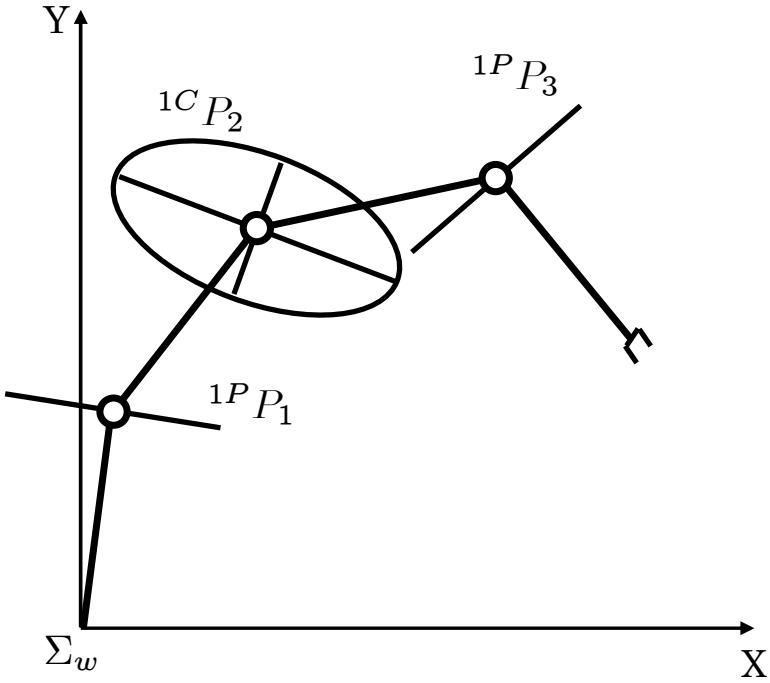

Fig. 7.4: Avoidance manipulability ellipsoids

denoted along each rotational axis as counterclockwise direction is positive. All links are 0.25 in length (unit is $[m]$).

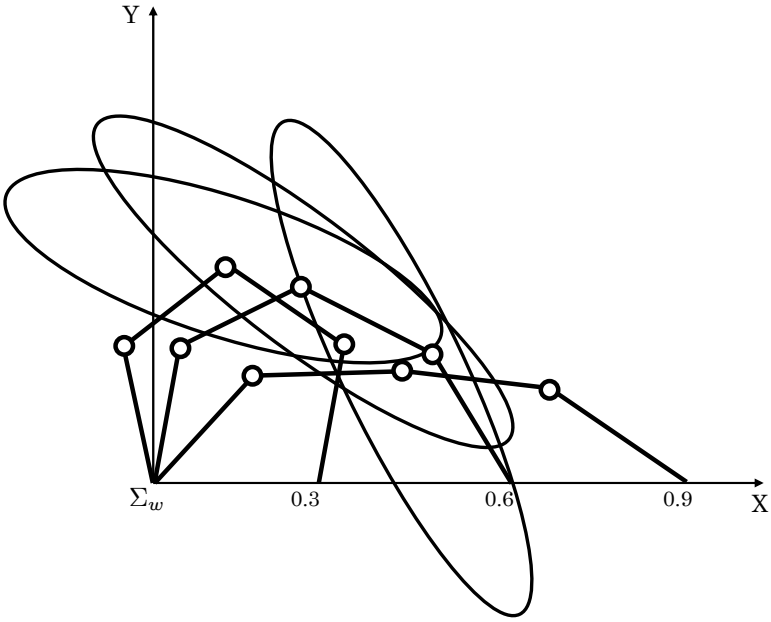

Fig. 7.5: Manipulability ellipsoid of the second link

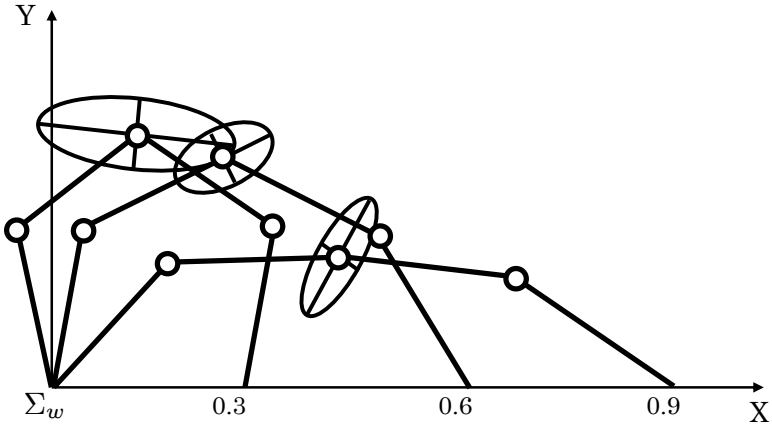

Fig. 7.6: Avoidance manipulability ellipsoid of the second link

When the manipulator's end-effector position is fixed at $\boldsymbol{r}_{4d} = (0.6, 0.3)$, the joint angles are confirmed as $q_1 = 1.396$, $q_2 = -0.524$, $q_3 = -0.631$ and $q_4 = -1.153$ respectively. In this given configuration, the manipulability ellipsoids and the avoidance manipulability ellipsoids are shown in Fig.7.3 and Fig.7.4 respectively. From Fig.7.3, we can find that the size of manipulability ellipsoids become bigger and bigger as the link order increases. However, from Fig.7.4, the avoidance manipulability ellipsoids corresponding to the first and the third links ($^{1P}P_1$ and $^{1P}P_3$) are denoted by two lines, which can be thought as segment of ellipsoid. The avoidance manipulability ellipsoid corresponding to the second link ($^{1C}P_2$) is complete ellipsoid in 2-dimensional space. By comparing Fig.7.3 with Fig.7.4, we can find that the

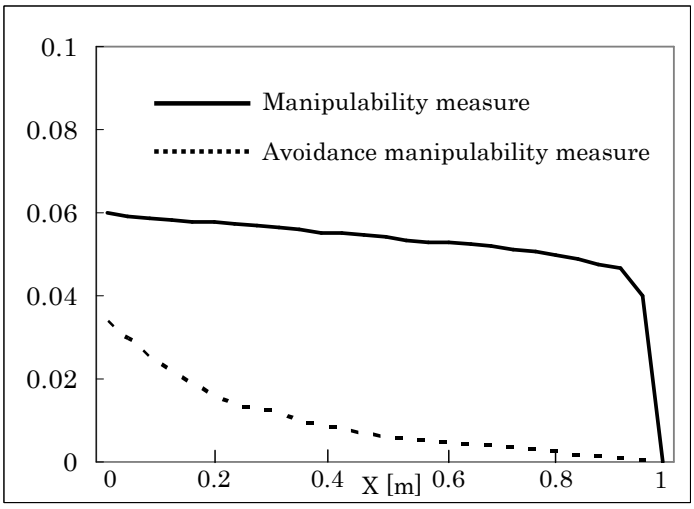

Fig. 7.7: Manipulability measure/avoidance manipulability measure

size of the avoidance manipulability ellipsoids does not spread according to the increment of the link order, which completely differs from the manipulability ellipsoids. Moreover, the size of each avoidance manipulability ellipsoid is smaller than the corresponding size of manipulability ellipsoid because the singular values of ${}^1\boldsymbol{M}_i$ are smaller than the ones of $\boldsymbol{J}_i$.

If the manipulator's end-effector position $\boldsymbol{r}_{4d}$ is designated at three different positions on the x-axis, as $(0.3, 0.0)$, $(0.6, 0.0)$, $(0.9, 0.0)$. The first configuration of manipulator is that $q_1 = 1.745$, $q_2 = -1.047$, $q_3 = -1.393$ and $q_4 = -1.037$. Fig.7.5 and Fig.7.6 show the manipulability ellipsoids and the avoidance manipulability ellipsoids of the second link when the manipulator's end-effector is fixed at these three different positions respectively. By comparing Fig.7.5 with Fig.7.6, we can see that the size of manipulability ellipsoid does not change so much, adversely, the size of avoidance manipulability ellipsoid changes remarkably. If we evaluate the manipulability measure and the avoidance manipulability measure by the sum of their ellipsoid areas. Fig.7.7 shows the change of manipulability measure and avoidance manipulability measure of the second link as the manipulator's end-effector position changes from $(0.0, 0.0)$ to $(1.0, 0.0)$ in x-axis, here please notice that manipulability measure [36] and avoidance manipulability measure [28] are evaluated by the area of manipulability ellipsoid and avoidance manipulability ellipsoid. From Fig.7.7, we find that the second link can keep the high manipulability measure in the whole moving extent. However, the avoidance manipulability measure of the second link decreases quickly as the manipulator's end-effector

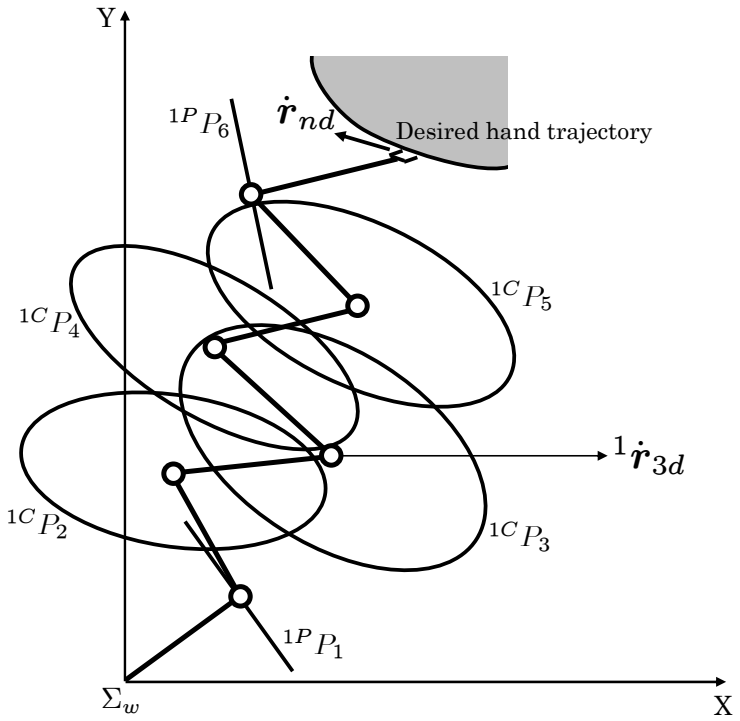

Fig. 7.8: First avoidance manipulability ellipsoids

position is far away the root of the first link, which indicates that it is better to make the manipulator's end-effector do something such as trajectory tracking or obstacle avoidance near the root of the first link for keep higher avoidance manipulability measure.

7.5.2 Comparison of Consecutive Avoidance Manipulability

Here, we use an 7-link manipulator in 2-dimensional space as an example to analyze the avoidance manipulability ellipsoid when the manipulator deals with plural avoidance tasks. The manipulator's configuration is that $q_1 = 0.698$, $q_2 = 1.396$, $q_3 = -1.920$, $q_4 = 2.094$, $q_5 = -1.920$, $q_6 = 1.745$ and $q_7 = -1.745$. All links are 0.2 in length. In this configuration, Fig.7.8 shows the first avoidance manipulability ellipsoids as ^1P_i $(i = 1, \cdots, 6)$. When the arbitrary first avoidance task (the first demanded avoidance velocity $^1\dot{\boldsymbol{r}}_{3d}$) is given to the third link, there exists the corresponding first avoidance velocity $\Delta^1\dot{\boldsymbol{r}}_{3d}$ in 2-dimensional space because $rank(^1\boldsymbol{M}_3) = 2$.

After $^1\dot{\boldsymbol{r}}_{3d}$ is realized, the second avoidance manipulability ellipsoids are shown in Fig.7.9 as ^2P_j $(j = 1, 2, 4, 5, 6)$. By comparing ^1P_i with ^2P_j, we can find that $^{2P}P_1$ and $^{2P}P_6$ are shorter than $^{1P}P_1$ and $^{1P}P_6$. Moreover, $^{2P}P_2$ and $^{2P}P_4$ become the partial avoidance

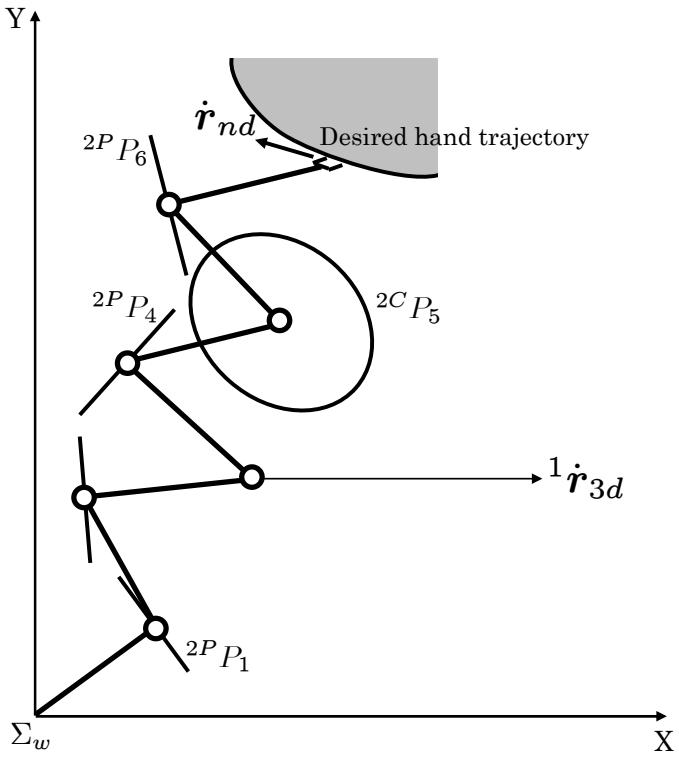

Fig. 7.9: Second avoidance manipulability ellipsoids

manipulability ellipsoids. The reason is that the given ${}^{1}\dot{\boldsymbol{r}}_{3d}$ has the effect of making the tips of the second and fourth links just move along one direction around the tip of the third link. ${}^{2C}P_5$ is still the complete avoidance manipulability ellipsoid, however the size of ${}^{2C}P_5$ is smaller than ${}^{1C}P_5$ because the singular values of ${}^{2}\boldsymbol{M}_5$ are smaller that the ones of ${}^{1}\boldsymbol{M}_5$. When we consider the second avoidance manipulability ellipsoids, $rank({}^{2}\boldsymbol{M}_j) = 1$ $(j = 1, 2, 4, 6)$ and $rank({}^{2}\boldsymbol{M}_5) = 2$, which indicates that only the tip of the fifth link can arbitrarily realize the second avoidance velocity in 2-dimensional space, the tips of the other links can realize the second velocity along one direction. For example, when we consider the fourth link, we can calculate the second avoidance matrix of the fourth link ${}^{2}\boldsymbol{M}_4$ with $rank({}^{2}\boldsymbol{M}_4) = 1$, and we can calculate ${}^{2}\boldsymbol{M}_4^{+}$ from (7.2), then we can calculate

$$ {}^{2}\boldsymbol{M}_4 {}^{2}\boldsymbol{M}_4^{+} = \begin{pmatrix} 0.586824 & 0.492404 \\ 0.492404 & 0.413176 \end{pmatrix} \neq \boldsymbol{I}_2. \tag{7.66} $$

According to (3.11), we can find that the second avoidance velocity of the fourth link can be realized along only one direction as

$$ \Delta {}^{2}\dot{\boldsymbol{r}}_{4d}^{*} = \begin{pmatrix} 0.586824 & 0.492404 \\ 0.492404 & 0.413176 \end{pmatrix} \boldsymbol{P},\ \boldsymbol{P} \in R^m. \tag{7.67} $$

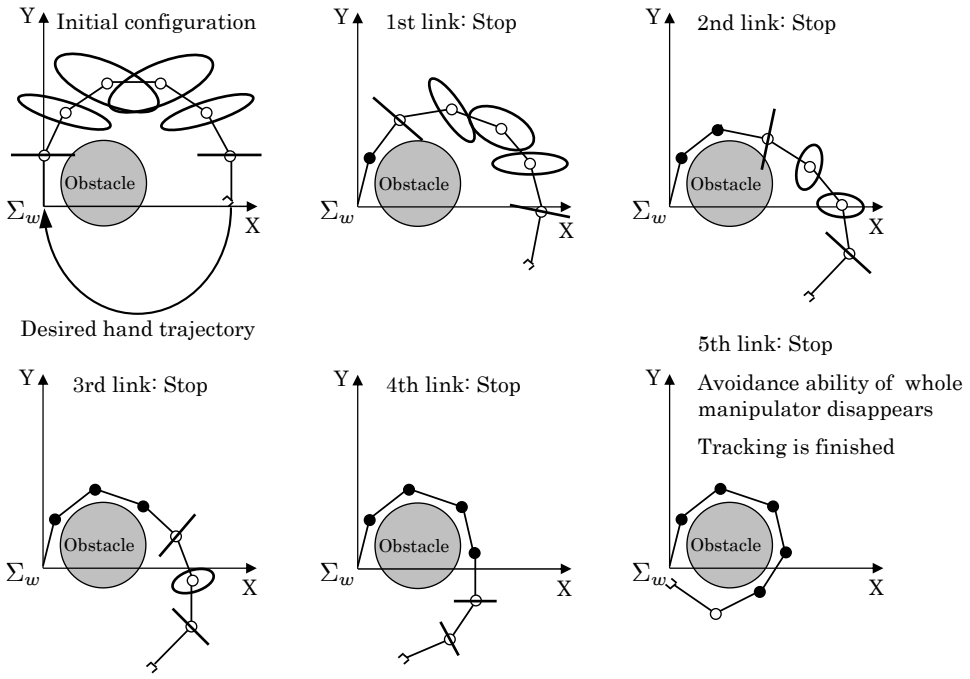

Fig. 7.10: Stoppage operation process 1

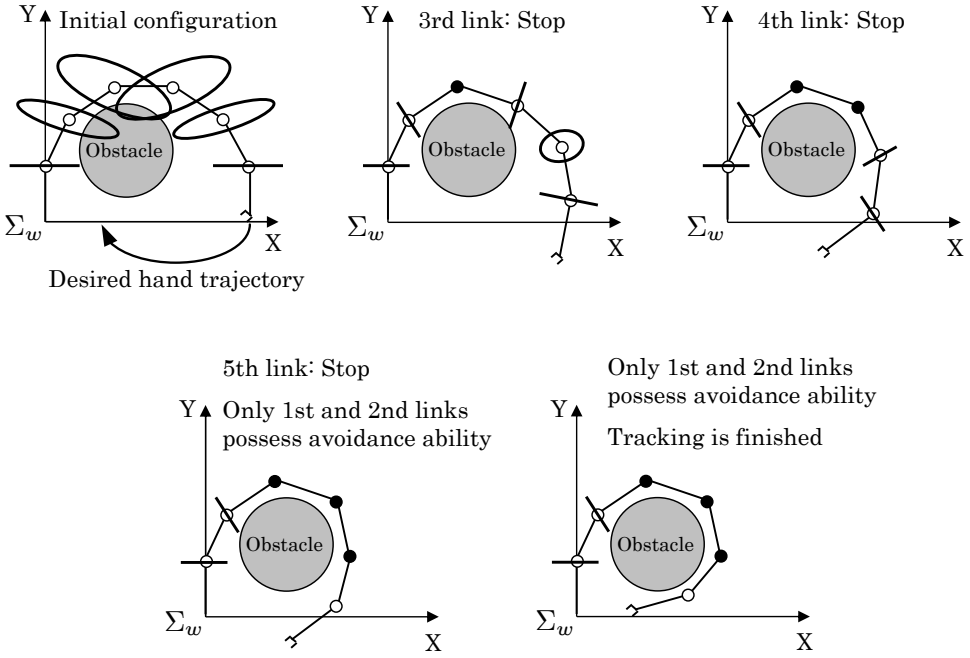

Fig. 7.11: Stoppage operation process 2

This example shows that it is impossible to arbitrarily realize the second avoidance velocity of the tip of the fourth link in 2-dimensional space. The second avoidance velocity of the tip of the fourth link just can realize along with the direction of ${}^{2P}P_4$, which is described by the partial avoidance manipulability ellipsoid.

7.5.3 Stoppage of Intermediate Links

Fig.7.10 and Fig.7.11 show the changing processes of the avoidance manipulability ellipsoids when a 7-link manipulator tracks the desired trajectory and avoids a circular obstacle in 2-dimensional space. The initial configuration is that $q_1 = 1.57$, $q_2 = -0.532$, $q_3 = -0.532$, $q_4 = -0.532$, $q_5 = -0.532$, $q_6 = -0.532$ and $q_7 = -0.532$, where this initial configuration satisfies "All-Non-Singular Configuration Assumption" given by (7.40). All links are 0.2 in length. The shape of obstacle is a circle with radius of $r = 0.19[m]$ shown in Fig.7.10, the center of obstacle is fixed at $(0.25, 0.10)$. In Fig.7.11, the center of obstacle is fixed at $(0.31, 0.25)$. In the process of trajectory tracking of the manipulator's end-effector, the i-th link will be stopped (the demanded avoidance velocity is zero discussed in subsection 7.4) for avoiding the collision with the obstacle once the distance between the tip of the i-th link $\boldsymbol{r}_i$ and the center of the obstacle is less than $1.25r$.

From Fig.7.10, in the process of trajectory tracking and obstacle avoidance, the tip of the first link is stopped when it nears the obstacle, that is to say, the first demanded avoidance velocity ${}^1\dot{\boldsymbol{r}}_{d1} = 0$ is realized (the first avoidance task is finished). Then, the sizes of the second avoidance ellipsoids change after finishing the first avoidance task. The second avoidance ellipsoid of the second link becomes a segment, and the others become smaller. In this way, the manipulator can execute the second (${}^2\dot{\boldsymbol{r}}_{2d} = 0$), third (${}^3\dot{\boldsymbol{r}}_{3d} = 0$), fourth (${}^4\dot{\boldsymbol{r}}_{4d} = 0$) and fifth demanded avoidance velocity (${}^5\dot{\boldsymbol{r}}_{5d} = 0$) in sequence. The changed sizes of the avoidance ellipsoids become segment or smaller after finishing the current avoidance task. Finally, the manipulator finish the desired trajectory tracking and obstacle avoidance, however, the avoidance ability of whole manipulator disappears and it can not continue to track trajectory and avoid obstacle simultaneously after these five demanded avoidance velocities have been realized (these five avoidance tasks are finished) because redundancy has disappeared. This specific example in Fig.7.10 just verifies "**Corollary c**".

In Fig.7.11, in the process of trajectory tracking and obstacle avoidance, the first avoidance task (${}^1\dot{\boldsymbol{r}}_{3d} = 0$) is given to the tip of the third link. After finishing this first avoidance task, the second avoidance ellipsoids become smaller, especially, the second avoidance ellipsoids of the second and fourth links become segments. Then, the second and third avoidance tasks

are given to the fourth and fifth links respectively, that is, ${}^{2}\dot{\boldsymbol{r}}_{4d} = 0$ and ${}^{3}\dot{\boldsymbol{r}}_{5d} = 0$. Finally, the manipulator finish the desired trajectory tracking and obstacle avoidance, it can not continue to track trajectory and avoid obstacle simultaneously after these three avoidance tasks are finished. However, the first and second links still possess the avoidance ability in Fig.7.11. This is the difference between Fig.7.10 and Fig.7.11.

8 General Discussion

In our previous works, the concept of avoidance manipulability was presented by referring to the concept of manipulability. The avoidance manipulability ellipsoid was presented as the evaluation of avoidance manipulability. AMSI was proposed as an index to optimize the avoidance manipulability of the whole manipulator. AMSIP was proposed to improve AMSI as an index to optimize the avoidance manipulability considering the distance between the manipulator and obstacle. Single preview control and 1-step GA were combined to use for on-line control system, where the redundant manipulator can on-line finish the tasks of trajectory tracking and obstacle avoidance with higher avoidance manipulability.

As for my contribution in this docotor thesis, I presented multiple preview control for improving single preview control. On the one hand, preview control concept includes unique idea as it utilizes future information to control current configuration. Single preview is a classic local method, by which the detected future information is still limited, so sometimes the system can not work safely by hazardous collision because of natural defect of local method although it is suitable for on-line system. On the other hand, path planning is only suitable for off-line system as a classic global method on the assumption of stationary environment. Multiple preview can improve the limitation of single preview through detecting the more future information. Multiple preview possesses their merits, on-line and non-collision. I discussed its effectiveness through simulations among multiple preview, single preview and path planning. Further, I verified the effectiveness of the presented on-line control system by simulation and experiment of real machine "PA10". In addition, I proposed the sufficient conditions that can guarantee mathematically the sustainability of the avoidance space of intermediate links by non-singular decomposition analyses of the first avoidance matrix ${}^{1}\boldsymbol{M}_{i}$.

However, there are remaining problems need to be solved in my current research. Firstly, sustainability of the plural avoidance space by non-singular decomposition analyses of plural avoidance matrices such as ${}^{2}\boldsymbol{M}_{j}$, ${}^{3}\boldsymbol{M}_{k}$ and so on. Secondly, solution of self-collision problem

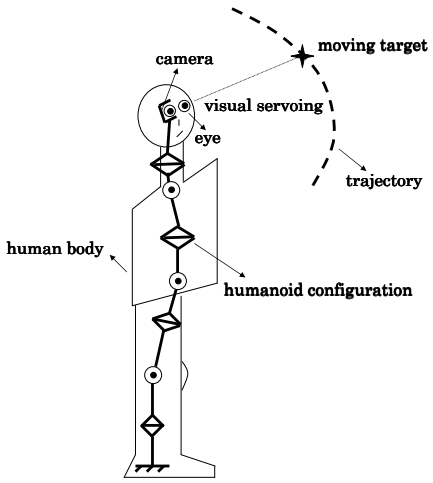

Fig. 8.1: Humanoid robot with visual servoing system

by adding the constraint conditions.

The concept of avoidance manipulability is main contribution in my current research, by which on-line control system of trajectory tracking and obstacle avoidance was designed. However, The current proposed work is not only applied to the on-line avoidance of obstacles for redundant manipulators following a specified end-effector path. We should potentially improve our perspectives, or lead to more impressive examples such as humanoid robotics as a potential application. So, "Reconfiguration Manipulability" is more suitable for embodying our idea than "Avoidance Manipulability".

Here, we will conceptually introduce the reconfiguration manipulability into the application of humanoid robot as an example. As shown in Fig.8.1, it is a humanoid robot with visual servoing system. The whole body of humanoid robot, from the foots to the head, can be described by a redundant manipulator. The foots touch the ground and are fixed at the base coordinate. The head may be thought to represent the end-effector of the redundant manipulator. Especially, the robot's eyes are used as visual servoing system by installing a camera or several ones. Humanoid robot mainly has two kinds of tasks. On the one hand, visual servoing system is used for executing the prior end-effector task, by which the camera can on-line track moving target to keep its head's pose as required. On the other hand, some appropriate shape-adjustments of the body by controlling the motion of the intermediate links for keeping the stability of humanoid robot are thought to be reconfiguration subtasks.

According to above discussion, the possibility of stabilizing control as the secondary sub-

tasks can be described in the reconfiguration space and restricted strictly in the range space of ${}^{1}\boldsymbol{M}_{i}$, which is the main result of this research. Therefore, based on the sufficient conditions to keep the expansion of the reconfiguration space, the dimension of the stabilizing motion of the humanoid robot can be maintained by "Part-Non-Singular Configuration Assumption" or "All-Non-Singular Configuration Assumption", since it guarantees the sustainability of stabilizing motion.

9 Conclusion

In this research, for simultaneously solving the problems of real-time trajectory tracking and obstacle avoidance for an unknown object, it is necessary and important to always keep high avoidance manipulability of the manipulator as much as possible when the manipulator's end-effector tracks the desired trajectory. Therefore, a new definition "AMSI" (Avoidance Manipulability Shape Index) as an index being able to evaluate the avoidance manipulability of the whole manipulator is presented. And "AMSIP" (AMSI with Potential) is presented as the optimal evaluation considering both avoidance manipulability ("AMSI") and potential (judging the distance between the manipulator and the target object). By combining preview control and 1-step GA, the effectiveness of real-time optimization of manipulator's configuration based on "AMSIP" is verified by simulations. Moreover, by comparing multiple preview control with single preview control, we can think that multiple preview control is gifted with both merits of single-preview control and path planning.

In addition, we analyzed the avoidance matrix and the avoidance manipulability ellipsoid. We discussed the possibility of realizing avoidance tasks. Moreover, we found the assumptions of manipulator's shape to determine explicitly and guarantee the sustainability of shape-changeable space. Further we have also proposed avoidance manipulability measure to evaluate shape-changeability of manipulator, which will be useful in control of trajectory tracking and obstacle avoidance for redundant manipulator in future research as a theoretical guidance.

REFERENCE

[1] Sanjeev Seereeram and John T., "A Global Approach to Path Planning for Redundant Manipulators", *IEEE Transactions on Robotics and Automation*, Vol.11, No.1, pp.152-160, 1995.

[2] Akira Mohri, DongXiang Yang and Motoji Yamamoto, "Collision Free Trajectory Planning for Manipulator Using Potential Function", *IEEE International Conference on Robotics and Automation*, Vol.3, pp.3069-3074, 1995.

[3] Shugen M. and Watanabe M., "Minimum time path-tracking control of redundant manipulators", *International Conference on Intelligent Robots and Systems*, Takamatsu, Vol.1, pp.27-32, 2000.

[4] Rodrigo S. Jamisola, Jr. Anthony A. Maciejewski and Rodney G. Roberts, "Failure-Tolerant Path Planning for Kinematically Redundant Manipulators Anticipating Locked-Joint Failures", *IEEE Transactions on Robotics*, Vol.22, No.4, pp.603-612, 2006.

[5] Jaesik Choi and Eyal Amir, "Factor-Guided Motion Planning for a Robot Arm", *International Conference on Intelligent Robots and Systems*, San Diego, pp.27-32, 2007.

[6] Juan Manuel Ahuactzin and Kamal K. Gupta, "The Kinematic Roadmap: A Motion Planning Based Global Approach for Inverse Kinematics of Redundant Robots", *Transactions on Robotics and Automation*, Vol.15, No.4, pp.653-669, 1999.

[7] Nagatani k, Hirayama T, Gofuku A and Tanaka Y, "Motion planning for mobile manipulator with keeping manipulability", *Proceedings of IEEE/RSJ International Conference on Intelligent Robots and Systems*, Lausanne, Vol.2, pp.1663-1668, 2002.

[8] Glass K., Colbaugh R., Lim D. and Seraji H, "Real-time collision avoidance for redundant manipulators", *IEEE Transactions on Robotics and Automation*, Vol.11, pp.448-457, 1995.

[9] Homayoun Seraji and Bruce Bon, "Real-Time Collision Avoidance for Position-Controlled Manipulators", *IEEE Transactions on Robotics and Automation*, Vol.15, No.4, pp.670-677, 1999.

[10] Leon Zlajpah and Bojan Nemec, "Kinematic Control Algorithms for On-line Obstacle Avoidance for Redundant Manipulator", *International Conference on Intelligent Robots and Systems*, Lausanne, Vol.2, pp.1898-1903, 2002.

[11] Kwang-Kyu Lee and Martin Buss, "Obstacle Avoidance for Redundant Robots Using Jacobian Transpose Method", *International Conference on Intelligent Robots and Systems*, San Diego, pp.3509-3514, 2007.

[12] Marani G and Jinhyun Kim, "A real-time approach for singularity avoidance in resolved motion rate control of robotic manipulator", *Proceedings of IEEE/RSJ International Conference on Robotics and Automation*, Washington, Vol.2, pp.1973-1978, 2002.

[13] Tsuneo Yoshikawa, "Measure of Manipulability for Robot Manipulators", (in Japanese) *Journal of the Robotics Society of Japan*, Vol.2, No.1, pp.63-71, 1984.

[14] Tsuneo Yoshikawa, "Manipulability of Robot Mechanisms", *The International Journal of Robotics Research*, Vol.4, No.2, pp.3-9, 1985.

[15] Anthony A.Maciejewski and Charles A.Klein, "Obstacle Avoidance for Kinematically Redundant Manipulators in Dynamically Varying Environments", *The International Journal of Robotics Research*, Vol.4, No.3, pp.109-117, 1985.

[16] Yoshihiko Nakamura, Hideo Hanafusa and Tsuneo Yoshikawa, "Task-Priority Based Redundancy Control of Robot Manipulators", *The International Journal of Robotics Research*, Vol.6, No.2, pp.3-15, 1987.

[17] S. Lee, "Dual Redundant Arm Configuration Optimization with Task-oriented Dual Arm Manipulability", *IEEE Transactions on Robotics and Automation*, Vol.5, No.1, pp.78-97, 1989.

[18] P. Chiaccho, S. Chiaverini, L. Sciavicco and B. Siciliano, "Global Task Space Manipulability Ellipsoids for Multiple-Arm System", *IEEE Transactions on Robotics and Automation*, Vol.7, No.5, pp.678-685, 1991.

[19] A. Bicchi, C. Melchiorri and D. Balluchi, "On the Mobility and Manipulability of General Multiple Limb Robots", *IEEE Transactions on Robotics and Automation*, Vol.11, No.2, pp.215-228, 1995.

[20] Ralf Koeppe and Tsuneo Yoshikawa, "Dynamic Manipulability Analysis of Compliant Motion", *Proceedings of IEEE/RSJ International Conference on Intelligent Robots and Systems*, Grenoble, vol.3, pp.1472-1478, 1997.

[21] Tsuneo Yoshikawa, "Dynamic Manipulability of Robot Manipulators", *IEEE International Conference on Robotics and Automation*, Vol.2, pp.1033-1038, 1985.

[22] Ryo Kurazume and Tsutomu Hasegawa, "Impedance Matching for Free Flying Robots", (in Japanese) *Proc. 20th Annu. Conf. Robot. Soc. Jpn.*, p. 3J16, 2002.

[23] Ryo Kurazume and Tsutomu Hasegawa, "A New Index of Serial-Link Manipulator Performance Combining Dynamic Manipulability and Manipulating Force Ellipsoid", *IEEE Transactions on Robotics*, Vol.22, No.5, pp.1022-1028, 2006.

[24] Alan Bowling and Oussama Khatib, "The Dynamic Capability Equations: A New Tool for Analyzing Robotic Manipulator Performance", *IEEE Transactions on Robotics*, Vol.21, No.1, pp.115-123, 2005.

[25] Mamoru Minami, Hitoshi Takagi and Toshiyuki Asakura, "Trajectory Tracking and Obstacle Avoidance Control to Unknown Objects for Redundant Manipulators Utilizing Preview Control", (in Japanese), *Transactions of the Japan Society of Mechanical Engineers*, Vol.64, No.621, pp.1749-1756, 1998.

[26] Mamoru Minami, Yoshihiro Nomura and Toshiyuki Asakura, "Preview and Postview Control System for Tajectry Tracking and Obstacle Avoidance to Unknown Objects for Redundant Manipulators", (in Japanese), *Journal of the robotics Society of Japan*, Vol.15, No.4, pp.573-580, 1997.

[27] Mamoru Minami, Yoshihiro Nomura and Toshiyuki Asakura, "Avoidance Manipulability for Redundant Manipulators", (in Japanese), *Journal of the Robotics Society of Japan*, Vol.17, No.6, pp.887-895, 1999.

[28] Hiroshi Tanaka, Mamoru Minami and Yasushi Mae, "Trajectory Tracking of Redundant Manipulators Based on Avoidance Manipulability Shape Index", *Proceedings of IEEE/RSJ International Conference on Intelligent Robots and Systems*, Edmonton, pp.1892-1897, 2005.

[29] Homayoun Seraji, "Configuration Control of Redundant Manipulators: Theory and Implementation", *IEEE Transactions on Robotics and Automation*, Vol.5, No.4, pp.472-490, 1989.

[30] Hidekazu Suzuki and Mamoru Minami, "Visual Servoing to Catch Fish Using Global/Local GA Search", *IEEE/ASME Transactions on Mechatronics*, Vol.10, No.3, pp.352-357, 2005.

[31] Bruno Siciliano and Jean-Jacques E. Slotine, "A General Framework for Managing Multiple Tasks in Highly Redundant Robotic Systems", *Fifth International Conference on Advanced Robotics*, Vol.2, pp.1211-1216, 1991.

[32] Keiji Ikeda, Hiroshi Tanaka, Tongxiao Zhang, Mamoru Minami and Yasushi Mae, "Online Optimization of Avoidance Ability for Redundant Manipulator", *Proceedings of IEEE/RSJ International Conference on Intelligent Robots and Systems*, Beijing, pp.592-597, 2006.

[33] Tongxiao Zhang, Mamoru Minami and Wei Song, "Multi-preview configuration control for redundant manipulator by future reachability evaluation", *Proceedings of IEEE/RSJ*

International Conference on Intelligent Robots and Systems, SanDiego, pp.3503-3508, 2007.

[34] Mamoru Minami and Masatoshi Takahara, "Avoidance Manipulability for Redundant Manipulators", *IEEE/ASME Int. Conf. on Advanced Intelligent Mechatronics*, No.140, pp.314-319, 2003.

[35] Masatoshi Sakawa, *Optimization of Nonlinear Systems - From Single Objective to Multiobjective*, (in Japanese), Morikita Publishing Co., Ltd, 1994.

[36] Tsuneo Yoshikawa, "Foundations of Robotics: Analysis and Control", The MIT Press, 1990.

Appendix

A. Proof of Lemma 1

(necessary condition)

According to $\Delta^1\dot{\boldsymbol{r}}_{id} = {}^1\boldsymbol{M}_i{}^1\boldsymbol{M}_i^+\Delta^1\dot{\boldsymbol{r}}_{id}$, when $(\boldsymbol{I}_m - {}^1\boldsymbol{M}_i{}^1\boldsymbol{M}_i^+)\Delta^1\dot{\boldsymbol{r}}_{id} = \boldsymbol{0}$ holds for $\forall\Delta^1\dot{\boldsymbol{r}}_{id} \in R^m$, it is necessary that ${}^1\boldsymbol{M}_i{}^1\boldsymbol{M}_i^+ = \boldsymbol{I}_m$. Then ${}^1\boldsymbol{M}_i \in R^{m\times n}$ should be row full rank, that is, $rank({}^1\boldsymbol{M}_i) = m$.

(sufficient condition)

Since $rank({}^1\boldsymbol{M}_i) = m$, ${}^1\boldsymbol{M}_i$ has m non-zero singular values $(\sigma_1, \sigma_2, \cdots, \sigma_m)$. Then, ${}^1\boldsymbol{M}_i$ can be decomposed by ${}^1\boldsymbol{M}_i = \boldsymbol{U}_i\boldsymbol{\Sigma}_i\boldsymbol{V}_i^T$, where $\boldsymbol{U}_i$ is the $m\times m$ unit orthogonal matrix satisfying $\boldsymbol{U}_i\boldsymbol{U}_i^T = \boldsymbol{U}_i^T\boldsymbol{U}_i = \boldsymbol{I}_m$, $\boldsymbol{\Sigma}_i = (\,diag(\sigma_k)\,|\,\boldsymbol{0}\,)$ $(k = 1, \cdots, m$ and $\sigma_k \neq 0)$ and $\boldsymbol{V}_i$ is the $n\times n$ unit orthogonal matrix satisfying $\boldsymbol{V}_i\boldsymbol{V}_i^T = \boldsymbol{V}_i^T\boldsymbol{V}_i = \boldsymbol{I}_n$. In addition, ${}^1\boldsymbol{M}_i^+ = \boldsymbol{V}_i\boldsymbol{\Sigma}_i^+\boldsymbol{U}_i^T$, where $\boldsymbol{\Sigma}_i^+ = (\,diag(\sigma_k^{-1})\,|\,\boldsymbol{0}\,)^T$ $(k = 1, \cdots, m$ and $\sigma_k \neq 0)$. In this way, $\Delta^1\dot{\boldsymbol{r}}_{id} = {}^1\boldsymbol{M}_i{}^1\boldsymbol{M}_i^+\Delta^1\dot{\boldsymbol{r}}_{id}$ follows from ${}^1\boldsymbol{M}_i{}^1\boldsymbol{M}_i^+ = \boldsymbol{U}_i\boldsymbol{\Sigma}_i\boldsymbol{V}_i^T\boldsymbol{V}_i\boldsymbol{\Sigma}_i^+\boldsymbol{U}_i^T = \boldsymbol{I}_m$.

B. Proof of Lemma 2

From "**Lemma 1**" and relation shown in (3.11), "**Lemma 2**" is proved.

C. Proof of Theorem 1

From "**Lemma 1**", (3.5) and (3.7), "**Theorem 1**" follows.

D. Proof of Theorem 2

From "**Lemma 2**", (3.5) and (3.7), "**Theorem 2**" follows.

E. Proof of Proposition a

$$\begin{aligned} {}^1\boldsymbol{M}_n &= \boldsymbol{J}_n(\boldsymbol{I}_n - \boldsymbol{J}_n^+\boldsymbol{J}_n) \\ &= \boldsymbol{J}_n - \boldsymbol{J}_n\boldsymbol{J}_n^+\boldsymbol{J}_n \\ &= \boldsymbol{J}_n - \boldsymbol{J}_n \\ &= \boldsymbol{0}. \end{aligned} \tag{1}$$

F. Proof of Proposition b

When $m < n$, Then, according to (2.20), (7.22) and (7.28), ${}^1\boldsymbol{M}_i$ can be decomposed as

$$\begin{aligned}
{}^1\boldsymbol{M}_i &= \boldsymbol{J}_i \boldsymbol{L}_n \\
&= \overset{i}{m}\left(\tilde{\boldsymbol{J}}_i\right) \quad \overset{n-i}{\left(\boldsymbol{0}\right)} \quad \overset{n-m}{n}\left(\boldsymbol{V}_{n-m}\right) \quad \overset{n}{n-m}\left(\boldsymbol{V}_{n-m}^T\right) \\
&= \overset{i}{m}\left(\tilde{\boldsymbol{J}}_i\right) \quad \overset{n-m}{i}\left(\boldsymbol{V}_{i,(n-m)}\right) \quad \overset{n}{n-m}\left(\boldsymbol{V}_{n-m}^T\right), \qquad (2)
\end{aligned}$$

then, we can obtain

$$\begin{aligned}
rank({}^1\boldsymbol{M}_i) &= rank(\tilde{\boldsymbol{J}}_i \boldsymbol{V}_{i,(n-m)} \boldsymbol{V}_{n-m}^T) \\
&\geq rank(\tilde{\boldsymbol{J}}_i) + rank(\boldsymbol{V}_{i,(n-m)} \boldsymbol{V}_{n-m}^T) - i \\
&\geq rank(\tilde{\boldsymbol{J}}_i) + rank(\boldsymbol{V}_{i,(n-m)}) + rank(\boldsymbol{V}_{n-m}^T) - (n-m) - i \\
&= rank(\tilde{\boldsymbol{J}}_i) + rank(\boldsymbol{V}_{i,(n-m)}) + (n-m) - (n-m) - i \\
&= rank(\tilde{\boldsymbol{J}}_i) + rank(\boldsymbol{V}_{i,(n-m)}) - i \qquad (3)
\end{aligned}$$

and

$$\begin{aligned}
rank({}^1\boldsymbol{M}_i) &= rank(\tilde{\boldsymbol{J}}_i \boldsymbol{V}_{i,(n-m)} \boldsymbol{V}_{n-m}^T) \\
&\leq min\{rank(\tilde{\boldsymbol{J}}_i),\, rank(\boldsymbol{V}_{i,(n-m)}),\, rank(\boldsymbol{V}_{n-m}^T)\} \\
&= min\{rank(\tilde{\boldsymbol{J}}_i),\, rank(\boldsymbol{V}_{i,(n-m)}),\, n-m\}. \qquad (4)
\end{aligned}$$

In (3) and (4), we use an important mathematical theory: assuming $\boldsymbol{A}$ is a $n \times m$ matrix and $\boldsymbol{B}$ is a $m \times l$ matrix, then,

$$rank(\boldsymbol{A}) + rank(\boldsymbol{B}) - m \leq rank(\boldsymbol{AB}) \leq min\{rank(\boldsymbol{A}),\, rank(\boldsymbol{B})\}. \qquad (5)$$

"**Proposition b**" follows.

G. Proof of Proposition c

Because $rank(\boldsymbol{J}_i) = rank(\tilde{\boldsymbol{J}}_i)$, substituting $rank(\boldsymbol{J}_i) = min\{i, m\}$ into (3) and (4), "**Proposition c**" follows.

H. Proof of Lemma a

Because $rank(\boldsymbol{J}_n^{n-m+1\to n}) = m$, we can obtain $rank(\boldsymbol{J}_n) = m$, so, referring to (7.10), $\boldsymbol{J}_n$ can be decomposed by

$$\begin{aligned} \boldsymbol{J}_n &= \boldsymbol{U}_m\boldsymbol{\Sigma}_m\boldsymbol{V}_m^T \\ &= \boldsymbol{R}_m\boldsymbol{V}_m^T. \end{aligned} \tag{6}$$

In (6), because $rank(\boldsymbol{U}_m) = m$ and $rank(\boldsymbol{\Sigma}_m) = m$, $rank(\boldsymbol{R}_m) = rank(\boldsymbol{U}_m\boldsymbol{\Sigma}_m) = m$. Then, according to (6), we can obtain

$$\boldsymbol{V}_m^T = \boldsymbol{R}_m^{-1}\boldsymbol{J}_n. \tag{7}$$

(7) can be rewritten by

$$(\boldsymbol{V}_{(n-m),m}^T,\ \boldsymbol{V}_{m,m}^T) = \boldsymbol{R}_m^{-1}\boldsymbol{J}_n. \tag{8}$$

According to (8) and the definition of $\boldsymbol{J}_n^{n-m+1\to n}$, we can obtain

$$\boldsymbol{V}_{m,m}^T = \boldsymbol{R}_m^{-1}\boldsymbol{J}_n^{n-m+1\to n}. \tag{9}$$

In (9), because $rank(\boldsymbol{R}_m^{-1}) = m$ and $rank(\boldsymbol{J}_n^{n-m+1\to n}) = m$, we can obtain

$$\begin{aligned} rank(\boldsymbol{V}_{m,m}^T) &= rank(\boldsymbol{V}_{m,m}) \\ &= m. \end{aligned} \tag{10}$$

In addition, from (7.25), $\boldsymbol{V}^T$ can be expressed as

$$\boldsymbol{V}^T = \begin{array}{c} \\ m \\ n-m \end{array} \begin{array}{c} \begin{array}{cc} n-m & m \end{array} \\ \begin{pmatrix} \boldsymbol{A}^T & \boldsymbol{B}^T \\ \boldsymbol{C}^T & \boldsymbol{D}^T \end{pmatrix} \end{array}, \tag{11}$$

then, we can obtain that

$$\boldsymbol{V}^T\boldsymbol{V} = \begin{array}{c} \\ m \\ n-m \end{array} \begin{array}{c} \begin{array}{cc} m & n-m \end{array} \\ \begin{pmatrix} \boldsymbol{A}^T\boldsymbol{A} + \boldsymbol{B}^T\boldsymbol{B} & \boldsymbol{A}^T\boldsymbol{C} + \boldsymbol{B}^T\boldsymbol{D} \\ \boldsymbol{C}^T\boldsymbol{A} + \boldsymbol{D}^T\boldsymbol{B} & \boldsymbol{C}^T\boldsymbol{C} + \boldsymbol{D}^T\boldsymbol{D} \end{pmatrix} \end{array} \tag{12}$$

and

$$\boldsymbol{V}\boldsymbol{V}^T = \begin{array}{c} \\ n-m \\ m \end{array} \begin{array}{c} \begin{array}{cc} n-m & m \end{array} \\ \begin{pmatrix} \boldsymbol{A}\boldsymbol{A}^T + \boldsymbol{C}\boldsymbol{C}^T & \boldsymbol{A}\boldsymbol{B}^T + \boldsymbol{C}\boldsymbol{D}^T \\ \boldsymbol{B}\boldsymbol{A}^T + \boldsymbol{D}\boldsymbol{C}^T & \boldsymbol{B}\boldsymbol{B}^T + \boldsymbol{D}\boldsymbol{D}^T \end{pmatrix} \end{array}. \tag{13}$$

And because of the condition that

$$\boldsymbol{V}^T\boldsymbol{V} = \boldsymbol{I}_n, \tag{14}$$

then, from (12), we can obtain

$$\boldsymbol{A}^T\boldsymbol{A} + \boldsymbol{B}^T\boldsymbol{B} = \boldsymbol{I}_m. \tag{15}$$

Because of the condition that

$$\boldsymbol{V}\boldsymbol{V}^T = \boldsymbol{I}_n, \tag{16}$$

then, from (13), we can obtain

$$\boldsymbol{A}\boldsymbol{A}^T + \boldsymbol{C}\boldsymbol{C}^T = \boldsymbol{I}_{n-m}. \tag{17}$$

$\boldsymbol{A}^T$ and $\boldsymbol{A}$ can be expressed by singular value decomposition as

$$\boldsymbol{A}^T = {}^A\boldsymbol{U}\,{}^A\boldsymbol{\Sigma}\,{}^A\boldsymbol{V}^T \tag{18}$$

and

$$\boldsymbol{A} = {}^A\boldsymbol{V}\,{}^A\boldsymbol{\Sigma}^T\,{}^A\boldsymbol{U}^T. \tag{19}$$

In (18) and (19), ${}^A\boldsymbol{U}$ is a $m\times m$ matrix satisfying ${}^A\boldsymbol{U}\,{}^A\boldsymbol{U}^T = {}^A\boldsymbol{U}^T\,{}^A\boldsymbol{U} = \boldsymbol{I}_m$, ${}^A\boldsymbol{\Sigma}$ is a $m\times(n-m)$ matrix including the singular values of $\boldsymbol{A}$, ${}^A\boldsymbol{V}$ is a $(n-m)\times(n-m)$ matrix satisfying ${}^A\boldsymbol{V}\,{}^A\boldsymbol{V}^T = {}^A\boldsymbol{V}^T\,{}^A\boldsymbol{V} = \boldsymbol{I}_{n-m}$. Then, we can obtain

$$\boldsymbol{A}^T\boldsymbol{A} = {}^A\boldsymbol{U}\,{}^A\boldsymbol{\Sigma}\,{}^A\boldsymbol{\Sigma}^T\,{}^A\boldsymbol{U}^T \tag{20}$$

and

$$\boldsymbol{A}\boldsymbol{A}^T = {}^A\boldsymbol{V}\,{}^A\boldsymbol{\Sigma}^T\,{}^A\boldsymbol{\Sigma}\,{}^A\boldsymbol{V}^T. \tag{21}$$

According to (15) and (20), we can obtain

$$\begin{aligned}
\boldsymbol{B}^T\boldsymbol{B} &= \boldsymbol{I}_m - \boldsymbol{A}^T\boldsymbol{A} \\
&= {}^A\boldsymbol{U}\,{}^A\boldsymbol{U}^T - {}^A\boldsymbol{U}\,{}^A\boldsymbol{\Sigma}\,{}^A\boldsymbol{\Sigma}^T\,{}^A\boldsymbol{U}^T \\
&= {}^A\boldsymbol{U}(\boldsymbol{I}_m - {}^A\boldsymbol{\Sigma}\,{}^A\boldsymbol{\Sigma}^T)\,{}^A\boldsymbol{U}^T,
\end{aligned} \tag{22}$$

then, we can obtain

$$\boldsymbol{I}_m - {}^A\boldsymbol{\Sigma}{}^A\boldsymbol{\Sigma}^T = {}^A\boldsymbol{U}^T\boldsymbol{B}^T\boldsymbol{B}{}^A\boldsymbol{U}. \tag{23}$$

In (23), because $rank(\boldsymbol{B}) = m$ (please notice $\boldsymbol{B} = \boldsymbol{V}_{m,m}$ and refer to (10)) and $rank({}^A\boldsymbol{U}) = m$ (${}^A\boldsymbol{U}$ is also a $m \times m$ matrix), so we can obtain

$$rank(\boldsymbol{I}_m - {}^A\boldsymbol{\Sigma}{}^A\boldsymbol{\Sigma}^T) = m. \tag{24}$$

If $n \geq 2m$, according to (17) and (21), we can obtain

$$\begin{aligned}
\boldsymbol{C}\boldsymbol{C}^T &= \boldsymbol{I}_{n-m} - \boldsymbol{A}\boldsymbol{A}^T \\
&= {}^A\boldsymbol{V}{}^A\boldsymbol{V}^T - {}^A\boldsymbol{V} \begin{matrix} \\ m \\ n-2m \end{matrix} \begin{matrix} \begin{matrix} m & n-2m \end{matrix} \\ \begin{pmatrix} {}^A\boldsymbol{\Sigma}{}^A\boldsymbol{\Sigma}^T & \boldsymbol{\emptyset} \\ \boldsymbol{\emptyset} & \boldsymbol{\emptyset} \end{pmatrix} \end{matrix} {}^A\boldsymbol{V}^T \\
&= {}^A\boldsymbol{V}(\boldsymbol{I}_{n-m} - \begin{matrix} m \\ n-2m \end{matrix} \begin{matrix} \begin{matrix} m & n-2m \end{matrix} \\ \begin{pmatrix} {}^A\boldsymbol{\Sigma}{}^A\boldsymbol{\Sigma}^T & \boldsymbol{\emptyset} \\ \boldsymbol{\emptyset} & \boldsymbol{\emptyset} \end{pmatrix} \end{matrix}){}^A\boldsymbol{V}^T \\
&= {}^A\boldsymbol{V} \begin{matrix} m \\ n-2m \end{matrix} \begin{matrix} \begin{matrix} m & n-2m \end{matrix} \\ \begin{pmatrix} \boldsymbol{I}_m - {}^A\boldsymbol{\Sigma}{}^A\boldsymbol{\Sigma}^T & \boldsymbol{\emptyset} \\ \boldsymbol{\emptyset} & \boldsymbol{I}_{n-2m} \end{pmatrix} \end{matrix} {}^A\boldsymbol{V}^T.
\end{aligned} \tag{25}$$

In (25), because of (24), we can obtain

$$rank(\begin{matrix} m \\ n-2m \end{matrix} \begin{matrix} \begin{matrix} m & n-2m \end{matrix} \\ \begin{pmatrix} \boldsymbol{I}_m - {}^A\boldsymbol{\Sigma}{}^A\boldsymbol{\Sigma}^T & \boldsymbol{\emptyset} \\ \boldsymbol{\emptyset} & \boldsymbol{I}_{n-2m} \end{pmatrix} \end{matrix}) = n - m. \tag{26}$$

and because $rank({}^A\boldsymbol{V}) = n - m$ and (26), we can obtain $rank(\boldsymbol{C}\boldsymbol{C}^T) = n - m$, that is, $rank(\boldsymbol{C}) = n - m$.

On the other hand, if $n < 2m$, according to (17) and (21), we can obtain

$$\begin{aligned}
\boldsymbol{C}\boldsymbol{C}^T &= \boldsymbol{I}_{n-m} - \boldsymbol{A}\boldsymbol{A}^T \\
&= {}^A\boldsymbol{V}{}^A\boldsymbol{V}^T - {}^A\boldsymbol{V}{}^A\boldsymbol{\Sigma}^T{}^A\boldsymbol{\Sigma}{}^A\boldsymbol{V}^T \\
&= {}^A\boldsymbol{V}(\boldsymbol{I}_{n-m} - {}^A\boldsymbol{\Sigma}^T{}^A\boldsymbol{\Sigma}){}^A\boldsymbol{V}^T.
\end{aligned} \tag{27}$$

In (27), because $m < n < 2m$, that is $n - m < m$, we can obtain the relation as

$$\boldsymbol{I}_m - {}^A\boldsymbol{\Sigma}^A\boldsymbol{\Sigma}^T = \begin{array}{c} \\ n-m \\ 2m-n \end{array} \begin{array}{c} \begin{array}{cc} n-m & 2m-n \end{array} \\ \begin{pmatrix} \boldsymbol{I}_{n-m} - {}^A\boldsymbol{\Sigma}^{TA}\boldsymbol{\Sigma} & \boldsymbol{\emptyset} \\ \boldsymbol{\emptyset} & \boldsymbol{I}_{2m-n} \end{pmatrix} \end{array}. \tag{28}$$

Because $rank(\boldsymbol{I}_m - {}^A\boldsymbol{\Sigma}^A\boldsymbol{\Sigma}^T) = m$ in (24) and $rank(\boldsymbol{I}_{2m-n}) = 2m - n$, we can obtain

$$\begin{aligned} rank(\boldsymbol{I}_{n-m} - {}^A\boldsymbol{\Sigma}^{TA}\boldsymbol{\Sigma}) &= m - (2m - n) \\ &= n - m. \end{aligned} \tag{29}$$

and because $rank({}^A\boldsymbol{V}) = n - m$ and (27), we can obtain $rank(\boldsymbol{C}\boldsymbol{C}^T) = n - m$, that is, $rank(\boldsymbol{C}) = n - m$.

According to above discussion, in the two conditions of $n \geq 2m$ and $m < n < 2m$, that is $m < n$, we can obtain (here, please notice $\boldsymbol{C} = \boldsymbol{V}_{(n-m),(n-m)}$ in (7.25))

$$rank(\boldsymbol{V}_{(n-m),(n-m)}) = n - m. \tag{30}$$

Then, when $1 \leq i < n-m$, we can obtain the relation between $\boldsymbol{V}_{i,(n-m)}$ and $\boldsymbol{V}_{(n-m),(n-m)}$ as

$$\boldsymbol{V}_{(n-m),(n-m)} = \begin{array}{c} \\ i \\ n-m-i \end{array} \begin{array}{c} n-m \\ \begin{pmatrix} \boldsymbol{V}_{i,(n-m)} \\ \boldsymbol{V}_{(n-m-i),(n-m)} \end{pmatrix} \end{array}. \tag{31}$$

According to (30) and (31), $\boldsymbol{V}_{(n-m),(n-m)}$ is a $(n-m)\times(n-m)$ matrix with full rank. Since $\boldsymbol{V}_{i,(n-m)}$ is a $i\times(n-m)$ matrix and $\boldsymbol{V}_{i,(n-m)}$ is one part of $\boldsymbol{V}_{(n-m),(n-m)}$, then the j-th $(j = 1, \cdots, i)$ row vectors of $\boldsymbol{V}_{i,(n-m)}$ are independent and we can obtain $rank(\boldsymbol{V}_{i,(n-m)}) = i$.

When $n - m \leq i \leq n$, we can obtain the relation between $\boldsymbol{V}_{i,(n-m)}$ and $\boldsymbol{V}_{(n-m),(n-m)}$ as

$$\boldsymbol{V}_{i,(n-m)} = \begin{array}{c} \\ n-m \\ i-n+m \end{array} \begin{array}{c} n-m \\ \begin{pmatrix} \boldsymbol{V}_{(n-m),(n-m)} \\ \boldsymbol{V}_{(i-n+m),(n-m)} \end{pmatrix} \end{array}. \tag{32}$$

According to (30) and (32), $\boldsymbol{V}_{(n-m),(n-m)}$ is one part of $\boldsymbol{V}_{i,(n-m)}$, then the j-th $(j = 1, \cdots, n-m)$ column vectors of $\boldsymbol{V}_{i,(n-m)}$ are independent and we can obtain $rank(\boldsymbol{V}_{i,(n-m)}) = n - m$. In this way, we can obtain

$$rank(\boldsymbol{V}_{i,(n-m)}) = \begin{cases} i & 1 \leq i < n-m \\ n-m & n-m \leq i \leq n \end{cases}. \tag{33}$$

"**Lemma a**" follows.

I. Proof of Lemma b

Substituting (7.35) into (7.32), "**Lemma b**" follows.

J. Proof of Theorem a

If $\{n \geq 2m\} \cap \{1 \leq i < m\}$ or $\{m < n < 2m\} \cap \{1 \leq i < n-m\}$, we know that $i < m \leq n-m$ or $i < n-m < m$, by inputting these conditions into "**Lemma b**" (7.36), we can obtain

$$rank({}^1\boldsymbol{M}_i) = i. \tag{34}$$

If $\{n \geq 2m\} \cap \{m \leq i \leq n-m\}$, we know that $m \leq i \leq n-m$, by inputting this condition into "**Lemma b**" (7.36), we can obtain

$$rank({}^1\boldsymbol{M}_i) = m. \tag{35}$$

If $\{m < n < 2m\} \cap \{n-m \leq i \leq m\}$, we know that $n-m \leq i \leq m$, by inputting this condition into "**Lemma b**" (7.36), we can obtain

$$rank({}^1\boldsymbol{M}_i) = n-m. \tag{36}$$

If $\{n \geq 2m\} \cap \{n-m < i \leq n-1\}$, we know that $m \leq n-m < i$, by inputting this condition into "**Lemma b**" (7.36), we can obtain

$$n-i \leq rank({}^1\boldsymbol{M}_i) \leq m. \tag{37}$$

If $\{m < n < 2m\} \cap \{m < i \leq n-1\}$, we know that $n-m < m < i$, by inputting this condition into "**Lemma b**" (7.36), we can obtain

$$n-i \leq rank({}^1\boldsymbol{M}_i) \leq n-m. \tag{38}$$

In this way, (7.38) and (7.39) are proved in above five rough conditions as shown (34), (35), (36), (37) and (38). "**Theorem a**" follows.

K. Proof of Corollary a

In (7.40), when $i = n$ and $\nu = n-m+1$, we can obtain

$$\begin{aligned} rank({\boldsymbol{J}_i}^{\nu \to \nu+m-1}) &= rank({\boldsymbol{J}_n}^{n-m+1 \to n}) \\ &= min\{n, m\} \\ &= m. \end{aligned} \tag{39}$$

By (39), we finished the proof that "All-Non-Singular Configuration Assumption" includes "Part-Non-Singular Configuration Assumption (a)".

From (7.40), when $i < m$ and $\nu = 1$, we can obtain

$$\begin{aligned} rank({\boldsymbol J_i}^{\nu\to\nu+m-1}) &= rank({\boldsymbol J_i}^{1\to m}) \\ &= rank((\underbrace{\tilde{\boldsymbol J}_i}_{i}, \underbrace{\boldsymbol 0}_{m-i})\}m) \\ &= rank(\tilde{\boldsymbol J}_i) \\ &= i, \end{aligned} \tag{40}$$

when $m < i$ and $\nu = i - m + 1$, we can obtain

$$\begin{aligned} rank({\boldsymbol J_i}^{\nu\to\nu+m-1}) &= rank({\boldsymbol J_i}^{i-m+1\to i}) \\ &= m, \end{aligned} \tag{41}$$

then, we can obtain

$$rank(\tilde{\boldsymbol J}_i) = m. \tag{42}$$

Then, (40) and (42) can be combined as

$$rank(\tilde{\boldsymbol J}_i) = min\{i, m\}, \tag{43}$$

that is

$$rank(\boldsymbol J_i) = min\{i, m\}, \tag{44}$$

which is identical to "Part-Non-Singular Configuration Assumption (b)" of "**Theorem a**". In this way, we finished the proof that "All-Non-Singular Configuration Assumption" includes "Part-Non-Singular Configuration Assumption (b)". "**Corollary a**" follows.

L. Proof of Corollary b

Put $\Delta^1\dot{\boldsymbol r}_{id} = -\boldsymbol J_i\boldsymbol J_n^+\dot{\boldsymbol r}_{nd}$. There exists ${}^1\boldsymbol l \in R^n$ such that $\Delta^1\dot{\boldsymbol r}_{id} = {}^1\boldsymbol M_i{}^1\boldsymbol l$ if and only if $\Delta^1\dot{\boldsymbol r}_{id} \in R({}^1\boldsymbol M_i)$. That is $\Delta^1\dot{\boldsymbol r}_{id} = {}^1\boldsymbol M_i{}^1\boldsymbol M_i^+\Delta^1\dot{\boldsymbol r}_{id}$, which is equivalent to $\boldsymbol J_i\boldsymbol J_n^+\dot{\boldsymbol r}_{nd} = {}^1\boldsymbol M_i{}^1\boldsymbol M_i^+\boldsymbol J_i\boldsymbol J_n^+\dot{\boldsymbol r}_{nd}$. Since $\dot{\boldsymbol r}_{nd}$ has been assumed to be given arbitrarily in m-dimensional space, it follows $\boldsymbol J_i\boldsymbol J_n^+ = {}^1\boldsymbol M_i{}^1\boldsymbol M_i^+\boldsymbol J_i\boldsymbol J_n^+$. "**Corollary b**" follows.

M. Proof of Corollary c

Assuming "Part-Non-Singular Configuration Assumption" or "All-Non-Singular Configuration Assumption" for all i satisfying $1 \leq i \leq n-m$. From "**Theorem a**", when $1 \leq i \leq n-m$, we can obtain $rank(\boldsymbol{J}_i) = rank({}^1\boldsymbol{M}_i) = min\{i, m\}$. In addition, $\boldsymbol{J}_i$ and ${}^1\boldsymbol{M}_i$ can be decomposed as $\boldsymbol{J}_i = \boldsymbol{B}'\boldsymbol{C}'$ and ${}^1\boldsymbol{M}_i = \boldsymbol{B}'\boldsymbol{D}'$. $\boldsymbol{B}'$ is a $m \times i$ matrix, $\boldsymbol{C}'$ and $\boldsymbol{D}'$ are $i \times n$ matrices. Referring to (2.20) and (7.30), $\boldsymbol{B}'$, $\boldsymbol{C}'$ and $\boldsymbol{D}'$ can be described as

$$\begin{cases} \boldsymbol{B}' = \tilde{\boldsymbol{J}}_i \\ \boldsymbol{C}' = (\boldsymbol{I}_i \ \boldsymbol{0}) \\ \boldsymbol{D}' = \boldsymbol{V}_{i,(n-m)}\boldsymbol{V}_{n-m}^T \end{cases}, \tag{45}$$

and it is easy to know

$$\begin{cases} rank(\boldsymbol{B}') = min\{i, m\} \\ rank(\boldsymbol{C}') = i \end{cases} \tag{46}$$

and

$$rank(\boldsymbol{D}') = min\{i, n-m\} = i \tag{47}$$

because $rank(\boldsymbol{V}_{i,(n-m)}) + rank(\boldsymbol{V}_{n-m}^T) - (n-m) \leq rank(\boldsymbol{D}') \leq min\{rank(\boldsymbol{V}_{i,(n-m)}), rank(\boldsymbol{V}_{n-m}^T)\}$, that is $rank(\boldsymbol{V}_{i,(n-m)}) \leq rank(\boldsymbol{D}') \leq min\{rank(\boldsymbol{V}_{i,(n-m)}), n-m\}$, that is $min\{i, n-m\} \leq rank(\boldsymbol{D}') \leq min\{min\{i, n-m\}, n-m\}$, resulting in $rank(\boldsymbol{D}') = i$ in this case referring to (33).

Then, if $\{1 \leq i < m \leq n-m\} \cup \{1 \leq i \leq n-m < m\}$, we can obtain

$$\begin{aligned} {}^1\boldsymbol{M}_i{}^1\boldsymbol{M}_i^+\boldsymbol{J}_i\boldsymbol{J}_n^+ &= \boldsymbol{B}'\boldsymbol{D}'[\boldsymbol{D}'^T(\boldsymbol{D}'\boldsymbol{D}'^T)^{-1}(\boldsymbol{B}'^T\boldsymbol{B}')^{-1}\boldsymbol{B}'^T]\boldsymbol{B}'\boldsymbol{C}'\boldsymbol{J}_n^+ \\ &= \boldsymbol{B}'[\boldsymbol{D}'\boldsymbol{D}'^T(\boldsymbol{D}'\boldsymbol{D}'^T)^{-1}(\boldsymbol{B}'^T\boldsymbol{B}')^{-1}\boldsymbol{B}'^T\boldsymbol{B}']\boldsymbol{C}'\boldsymbol{J}_n^+ \\ &= \boldsymbol{B}'\boldsymbol{C}'\boldsymbol{J}_n^+ \\ &= \boldsymbol{J}_i\boldsymbol{J}_n^+. \end{aligned} \tag{48}$$

If $m \leq i \leq n-m$, because ${}^1\boldsymbol{M}_i$ is row full rank matrix, that is $rank({}^1\boldsymbol{M}_i) = m$, we can simply obtain

$$\begin{aligned} {}^1\boldsymbol{M}_i{}^1\boldsymbol{M}_i^+\boldsymbol{J}_i\boldsymbol{J}_n^+ &= {}^1\boldsymbol{M}_i{}^1\boldsymbol{M}_i^T({}^1\boldsymbol{M}_i{}^1\boldsymbol{M}_i^T)^{-1}\boldsymbol{J}_i\boldsymbol{J}_n^+ \\ &= \boldsymbol{J}_i\boldsymbol{J}_n^+. \end{aligned} \tag{49}$$

"**Corollary c**" follows.

Acknowledgement

I would like to say special thanks to my supervisor, Professor Mamoru Minami. With his instruction and encouragement, I can get well along with this research. Prof. Minami taught me many things such as research direction, research methods and research attitude. These will be very helpful in my future.

Then, I would like to say thanks to Prof. Osami Yasukura, Associate Prof. Yasushi Mae and Associate Prof. kenji Tanaka, they gave me many advices about my research. Especially Prof. Osami Yasukura helped me in finishing many mathematical proofs in my research. Also, I would like to say thanks to my professors in China University of Mining and Technology, Prof. Xiaoping Ma and Prof. Xijin Guo.

Moreover, I wish to express my gratitude to Mrs. Wei Song, Mr. Keiji Ikeda, Mr. Hiroshi Tanaka and Mr. Yusaku Nakamura who gave me profitable advice and helped me in my experiments. Especially Mr. Keiji Ikeda did much essential and important work for my research previously. Finally, I want to say thanks to all students in my laboratory, thanks to them, I have a good study and a happy living time.

Finally, I wish to express my gratitude to my grandfather Mr. Kongzhang Zhang, my parents Mr. Jianer Zhang, Mrs. Yan Jin, Mrs. Yin Liang, Mr. Xuan Shen, Mrs. Jianhua Chen, my uncles Mr. Buer Zhang, Mr. Guobin Yang, Mr. Bin Meng and my wife Jingjing Shen, they supported me in living and soul. Especially my grandfather Mr. Kongzhang Zhang gave me the huge spirited energy to help me in overcoming all difficulties.

Sept. 2009

Tongxiao Zhang